

University of Windsor

Scholarship at UWindor

Electronic Theses and Dissertations

Theses, Dissertations, and Major Papers

2011

EXPLORING THE REACTIVITY OF INDIUM(I) TRIFLATE AND RELATED LOW OXIDATION STATE INDIUM SALTS

Benjamin Cooper
University of Windsor

Follow this and additional works at: <https://scholar.uwindsor.ca/etd>

Recommended Citation

Cooper, Benjamin, "EXPLORING THE REACTIVITY OF INDIUM(I) TRIFLATE AND RELATED LOW OXIDATION STATE INDIUM SALTS" (2011). *Electronic Theses and Dissertations*. 388.
<https://scholar.uwindsor.ca/etd/388>

This online database contains the full-text of PhD dissertations and Masters' theses of University of Windsor students from 1954 forward. These documents are made available for personal study and research purposes only, in accordance with the Canadian Copyright Act and the Creative Commons license—CC BY-NC-ND (Attribution, Non-Commercial, No Derivative Works). Under this license, works must always be attributed to the copyright holder (original author), cannot be used for any commercial purposes, and may not be altered. Any other use would require the permission of the copyright holder. Students may inquire about withdrawing their dissertation and/or thesis from this database. For additional inquiries, please contact the repository administrator via email (scholarship@uwindsor.ca) or by telephone at 519-253-3000ext. 3208.

EXPLORING THE REACTIVITY OF INDIUM(I) TRIFLATE AND RELATED LOW
OXIDATION STATE INDIUM SALTS

By
Benjamin F. T. Cooper

A Dissertation
Submitted to the Faculty of Graduate Studies
Through Chemistry and Biochemistry
in Partial Fulfillment of the Requirements for
the Degree of Doctor of Philosophy at the
University of Windsor

Windsor, Ontario, Canada
2011
© 2011 Benjamin F. T. Cooper

“Exploring the reactivity of indium(I) triflate and related low oxidation state indium salts”

By

Benjamin F. T. Cooper

APPROVED BY:

Dr. D. S. Richeson
University of Ottawa

Dr. C. G. Weisener
Department of Earth and Environmental Sciences

Dr. S. J. Loeb
Department of Chemistry and Biochemistry

Dr. R. W. Schurko
Department of Chemistry and Biochemistry

Dr. C. L. B. Macdonald, Advisor
Department of Chemistry and Biochemistry

Chair of Defense

Declaration of Co-Authorship / Previous Publication

I. Co-Authorship Declaration

I hereby declare that this thesis incorporates material that is result of joint research, as follows:

This thesis also incorporates the outcome of joint research undertaken in collaboration with Hiyam Hamaed under the supervision of Professor Robert Schurko. The collaborative work is present in Chapters 5 and 7 of the thesis. In all cases the key ideas, primary contributions, experimental designs, data analysis, and interpretation, were performed by the author, and the contribution of the co-authors was primarily through the provision of solid state nuclear magnetic resonance spectra.

I am aware of the University of Windsor Senate Policy on Authorship and I certify that I have properly acknowledged the contribution of other researchers to my thesis, and have obtained written permission from each of the co-author(s) to include the above material(s) in my thesis.

I certify that, with the above qualification, this thesis, and the research to which it refers, is the product of my own work.

II. Declaration of Previous Publication

This thesis includes a book chapter and 6 original papers that have been previously published/submitted for publication in peer reviewed journals, as follows:

Thesis Chapter	Publication title/full citation	Publication status
Chapter 1	Benjamin F.T]. Cooper and Charles L.B. Macdonald; Mixed or Intermediate Valence Group 13 Metal Compounds. In <i>The Group 13 Metals Aluminium, Gallium, Indium, and Thallium: Chemical Patterns and Peculiarities</i> ; Aldridge, S.; Downs, A.J.; 2011	Published
Chapter 2	Alternative syntheses of univalent indium salts including a direct route from indium metal / Benjamin F.T. Cooper, and Charles L.B. Macdonald; <i>New Journal of Chemistry</i> , 2010 , 34, 8, 1551-1555	Published
Chapter 3	Synthesis and structure of an indium(I) "crown sandwich" / Benjamin F.T. Cooper, and Charles L.B. Macdonald; <i>Journal of Organometallic Chemistry</i> , 2008 , 693, 1707-1711	Published

ABSTRACT

This dissertation's primary focus is on expanding the chemistry of the unusually soluble inorganic indium(I) salt, indium trifluoromethanesulfonate (Indium triflate, InOTf). The utility of InOTf as a reagent required the development of a clean synthetic protocol in which the desired salt is produced in a reaction directly from indium metal.

The ability to ligate this salt with cyclic ethers has been previously reported, however, the unique structural and chemical features observed upon tuning the crown ether cavity size are elucidated. The sandwich-like structure of the [15]crown-5 adduct is reported, and the temperature dependence of the crystalline phase is investigated.

The affinity of crown ethers for alkali metals should allow a synthetic route for removal of the indium center from the ligand. Toward this end reactions of [In([18]crown-6)][OTf] with various potassium salts are reported.

The ability to ligate InOTf with cyclic ethers has been found to drastically alter the reactivity of the triflate salt, specifically with respect to insertion reactions into carbon-chlorine bonds in halogenated solvents. The reactions of "crowned" InOTf complexes with CH_2Cl_2 and CHCl_3 are reported.

The mixed valent nature of E_2X_4 species, indium(+2) chloride for example, was used as a model for an improved synthesis of [In][EX₄] salts. These salts also form crown ether complexes and produce the first new valence isomer of In_2X_4 observed in over 50 years. The structural features of these "crowned" species are found to depend on both the cavity size of the crown ether and the element E. Computational analyses of these complexes suggest that the covalent nature of the anion plays a role in the donor capabilities of the crowned indium(+1) fragment.

The reactivity of InOTf with α -diimine ligands is also discussed along with preliminary structural evidence and computational analyses. The nature of both the anion and the ligand are found to have an impact on the energy and reactivity of the "lone pair" of electrons on the univalent indium center.

ACKNOWLEDGEMENTS

First and foremost I need to extend my gratitude to Chuck Macdonald for his guidance and support throughout the course of my doctorate degree. On top off all the nice things I can say about Chuck, I can add that he and his wife Inga make an excellent Mr. and Mrs. Claus.

Over the years there have been many graduate students throughout the department that I would like to thank. Whether they provided fruitful discussions or necessary distractions, it helped create a great environment to be around. I would specifically like to thank Hiyam Hamaed for our collaborations.

I would also like to thank the many faculty and staff members here in the Chemistry department that have helped me along the way. Whether it was helping me learn how to use an instrument, file paperwork, or helping with my GA requirements, there have been many people that have made being a part of this department enjoyable. Special thanks to Joe Lichaa for all of his help with maintenance and computer issues. Also, thanks to the woman I call the “departmental mother”, Marlene Bezaire, for looking after all of the graduate students.

Thank you to my family for their support over the years. Even though they may not understand what I do, they’ve always been excited to hear about my accomplishments. My grandmother can finally tell her bridge group that her grandson is done his doctorate. Finally, I would like to express my gratitude to Jaclyn Dupuis for always being there to encourage and revitalize me.

You have all contributed to this work in one way or another, and so I thank you.

Table of Contents

Declaration of Co-Authorship / Previous Publication	iii
ABSTRACT.....	vi
ACKNOWLEDGEMENTS	vii
Glossary of Terms.....	xviii
Chapter 1: Introduction	1
1.1 Oxidation States vs. Valence States	1
1.2 Low Oxidation State Chemistry of Group 13 Species	5
1.3 Mixed Valent Species	10
1.4 Mixed Valent Nature of Group 13 Halides.....	13
1.5 Group 13 Donor-Acceptor Compounds.....	27
1.6 Conclusions.....	38
References.....	41
Chapter 2: Improved Synthesis of Indium (I) Starting Materials	44
2.1 Introduction.....	44
2.2 Experimental.....	53
References.....	57
Chapter 3: Structural Dependency on Crown Ether Cavity Sizes	59
3.1 Introduction.....	59
3.2. Results and Discussion	61
3.3. Experimental	72
3.4. Supplementary Material.....	76
References.....	76
Chapter 4: Insertion Chemistry of "Crowned" Indium Triflate	78
4.1. Introduction.....	78
4.2 Results and Discussion	80
4.3 Experimental.....	91
4.4 Supplementary Material.....	95
References.....	95
Chapter 5: Metathesis Reactions With "crowned" Indium Salts	97
5.1 Introduction.....	97
5.2. Experimental	98
5.3. Results and Discussion	103
5.4. Conclusions.....	115

References.....	116
Chapter 6: Experimental and computational insights on the valence isomers of $EE'X_4$ species	118
6.1 Introduction.....	118
6.2 Results and Discussion	122
6.3 Conclusion	149
6.4 Experimental Section	150
References.....	159
Chapter 7: Ligand and Anion Effect on Low Oxidation State Indium Complexes	162
7.1 Introduction.....	162
7.2. Reactivity of Trier Centers Towards Diazabutadiene Ligands	164
7.3. Role of the Anion in $[In([18]crown-6)][A]$ species	175
7.4 Conclusions.....	178
7.5 Experimental	179
References.....	181
Chapter 8: Conclusions and Future Work.....	182
References.....	185
Vita Auctoris.....	186

List of Figures

Chapter 1

Figure 1.1: Assigned formal oxidation states and valence states of Al ₂ R ₄ isomers.	3
Figure 1.2: Oxidation States of Group 13 Species (E).....	7
Figure 1.3: Disproportionation of InX	7
Figure 1.4: Early postulated isomers of E ₂ X ₄	14
Figure 1.5: Solid State structure of GaCl ₂ (Ga ₂ Cl ₄ : [Ga ⁺][GaCl ₄ ⁻], 1.1).....	14
Figure 1.6: “Dumbbell” shaped E(+2)-E(+2) anion.	17
Figure 1.7: Solid state structure of the dioxane-stabilized isomer of Ga ₂ Cl ₄ (1.14).....	18
Figure 1.8: General schematic representation of donor stabilized E(+2)-E(+2) species. ...	19
Figure 1.9: Solid state structure of the dianion [Ga ₂ I ₄ ·2PCy ₂ ⁻²] from (1.30).....	21
Figure 1.10: ^{Mes} NHC-stabilized In ₂ Br ₄ (1.33).....	22
Figure 1.11: Solid state structure of In ₆ I ₈ ·4(TMEDA) (1.35).....	23
Figure 1.12: Solid State structure of the anion [In ₅ Br ₈ (quin) ₄ ⁻] (1.36).....	24
Figure 1.13: Solid state structure of In ₂ Cl ₄ (dibenzo[18]crown-6) (1.37).	25
Figure 1.14: Three structural isomers of E ₂ X ₄	26
Figure 1.15: Formally vacant orbitals on the E(+1) centre in the donor-acceptor isomer of In ₂ Cl ₄	27
Figure 1.16: Solid state structure of the salt [Cp* ₂ Al ₃ I ₂][Cp*Al ₂ I ₄] (1.38).....	29
Figure 1.17: Solid state structure of Cp*Al-Al(C ₆ F ₅) ₃ (1.39).....	31
Figure 1.18: General representation of group 13-group13 donor acceptor complexes of Cp*E donors	31
Figure 1.19: Mixed valent donor-acceptor gallium subtriflate (1.42).	34
Figure 1.20: Solid state structure of the anion from [Ga(toluene) ₂][Ga ₅ (OTf) ₆ (Cp*) ₂] (1.43).....	35
Figure 1.21: state structure of [K(TMEDA) ₂][((^{Dipp} DAB)Ga) ₂ GaH ₂] (1.45).	36
Figure 1.22: Solid state structures of TpzGa-GaI ₃ (1.46) (left) and an indium analogue ^{tBu} Tpz(pz)In-InI ₃ (1.47) (right).	37

Chapter 2

Figure 2.1: Some examples of indium(+1) triflate, 2.1 as a reagent. (a) [Cp ₂ Fe][PF ₆], by products; ^[12] (b) LiSi(SiMe ₃) ₃ ·3thf, by products; ^[18] (c) L = 2 [15]crown-5 or [18]crown-6; ^[15, 16] (d) Cp ₂ Mn, by products; ^[12] (e) [{2,4-tBu ₂ C ₆ H ₃ NCPh} ₂ (NC ₅ H ₃)] ^[17]	45
Figure 2.2: Solid-state molecular structure of [In([18]crown-6)][TFA] (2.3) with 30% probability ellipsoids (hydrogen atoms are omitted for clarity). Selected	

metrical parameters including bond distances (Å) and angles (°): C(1)-O(1) 1.218(8), C(1)-O(2) 1.221(8), In-O(1) 2.272(5), In-O(21) 2.785(5), In-O(22) 2.825(4), In-O(23) 2.951(4), In-O(24) 2.985(5), In-O(1)-C(1) 144.0(5), O(1)-C(1)-O(2) 132.4(7).....48

Figure 2.3: (i) experimentally observed pattern for **2.2** prepared by the metal-“crowned-acid” protocol; (ii) calculated powder pattern for **2.2** on the basis of the single crystal structure.^[15]52

Chapter 3

Figure 3.1: Drawings depicting the differing behavior of compounds containing group 13 elements (E) in the +3 and +1 oxidation states with electron donors (D) or acceptors (A).....60

Figure 3.2: Thermal ellipsoid plot (30% probability surface) of the molecular structure of the salt **3.3**[OTf]. Important bond distances (Å): In-O(1) 2.9819(18), In-O(2) 3.0954(18), In-O(3) 3.0103(19), In-O(4) 2.9802(19), In-O(5) 3.0857(19).....63

Figure 3.3: Cation of mesitylene stabilized indium salt, **3.4**64

Figure 3.4: Original VT pXRD Experiments of **3.3**[OTf]; (a) ambient temperature, (b) 40 °C, (c) 100 °C.66

Figure 3.5: DSC data of original sample of **3.3**[OTf].....67

Figure 3.6: Thermal ellipsoid plot (30% probability surface) of the molecular structure of the salt **3.3**[OTf] at room temperature.68

Figure 3.7: Powder XRD patterns of **3.3**[OTf]: Experimental (a); (i) InOTf synthesized directly from indium metal, (ii) InOTf synthesized from InCl₃; (arrows indicate presence of impurity) (iii) Simulated pattern from **3.3**[OTf] at room temperature.69

Figure 3.8: VT pXRD patterns of **3.3**[OTf]: (a) ambient conditions; (b) 40 °C; (c) after cooling from 40 °C to ambient conditions; (d) above 100 °C.....70

Figure 3.9: Variable temperature ¹¹⁵In NMR spectra of **3.3**[OTf]. (a) MAS at 21.1 T; (b) Static at 21.1 T; (c) Static at 9.4 T.....71

Chapter 4

Figure 4.1: Ball and stick representation of the connectivity in the cation **4.3b** from a diffraction experiment on a crystal of very poor quality.82

Figure 4.2: Ball and stick representation of the salt **4.4a**[OTf] from a crystal with disordered refinement; most of the hydrogen atoms have been omitted. Important bond distances (Å) and angles (°): In-C(1) 2.182(15), In-Cl(1) 2.329(4), In-O(11) 2.492(12), In-O(12) 2.409(9), In-O(13) 2.531(8),

H(1)···O(14) 2.25(2), C(1)···O(14) 3.13(2), C(1)-In-Cl(1) 167.8(4), O(14)-H(1)-C(1) 146.0(9).86

Figure 4.3: Ball and stick representation of the salt **4.4b**[OTf] from crystal with disordered refinement; most of the hydrogen atoms have been omitted for clarity. Important bond distances (Å) and angles (°) C(11)-In(1) 2.174(7), Cl(1)-In(1) 2.304(2), O(11)-In(1) 2.528(5), O(12)-In(1) 2.517(5), O(13)-In(1) 2.738(5), O(14)-In(1) 2.756(5), O(15)-In(1) 2.533(5), O(16)-In(1) 2.550(5), C(11)-In(1)-Cl(1) 171.81(19).....88

Chapter 5

Figure 5.1: pXRD patterns of: (a) (i) excess [In([18]crown-6)][OTf] + [K][OTf] from MeCN, (ii) [K][OTf] + MeCN, (iii) [K([18]crown-6)][OTf], (iv) [In([18]crown-6)][OTf]; (b) (i) [In([18]crown-6)][OTf] + [K][OTf] from toluene (Note the presence of a large d-spacing ipurity or layer effect in the solid), (ii) [K([18]crown-6)][OTf]..... 104

Figure 5.2: Thermal ellipsoid plot (30% probability surface) of the molecular structure of [K([18]crown-6)][OTf]. Important bond distances (Å): K(1)-O(101) 2.948, K(1)-O(102) 2.887(17), K(1)-O(103) 2.768(14), K(1)-O(104) 2.751(15), K(1)-O(105) 2.700(13), K(1)-O(105) 2.700(13), K(1)-O(106) 2.883(13) , K(1)-O(107) 2.877(5), K(1)-O(108) 2.984(5). 106

Figure 5.3: Crystal packing diagrams of [K([18]crown-6)][OTf] (i) and [In([18]crown-6)][OTf] (ii); (ii) exhibits features that are consistent with a stereochemically-active "lone pair" of electrons on the InI ion..... 107

Figure 5.4: pXRD patterns of: (i) [In([18]crown-6)][OTf] + [K][PF₆] from MeCN, (ii) [K][PF₆] + [18]crown-6 from MeCN, (iii) [In([18]crown-6)][OTf], (iv) [K([18]crown-6)][OTf]..... 109

Figure 5.5: pXRD patterns of: (i) [In([18]crown-6)][OTf] + KCl from MeCN, (ii) [K([18]crown-6)][OTf], (iii) [In([18]crown-6)][OTf]..... 111

Figure 5.6: pXRD patterns of: (a) (i) [In([18]crown-6)][OTf] + KCp* from toluene (Note the presence of a large d-spacing ipurity or layer effect in the solid), (ii) [K([18]crown-6)][OTf] , (iii) [In([18]crown-6)][OTf]; (b) (i) [In([18]crown-6)][OTf] + KCp* from thf (Note the presence of a large d-spacing ipurity or layer effect in the solid), (ii) [K([18]crown-6)][OTf]. 113

Chapter 6

Figure 6.1: Thermal ellipsoid plot (30% probability surface) of the molecular structure of **6.3**, **6.3·CH₂Cl₂**, **6.3·[18]crown-6**, **6.4**, **6.5**. (Most hydrogen atoms have been removed for clarity)..... 125

Figure 6.2: Thermal ellipsoid plot (30% probability surface) of the molecular structure of 6.9 (hydrogen atoms on the crown ether ligand are not shown for clarity). Selected bond distances (Å) and angles (°): Ga(1)–O(1), 1.863(2); Ga(2)–O(1), 1.878(2); Ga(1)–Cl(11), 2.1374(11); Ga(1)–Cl(12), 2.1539(11); Ga(1)–Cl(13), 2.1519(10); Ga(2)–Cl(21), 2.1539(10); Ga(2)–Cl(22), 2.1554(10); Ga(2)–Cl(23), 2.1463(9); In(1)–O(1), 3.089(3); In(1)–O(2), 2.939(3); In(1)–O(3), 2.852(2); In(1)–O(4), 2.841(3); In(1)–O(5), 2.878(3); In(1)–O(6), 2.901(3); In(1)–Cl(11) 3.244(1); O–H...O(1), 1.96(4); Ga(1)–O(1)–Ga(2), 130.89(14).....	130
Figure 6.3: Thermal ellipsoid plot (30% probability) of the molecular structure of 6.12 (hydrogen atoms are not shown for clarity). Selected bond distances (Å) and angles (°): In(1)–O(101), 2.644(2); In(1)–O(102), 2.608(3); In(1)–O(103), 2.615(3); In(1)–O(104), 2.777(3); In(1)–O(105), 2.657(3); In(1)–Cl(1), 3.731(1); In(1)–Cl(4), 3.957(1); In(1)–Cl(3), 4.275(1).	136
Figure 6.4: Powder X-ray diffraction patterns of: (a) [In][GaCl ₄] + 1.2 [15]crown-5; (b) [In][GaCl ₄] + 1 [15]crown-5; (c) [In][GaCl ₄] + 2 [15]crown-5.	137
Figure 6.5: Solid state structure of 6.13 (hydrogen atoms are not shown for clarity). Selected bond distances (Å): In(2)–In(2A), 2.7242(8); In(2)–Cl(1), 2.4142(15); In(2)–Cl(2), 2.4058(15); In(2)–Cl(3), 2.4046(15); In(1)–Cl(1A), 3.6330(19); In(1)–Cl(2), 3.9999(19); In(1)–Cl(3), 3.7158(17); In(1)–O(crown) 2.608(5)–2.806(4).	138
Figure 6.6: Metrical parameters of fully geometry-optimized In–E donor-acceptor complexes	147
Chapter 7	
Figure 7.1: Low quality solid state structure of InOTf· ^{Mes} DAB. Selected bond distances (Å): In(1)–N(1), 2.5091(4); In(1)–N(2), 2.4925(4); In(1)–O(1), 2.4617(4); N(1)–C(1), 1.2274(2); N(2)–C(2), 1.2814(2); C(1)–C(2), 1.5100(3); S–O _(range) , 1.417–1.441.	167
Figure 7.2: Optimized structures of EOTf ^H DAB; (a) E = In, (b) E = Ga	169
Figure 7.3: Optimized structures of ECl· ^H DAB; (a) E = In; (b) E = Ga.....	172
Figure 7.4: Highest Occupied Molecular Orbital of; (a) InCl· ^H DAB; (b) GaCl· ^H DAB..	174

List of Schemes

Chapter 2

Scheme 2.1: Preparation of InOTf via protonolysis of In^I-containing precursors.46

Scheme 2.2: Metal-acid syntheses of indium(+1) salts **2.1** and **2.2**.....50

Chapter 3

Scheme 3.1: Reaction of InOTf with [15]crown-562

Chapter 4

Scheme 4.1: Insertion reactions of "crowned" indium(+1) cations.....81

Scheme 4.2: Potential stepwise reaction pathways for C-Cl bond insertion.90

Chapter 5

Scheme 5.1: Crowned complexes of InOTf.....98

Scheme 5.2: Summary of potassium salt reactions with **5.1**..... 114

Chapter 6

Scheme 6.1: Simplified illustration of the different electronic structure for E^{III} vs. E^I valence states and selected examples of univalent group-13 species that have been used as donors (E= B, Al, Ga, Tl)..... 120

Scheme 6.2: Valence isomers of E₂X₄ (X = Cl, Br or I) including idealized parent valence isomers (top row) and selected examples observed experimentally (bottom row) for: (a) the ionic isomer; (b) the "covalent" isomer; (c) the donor-acceptor isomer. 121

Scheme 6.3: Some possible routes from **6.2** to **6.3** (X = Cl), **6.4** (X = Br), or **6.5** (X = I).
..... 127

Scheme 6.4: Metathetical synthesis of In-In donor-acceptor complexes..... 128

Scheme 6.5: Direct synthetic route to "crowned" indium(I) complexes; the circle represents the [18]crown-6 ligand. 135

Scheme 6.6: Graphical depiction of energies determined in this work. The bond snapping energy is calculated as the difference in energy between the energies of the component donor and acceptor fragments fixed in the geometry they possess in the complex; the reaction energy is determined by the energy difference between the optimized donor and acceptor molecules and the adduct they form..... 144

Chapter 7

Scheme 7.1: Group 13 NHC analogues	164
Scheme 7.2: Synthesis of a gallium NHC analogue	164
Scheme 7.3: Potential canonical forms for DAB complexes of E-X species; (i) ligand reduction and covalent bonding; (ii) donor-acceptor complex formation ..	165
Scheme 7.4: ^R DAB and ^R BIAN Ligands	166
Scheme 7.5: Formal ligand reduction during the complexation of EOTf species by DAB ligands	168

Chapter 8

Scheme 8.1: Potential metathesis reactions involving [In][GaCl ₄] species.	184
---	-----

List of Tables

Chapter 1

Table 1.1: Characteristics of the Four Classes of Mixed Valence Compounds..... 12

Table 1.2: Bond distances of E(+1)-E(+3) complexes..... 32

Chapter 2

Table 2.1: Crystal data and structure refinement for [In([18]crown-6)][TFA]..... 55

Chapter 3

Table 3.1: Summary of collection and refinement data for the X-ray diffraction investigation of **3.3**[OTf]. 75

Chapter 4

Table 4.1: Summary of collection and refinement data for the X-ray diffraction investigations of **4.4a** and **4.4b**. 94

Chapter 5

Table 5.1: Summary of X-ray crystallographic data for [K([18]crown-6)][OTf]..... 102

Chapter 6

Table 6.1: Selected metrical parameters for compounds **6.3**, **6.3·CH₂Cl₂**, **6.3·[18]crown-6**, **6.4**, and **6.5**. 125

Table 6.2: Solution ¹¹⁵In NMR data for [In][ECl₄] and [In([18]crown-6)][ECl₄] salts... 133

Table 6.3: Selected data from DFT calculations for geometry optimized crowned univalent indium model compounds(see experimental for details). 141

Table 6.4: Computational results for indium-indium donor-acceptor complexes. E_{snap} and E_{rxn} are illustrated in Scheme 6.6. 147

Table 6.5: Bond lengths, Wiberg bond indices, and MO orbital contributions for optimized donor-acceptor complexes. 149

Table 6.6: Crystallographic Information for **6.3**, **6.3·CH₂Cl₂**, **6.3·[18]crown-6**, and **6.4** 155

Table 6.7: Crystallographic Information for **6.5**, **6.9**, **6.12**, and **6.13** 1577

Chapter 7

Table 7.1: Diimine reactions with InOTf.....	166
Table 7.2: Lone pair and WBI data of DAB speices	175
Table 7.3: Computational data for a series of "crowned" indium salts.....	177

Glossary of Terms

Å	angstroms
A	anion
²⁷ Al	aluminum-27
Bu	butyl
CSD	Cambridge structural database
°C	degrees Celsius
CCDC	Cambridge Crystallographic Data Center
CCD	charge-coupled device
δ	chemical shift
DSC	differential scanning calorimetry
d	doublet
λ	wavelength
E	Group 13 metal center
eV	electron volts
X	Halogen
D	Donor
K	degrees Kelvin
Dipp	2,6-diisopropylphenyl
NHC	N-heterocyclic carbene
R	Substituent
FT	fourier transform
IR	Infrared

${}^nJ_{a-b}$	n-bond coupling between nuclei a and b
UV	Ultraviolet
NMR	Nuclear Magnetic Resonance
${}^{19}\text{F}$	fluorine-19
${}^{71}\text{Ga}$	gallium-71
g	gram
${}^1\text{H}$	hydrogen-1
HSAB	hard soft acid base theory
HOMO	highest occupied molecular orbital
kJ	kiloJoules
${}^{115}\text{In}$	Indium-115
ppm	parts per million
Me	methyl
Mes	mesityl
mg	milligram
mmol	milimole
mol	mole
mL	millilitre
mp	melting point
MO	molecular orbital
NBO	Natural Bond Orbital
Et	ethyl
${}^i\text{Pr}$	iso-propyl
${}^n\text{Pr}$	n-propyl

^t Bu	tertiary butyl
Cy	cyclohexyl
LUMO	lowest unoccupied molecular orbital
LP	lone pair
DMF	dimethylformamide
SS-NMR	solid-state nuclear magnetic resonance
THF	tetrahydrofuran
TMEDA	tetramethylethylenediamine
T	Tesla
Quin	quinuclidine
Ch	chalcogen
cm	centimeter
Cp	cyclopentadienyl
Cp'	substituted cyclopentadienyl
Cp*	pentamethylcyclopentadienyl
Nacnac	β -diketiminato ligand
NCA	Non-coordinating anion
OTf	trifluoromethanesulfonate, triflate
HOTf	trifluoromethanesulfonic acid
HRMS	high resolution mass spectrometry
ESI	electrospray ionization
TOF	time of flight
Ph	phenyl
DAB	diazabutadiene ligand

Tpz	tris(pyrazolyl)borate
TFA	trifluoroacetate
Pn	pnictogen
MeCN	acetonitrile
pXRD	powder X-Ray diffraction
s	singlet
t	triplet
WBI	Wiberg Bond Index
VAC	Vacuum Atmospheres Company

Chapter 1: Introduction

1.1 Oxidation States vs. Valence States

The concept of an element existing in a particular oxidation state^[1] is one of the oldest and most fundamental models employed to rationalize the chemical behaviour of a system. The inherent logic that underlies this approach stems from the understanding that the oxidation state provides a measure of the number of electrons associated with, and thus the chemistry of, a given element. While there are many methods that may be employed to assign an oxidation state to a particular element in any given compound, the majority of the approaches used involve the use of some sort of electron counting rules underpinned by certain axioms (such as: oxygen atoms typically must be counted as O(-2); hydrogen atoms must be treated as H(+1), protonation or deprotonation does not change the oxidation number, etc.). While the "formal oxidation states" that are provided by such counting rules have proven to be effective for the balancing of redox equations and are used frequently, they do not necessarily provide any useful information in regard to the structural features of the molecule or the chemistry of the element of interest, especially in the case of the p-block elements. For example, the formal oxidation states of the carbon atoms in the molecules $\text{CH}_{4-n}\text{F}_n$ (for $n = 0$ to 4) range from -4 to $+4$ in spite of the similar descriptions of the geometrical features (i.e., tetrahedral geometry, hybridization at carbon (sp^3), bonding (e.g., $a_1 + t_2$ molecular orbitals for CH_4 and CF_4)) and the relatively inert nature of each of the compounds. Along a similar line of reasoning, the assignment of a similar formal oxidation state of 0 to the carbon atoms in each of the following species: $\text{O}=\text{CH}_2$ (formaldehyde), CH_2Cl_2 , CHCl (chlorocarbene), diamond and graphite, clearly does not imply any similarity in the nature of the structures,

bonding models or reactivities exhibited by the compounds. Given the foregoing, while it is easy to assign a formal oxidation state or number to an element – knowledge of the empirical formula of the molecule is usually sufficient for the task – it is often wise to avoid ascribing too much importance to any formal oxidation state assigned by such rules.

A related but distinct model that may be used to understand the distribution of electrons about an element is that of the valence state.^[2] The valence state is a measure of the number of valence electrons used by an element for bonding; specifically, it is defined by subtracting the number of non-bonding electrons from the number of electrons in the free atom and is often more suitable for understanding the structural features of the element in a molecule. As indicated by the definition, and in contrast to a formal oxidation state, it is often impossible to assign a valence state to an element without knowledge of the actual electron distribution in the molecule in which the element is located. In particular, the presence (or absence) and location of non-bonding ("lone pair") electrons in the molecule is crucial to the correct assignment of a valence state. Such information is often only able to be inferred upon examination of molecular structural data or obtained by computational investigations of the compounds.^[3] Furthermore, because the valence state of an element is intimately connected to the actual distribution of electrons in a molecule, it often provides superior insight into the structural features and chemical behaviour that one may anticipate for the compound.

Unfortunately, the terms "oxidation state" and "valence state" are often treated as being interchangeable in the chemical literature. This situation likely arose because transition metals are often able to form coordination complexes in which the formal oxidation state and the valence state of the metal are identical. Furthermore, as indicated by Parkin,^[2] the term "valence" has also been used in some instances to indicate the

number of bonds to an atom or the coordination number of an atom. Although the valence does sometimes correspond to those numbers, there are many cases in which it does not; hence, to avoid confusion the term valence should not be used in that manner.

In order to illustrate the difference between formal oxidation numbers and valence states and the potential for confusion between the two, a few examples are provided in Figure 1.1.

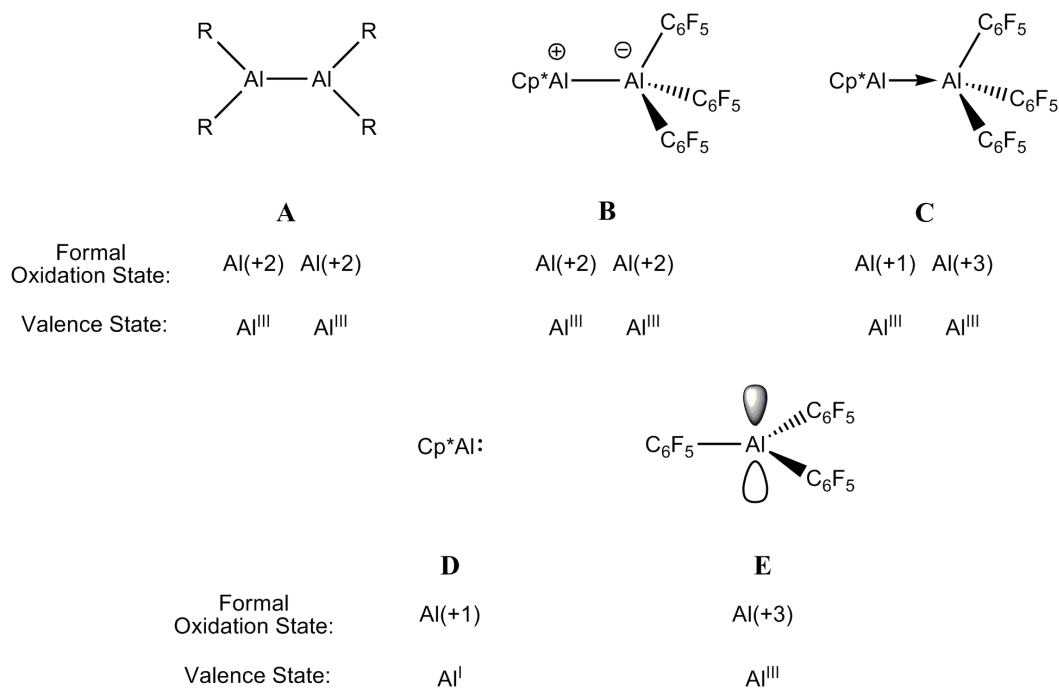


Figure 1.1: Assigned formal oxidation states and valence states of Al₂R₄ isomers.

An important low oxidation-state organoaluminum compound is the dialane R₂Al-AlR₂ (R = CH(SiMe₃)₂), **A**. A formal oxidation state of +2 may be assigned to each aluminum atom in the compound: the 4 ligands each bearing a -1 charge are balanced equally by 2 aluminum atoms to give the neutral molecule. However, both of the aluminum atoms in the compound are properly described as being trivalent in that all three valence electrons on each Al atom is involved in bonding and there are no non-bonding electrons. While the valence state certainly provides the best description of the

structural features and electron distribution of the molecule, the interesting and diverse reactivity of the dialane suggests that the presence of the Al-Al bond, indicated by the assignment of the +2 oxidation state to Al, truly does render the chemistry of this molecule different from that of other trivalent aluminum compounds. It is very likely that the reactivity is a consequence of the relative weakness and non-polarity of the metal-metal bond, rather than because of the presence of "+2 oxidation state" for Al; however, the unusual formal oxidation state does at least suggest that there is something unusual about the molecule. In a similar vein, the compound $\text{Cp}^*\text{Al}-\text{Al}(\text{C}_6\text{F}_4)_3$, **B** or **C**, has been called "mixed valent", not in the least because it is formed by mixing the univalent aluminum compound Cp^*Al **D** (in which Al is also in the +1 oxidation state) with the trivalent aluminum compound $\text{Al}(\text{C}_6\text{F}_4)_3$ **E** (in which Al is also in the +3 oxidation state). In the complex, the average oxidation state for Al is +2 for the same reason described for the dialane and the formal oxidation states assigned to the Al atoms remain +1 and +3, respectively (**C**). The compound can be treated as a donor-acceptor complex with a dative Al-Al bond, or equally validly, it could be considered as a dicoordinate $\text{Al}(+2)$ cation that is bonded to a tetracoordinate $\text{Al}(+2)$ anion (**B**). Regardless of the formal oxidation states on the Al atoms in such a compound, Parkin correctly argues that each of the aluminum atoms is again properly described as *trivalent* because all of the electrons on each atom are involved in bonding and there are no non-bonding electrons. Again, it must be emphasized that the proper description of the valence state, while generally a superior tool for understanding the distribution of electrons in a molecule, can sometimes mask interesting features of the compound that are suggested by formal oxidation states; the concepts of oxidation or valence states are simply models that are employed to assist

chemists in understanding the nature of molecules and both have strengths and weaknesses that must be taken into consideration.

In light of the foregoing discussion, the use of the valence and oxidation state terminology in the literature is far from ideal. For the purposes of this dissertation, the term "mixed valent" will be used in the colloquial sense to indicate a compound that contains a single group 13 element in more than one oxidation state or valence state. It should also be noted that the term "subvalent" (usually indicating that there are not enough ligands to bond with the elements of interest they were all in its highest valence state) has also often been used to describe such compounds. When appropriate, the valence state will be indicated with superscripted Roman numerals (e.g., In^{I} indicates univalent indium) and the formal oxidation state will be indicated with Arabic numerals in parentheses (e.g., $\text{Ga}(+2)$ indicates gallium in the +2 formal oxidation state.)

1.2 Low Oxidation State Chemistry of Group 13 Species

The chemistry of group 13, also referred to as the triels, can differ quite drastically from the low oxidation state species to their higher oxidation state analogues. As illustrated in Figure 1.2, while higher oxidation state species (+2, +3) have a vacant p-orbital associated with the group 13 center (E), the +1 oxidation state has both vacant p-orbitals and a "lone pair" of electrons associated with the triel element. The electron rich nature of the E(+1) center, coupled with the fact that E(+1) centers are typically coordinatively unsaturated, generally make E(+1) centers weak Lewis acids, stronger Lewis bases, and allow for unique reactivities only available to low oxidation state species. The +1 oxidation state becomes increasingly stable as you move down the periodic table (i.e., $\text{Al} < \text{Ga} < \text{In} < \text{Tl}$), with it being the preferred oxidation state for

thallium. This increased stability occurs due to a phenomenon called the "inert pair effect", and arises, in part, due to the energy difference between the ns orbital and the np orbitals. The valence electron configuration of the triel centers is ns^2np^1 , and as the principle quantum number (n) increases, the energy gap between the s and p orbitals increases. For the lighter elements the energy required to promote the ns^2 electrons is compensated for by the formation of relatively strong E-R bonds; however, for the heavier congeners, the increased radii of the triel center results in the formation of weaker bonds.^[4] As a result, it can be energetically favourable for the triel center to form a compound with a "lone pair" of electrons on the metal center, rather than to form two extra bonds. For thallium, the lone case where the +1 oxidation state is favoured over the +3 oxidation state, relativistic effects also must be considered. The electrons in the 6s orbital of thallium are traveling at such high velocities that the orbital size is decreased: this is known as relativistic contraction,^[5] which lowers the energy of the contracted 6s orbital. While relativistic effects play a role in the physical properties of thallium, the "inertness" of the 6s electrons is primarily attributed to the weakness of E-R bonds formed with the thallium center. Finally, it is worth emphasizing that because E(+1) cations are less electronegative than E(+3) cations, the nature of the interactions between the group 13 element and substituents from the top right-hand side of the p-block tend to be more ionic for E(+1) than for E(+3).

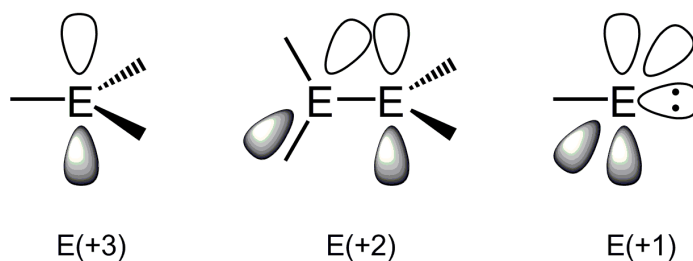


Figure 1.2: Oxidation States of Group 13 Species (E)

While the electron rich nature and coordinative unsaturation of low oxidation state indium species allow interesting chemistry to be performed, they also contribute to one of the leading obstacles to its development, which is disproportionation, the formation of elemental indium and higher oxidation state species from lower oxidation state derivatives (Figure 1.3). The relatively high energy of the $5s^2$ "lone pair" of electrons (i.e., basicity of the indium center) makes indium(+1) species susceptible to reactivity such as oxidation, and insertion reactions. Evidence suggests oxidation reactions involving indium(+1) compounds typically proceed through a one electron process to an indium(+2) intermediate, followed by a rapid oxidation to the final indium(+3) product.¹⁶

71



Figure 1.3: Disproportionation of InX

Perhaps some of the first compounds to come to mind when discussing low oxidation state main group species are metalloids clusters, complexes where the number of metal-metal bonds outnumber the ligand-metal bonds, which have been extensively

investigated by Schnöckel.^[8-10] Cluster formation is usually achieved via the use of bulky substituents which are required to impede disproportionation pathways (at least to complete disproportionation) and are particularly interesting as investigations into metalloid clusters can provide insight into solid-state bonding environments and properties of bulk materials and nanoparticles. While the numbers of structurally characterized aluminum and gallium clusters are well represented in the literature, the low solubility of InX (X = halide) starting materials impedes investigations into the analogous indium compounds, and illustrates the need of appropriate InR starting materials.

The synthesis of monomeric InR compounds has historically been plagued by aggregation and disproportionation. However, InR species can be stabilized by manipulating either the environment they exist in or the nature of the substituent R. For example, InR species can be synthesized in the gas phase at low pressures, or by trapping the compound in a solid inert matrix, both sets of conditions lead to the retention of the desired InR product.^[11] Alternatively, selection of an appropriately bulky, non-oxidizing substituent, R, can also yield a stable, monomeric InR species which resist aggregation into oligomers and/or disproportionation. Ligands prevalent in the literature for the formation of lower oxidation state species (0 to +2) include cyclopentadienyl, supersilyl, bulky aryl groups, terphenyl, β -diketiminates, diazabutadienes, and poly(pyrazolyl)borates.^[11-25] As the steric bulk of the substituent is decreased, the formation of weak metal-metal bonds affords oligomeric structures, as is illustrated by the Cp*E (E = Al, Ga, In) series which forms a tetramer (E = Al),^[26] or hexamers (E = Ga, In) in the solid state.^[27, 28] While these Cp*E compounds form clusters in the solid state, the resultant chemistry suggests monomeric species in solution, as they have been found to act as Lewis bases in the formation of transition metal complexes, as well as main group

acceptors.^[29-34] The presence of the “lone pair” of electrons on the metal center, and the potential ability to act as a π -backbonding acceptor, make E^I species particularly interesting in their use as transition metal ligands, as they are isovalent with CO.

Research into the development of indium chemistry has partially been driven by interest in III-V semiconductors, such as InP, indium oxide and its tin/zinc doped derivatives, and their potential uses in solar cells and other optoelectronic devices.^[4, 11] Development of low oxidation state indium species, excluding gas phase reactions, is primarily initiated by the use of monohalides or cyclopentadienyl derivatives. However, solubility and stability of these species hampers further development of indium chemistry and thus new materials are desirable. Previously in the Macdonald group, an exciting development in the field came via the synthesis of a structurally characterized, stable, soluble low oxidation state indium salt, indium(+1) trifluoromethanesulfonate (indium triflate, InOTf).^[35] This salt is particularly interesting as it has improved solubility over the starting halides, is stable in a variety of organic solvents, and can be reacted with an appropriately sized crown ether, [18]crown-6, to synthesize $[\text{In}([\text{18}]\text{crown-6})][\text{OTf}]$,^[36] the first structurally characterized monomeric indium(+1) species with indium acting as a Lewis acid. This is an encouraging synthetic development as attempts to ligate the indium(+1) halides has been met with rapid disproportionation, as is discussed in section 1.4.^[37] While certain aspects of the chemistry of this particular reagent, and its "crowned" analogue, will be discussed in detail in this dissertation, it should be noted that InOTf has also found utility as an organic transformation catalyst.^[38, 39] Kobayashi et al. found remarkable selectivity is obtained using InOTf for carbon-carbon bond formation reactions with allylboronates and acetals or ketals. They hypothesize that it is the amphoteric nature of indium(I) triflate that allows for the activation and selectivity within

these systems. While indium metal, and both mono- and trihalides have been used as catalysts for Barbier and Friedl-Crafts reactions, C-C bond formation, and transmetallations, this is an important discovery in the catalytic use of indium as Kobayashi et al. found that InOTf was the only compound to successfully catalyze the reaction.

The synthesis of InOTf helps illustrate a void in the development of low oxidation state indium chemistry, the isolation of indium(+1) salts with “common” anions (e.g., the lack of a structurally characterized "simple" amidoindium(+1) compound). While catalysis, optoelectronic devices, and semiconductor research continues to advance, the synthesis of other stable, soluble indium(+1) reagents could provide some of the greatest impact into the development of these fields by allowing for reactions to be performed under conditions that would previously cause disproportionation of the indium reagents. As such, the development of simple, stable salts and their structural properties merits increased investigation.

1.3 Mixed Valent Species

Using the most general definition, mixed valent species are an intriguing class of compounds that incorporates the same element in more than one oxidation or valence state. These compounds often exhibit significantly different properties when compared against relevant "parent" compounds. For example, while the parent tungsten compounds WO_3 and LiWO_3 are insulators, they may be combined to produce the mixed valent salt $\text{Li}_x\text{W}^{\text{V}}_x\text{W}^{\text{VI}}_{1-x}\text{O}_3$ that is a conductor.^[40] The impact of the presence of elements in two different oxidation states on the electronic, structural, and magnetic properties of numerous examples of such compounds, in conjunction with the prior absence of a

system of categorization for such species, led Robin and Day in 1967 to formulate a convention to classify the growing group of mixed valent compounds (primarily containing transition metals) that were being reported at the time.^[40]

Robin and Day classified mixed valence species by looking at the symmetry and strength of the ligand fields associated with the metal sites in the compound. A table outlining the full classification system from their article in *Advances in Inorganic Chemistry* is reproduced here in Table 1.1. In essence, the difference between the different classes of mixed valent compounds in their system is related to the amount of electronic communication between the different metal centers. If there is no electronic communication between the metal centers (i.e., $\alpha = 0$, where α is the coefficient describing the probability of electron transfer from one redox center to another and is thus a measure of the degree of delocalization of the electrons between the metals), then the number of electrons on each metal remains fixed and the compound is assigned to Class I: this is typically the case when the two metals are in very different coordination environments. Class II is used to describe situations in which there is some electronic communication between the metal centers in different oxidation states (i.e., $\alpha > 0$, "partially delocalized") and Class III describes complete delocalization (i.e., $\alpha \approx 1$, "fully delocalized") of the charge/electrons between the redox centers. Class III is divided into type A, which is used to describe systems containing "islands" of complete delocalization that are isolated from each other (such as solids containing isolated metal clusters), and type B, in which the delocalization extends throughout the solid.

Table 1.1: Characteristics of the Four Classes of Mixed Valence Compounds^[40]

Class I	Class II	Class III-A	Class III-B
(1) Metal ions in ligand fields of very different symmetry and/or strength, i.e., tetrahedral vs. octahedral	(1) Metal ions in ligand fields of nearly identical symmetry, differing from one another by distortions of only a few tenths Å	(1) Metal ions indistinguishable but grouped into polynuclear clusters	(1) All metal ions indistinguishable
(2) $\alpha = 0$; valences very firmly trapped	(2) $\alpha > 0$; valences distinguishable, but with slight delocalization	(2) α maximal locally	(2) α maximal; complete delocalization over the cation sublattice
(3) Insulator; resistivity of 10^{10} ohm cm or greater	(3) Semiconductor; resistivity in the range 10 - 10^7 ohm cm	(3) Probably insulating	(3) Metallic conductivity; resistivity in the range 10^{-2} - 10^{-6} ohm cm
(4) No mixed valence transitions in the visible region	(4) One or more mixed valence transitions in the visible region	(4) One or more mixed valence transitions in the visible region	(4) Absorption edge in the infrared, opaque with metallic reflectivity in the visible region
(5) Clearly shows spectra of constituent ions, IR, UV, Mössbauer	(5) Shows spectra of constituent ions at very nearly their normal frequencies	(5) Spectra of constituent ions not discernible	(5) Spectra of constituent ions not discernible
(6) Magnetically dilute, paramagnetic or diamagnetic to very low temperatures	(6) Magnetically dilute, with both ferromagnetic and antiferromagnetic interactions at low temperatures	(6) Magnetically dilute	(6) Either ferromagnetic with a high Curie temperature or diamagnetic, depending upon the presence or absence of local moments

In compounds, the group 13 elements are commonly found in the E(+1), E(+2), or E(+3) oxidation states, and the E(0) oxidation state is only observed in certain instances. Mixed valence species of this group incorporate atoms in at least two of these oxidation states. While an element by element discussion was included following the Robin-Day classification system, the group 13 section was relatively undeveloped because only four mixed valence species incorporating gallium, indium, or thallium had been characterized structurally at the time.^[40] The number of well-characterized mixed valence group 13 compounds has increased significantly since then and will be discussed in the following sections.

1.4 Mixed Valent Nature of Group 13 Halides

In general in this section, the group 13 elements (E = Al, Ga, In, Tl) will be examined from lightest to heaviest. Aluminum is the most electropositive element in group 13 and there are no stable base-free subhalides of the formula "AlX₂" known; hence, the discussion will begin with gallium. It should also be noted that the presence of fluorine typically favours the adoption of the highest available oxidation state. While TlF is a known salt, as Tl(+1) is favoured for reasons mentioned above, no mixed valent element fluorides have been structurally characterized. Thus, for the purposes of the discussion that follows, the halogen X is limited to Cl, Br and I only.

Early investigations into the nature of E(+2)X₂ salts began when it was discovered that these species were not paramagnetic, as would be expected on the basis of simple electron counting.^[41] It was reasoned that the diamagnetic nature of the species could

arise from the adoption of either of two valence isomer alternatives. Both possibilities have the formula E_2X_4 and are illustrated in Figure 1.4.

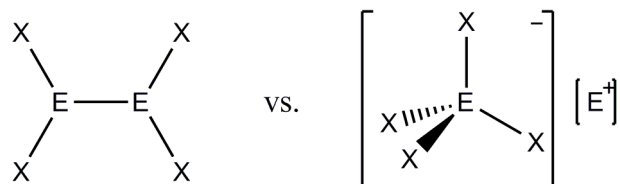


Figure 1.4: Early postulated isomers of E_2X_4 .

Initial results suggested that the ionic mixed valent formulation was the most appropriate; for example, the Raman spectrum of $GaCl_2$ (**1.1**), synthesized through the reaction of the proper stoichiometries of $GaCl_3$ with Ga metal, proved to be very similar to the spectrum obtained for salts containing the $[GaCl_4]^-$ anion.^[42] Furthermore, the Raman spectrum showed no evidence of a gallium-gallium bond. Any ambiguity as to the nature of the salt was removed completely upon the solution of the solid state structure of " $GaCl_2$ " (Ga_2Cl_4) by Garton in 1957 (Figure 1.5), confirming that it exists as a Robin-Day Class I mixed valent salt.

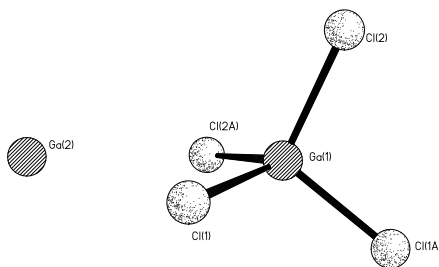


Figure 1.5: Solid State structure of $GaCl_2$ (Ga_2Cl_4 : $[Ga][GaCl_4]$, **1.1**).

Crystallizing in the orthorhombic space group *Pnna*, the structure consists of a tetrahedral $[\text{GaCl}_4^-]$ anion and a Ga-Cl distances of 2.160 and 2.184 Å and a Ga^+ cation with eight nearest neighbour chlorine atoms (at distances of at least 3.196 Å) resting at the corners of a dodecahedron.^[43] The adoption of an ionic structure rather than the covalent molecular $\text{Cl}_2\text{Ga-GaCl}_2$ alternative in the solid state is certainly favored by the greater lattice energy of the ionic alternative; however, other investigations reveal that lattice energy is not the only important factor. Consistent with the solid-state structural and spectroscopic data showing the mixed valent ionic nature of gallium(+2) halides, a molten-state ^{71}Ga NMR investigation found two distinct gallium resonances for each of the salts investigated.^[44] The chemical shifts were compared to that of $[\text{GaCl}_4^-]$ in aqueous HCl and were found to be shielded in comparison to the reference signals at 60 ppm ($[\text{GaCl}_4^-]$) and 750 ppm (Ga^+) for a GaCl_2 melt. Similarly, a GaBr_2 melt showed two gallium resonances at 130 ppm ($[\text{GaBr}_4^-]$) and 670 ppm (Ga^+). Interestingly, solution NMR studies in benzene showed a drastic shift in the Ga^+ resonances to 909 ppm and 942 ppm for GaBr_2 and GaCl_2 , respectively.^[44] While the effects of benzene on mixed valent halides will be discussed in the next section, these studies provide further evidence confirming the mixed valent nature of not only GaCl_2 but also GaBr_2 .

An interesting reaction of the salt GaCl_2 with gallium metal and AlCl_3 affords the structurally- and conceptually-related salt $[\text{Ga}][\text{AlCl}_4]$ (**1.2**):^[45, 46]



While the salt is not a mixed valent salt in the traditional sense – in that it contains two different group 13 elements in the two different oxidation states – it demonstrates the favorability of the univalent-trivalent motif and illustrates that such compounds follow

the anticipated periodic trend that heavier elements will prefer the +1 oxidation state over the lighter group 13 elements.

Although the initial investigations into the preparation and characterization of gallium(+2) iodide and the indium(+2) halides were pursued in the 1950's, structural authentication of the salts was not obtained until the 1980's. In fact, several subiodides of gallium were synthesized by heating various stoichiometries of gallium metal and iodine. In spite of the formula, even the material known as "GaI" obtained from the sonication of gallium metal with one half equivalent of I₂ undoubtedly exists as a mixed-valent compound, although the structure has not been elucidated.^[47] Not surprisingly, the crystal structure of Ga₂I₄ consists of the mixed valent salt [Ga][GaI₄] (1.3) packed in the rhombohedral space group *R3c*.^[48] The structure for the subhalide Ga₂I₃ was also elucidated and found to be a mixed valence salt of the formula [Ga⁺]₂[Ga₂I₆⁻²] (1.4) packing in the monoclinic space group *P2₁/c*. The salt also incorporates a gallium(+2)-gallium(+2) bond in the form of a staggered "dumbbell" shaped anion with a measured Ga-Ga distance of 2.387(5) Å. The "dumbbell" is a structural motif that is relatively common amongst ionic mixed valent group 13 species and is reported frequently in the literature; the propensity of Ga (and In) to form such E-E linked fragments is perhaps to be expected, given that related fragments (or distortions) are observed even in some polymorphs of the elements themselves.^[49, 50]

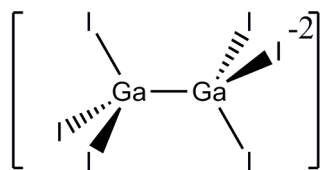


Figure 1.6: “Dumbbell” shaped E(+2)-E(+2) anion.

Tuck and co-workers reported simple synthetic routes to the indium(+2) halides through the reflux of InX_3 with excess indium metal in xylene for 18 hours.^[51] The iodide salt exists as pale yellow crystals with the composition $[\text{In}][\text{InI}_4]$ (**1.5**), which is similar to the analogous gallium salt.^[52] The tetraiodoindate anion contains indium in a tetrahedral environment, while the indium cation has eight nearest neighbour iodine atoms at distances ranging from 3.588(2) to 3.673(2) Å. Similarly, the thallium analogues TlCl_2 (**1.6**) and TlBr_2 (**1.7**) were confirmed to be mixed valent species of the form $[\text{Tl}][\text{TlX}_4]$ on the basis of X-ray diffraction studies and solid state ^{205}Tl NMR studies.^[53, 54]

Other subhalides of indium were prepared by Meyer through the reduction of InX_3 with In metal in various stoichiometries, and all are similarly found to exist as mixed valent salts. The chloride species In_5Cl_9 (**1.8**) and In_2Cl_3 (**1.9**), are characterized as the ionic species $[\text{In}]_3[\text{In}_2\text{Cl}_9]$ and $[\text{In}]_3[\text{InCl}_6]$, respectively, while In_2Br_3 (**1.10**) adopts the formula $[\text{In}]_2[\text{In}_2\text{Br}_6]$ and In_5Br_7 (**1.11**) is found to be $[\text{In}]_3[\text{In}_2\text{Br}_6][\text{Br}]$. Both of the bromides again contain the dianionic “dumbbell” E(+2)-E(+2) bonded ionic species, with the E-E bond distances of 2.67 Å and 2.74 Å for the distinct anions.^[55] A more recent structural investigation by Ruck and co-workers of In_5Br_7 revealed that the compound may exist as different polymorphs, both which consists of the same constituent ions in a different packing arrangement.^[56] Both the tetragonal and monoclinic packed polymorphs exhibit indium-indium bond lengths of 2.707 Å, 2.707(3) Å and 2.707(1) Å,

respectively. Somewhat more simply, for thallium, the halide of the composition Tl_2X_3 is also known and exists as mixed valent salts of the form $[Tl^+]_3[TlX_6^{-3}]$ for both $X = Cl$ (**1.12**) and Br (**1.13**).^[57, 58]

The numerous investigations into the nature of E_2X_4 species reveal that, in the absence of donor species, E_2X_4 tend to exist as mixed-valent salts of the general form $[E^I][E^{III}X_4]$. However, it has been found that, in the presence of many types of donors, the neutral X_2E-EX_2 alternative is isolated instead. While the X_2E-EX_2 moiety had been observed initially in the $[E_2X_6^{-2}]$ dianions in certain subhalides described above, the first reported neutral species incorporating a gallium-gallium bond was the dioxane-stabilized halide of the form $Cl_2Ga-GaCl_2 \cdot 2(diox)$ (**1.14**).^[59]

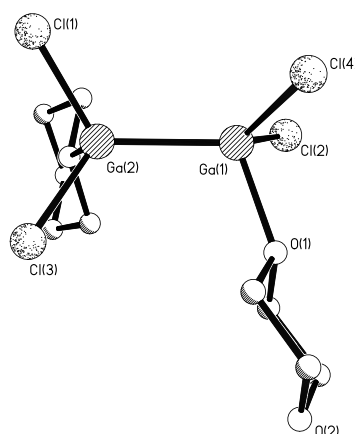


Figure 1.7: Solid state structure of the dioxane-stabilized isomer of Ga_2Cl_4 (**1.14**).

As illustrated in Figure 1.7, the dioxane acts as a monodentate ligand and acts to stabilize the vacant orbital on each Ga centre and yields the neutral isomer with a gallium-gallium bond distance of $2.406(1) \text{ \AA}$. Raman and conductivity investigations of

the heavier congeners suggest that the bromide and iodide analogues are structurally similar.^[60-62] The existence of numerous other examples of this type of donor-stabilized EX_2 species attests to the generality of the neutral, ethane-like "dumbbell" species illustrated in Figure 1.8.

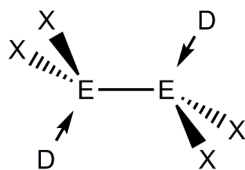


Figure 1.8: General schematic representation of donor stabilized $\text{E}(+2)\text{-E}(+2)$ species.

This more general depiction allows for the description of most of the neutral and ionic species reported in the literature. It must be emphasized at this point that while base-free " AlX_2 " salts are not known, examples of such donor-stabilized species have been characterized for $\text{X} = \text{Cl}, \text{Br}, \text{and I}$. In particular, Schnöckel and co-workers reported the adducts: $\text{Al}_2\text{Br}_4 \cdot 2(\text{PhOMe})$ (**1.15**) ($d(\text{Al-Al}) = 2.526 \text{ \AA}$),^[63] $\text{Al}_2\text{Cl}_4 \cdot 2(\text{NMe}_2\text{SiMe}_3)$ (**1.16**) ($d(\text{Al-Al}) = 2.573 \text{ \AA}$), $\text{Al}_2\text{Br}_4 \cdot 2(\text{NMe}_2\text{SiMe}_3)$ (**1.17**) ($d(\text{Al-Al}) = 2.564 \text{ \AA}$), $\text{Al}_2\text{I}_4 \cdot 2(\text{OEt}_2)$ (**1.18**) ($d(\text{Al-Al}) = 2.528 \text{ \AA}$), $\text{Al}_2\text{I}_4 \cdot 2(\text{PEt}_3)$ (**1.19**) ($d(\text{Al-Al}) = 2.546 \text{ \AA}$),^[64] $\text{Al}_2\text{Br}_4 \cdot 2(\text{NEt}_3)$ (**1.20**) ($d(\text{Al-Al}) = 2.571 \text{ \AA}$),^[65] and $\text{Al}_2\text{I}_4 \cdot 2(\text{THF})$ (**1.21**) ($d(\text{Al-Al}) = 2.520 \text{ \AA}$).^[66] These compounds were typically obtained by the disproportionation of meta-stable " Al-X " precursors, and the same approach was employed for the preparation of the gallium analogues, including: $\text{Ga}_2\text{Br}_4 \cdot 2(\text{THF})$ (**1.22**) ($d(\text{Ga-Ga}) = 2.412 \text{ \AA}$), $\text{Ga}_2\text{Br}_4 \cdot 2(\text{NHEt}_2)$ (**1.23**) ($d(\text{Ga-Ga}) = 2.435 \text{ \AA}$), $\text{Ga}_2\text{Br}_4 \cdot 2(4\text{-}^t\text{Bu-pyridine})$ (**1.24**) ($d(\text{Ga-Ga}) = 2.413 \text{ \AA}$), $\text{Ga}_2\text{Br}_4 \cdot 2(\text{NEt}_3)$ (**1.25**) ($d(\text{Ga-Ga}) = 2.4528(5) \text{ \AA}$),

$\text{Ga}_2\text{Cl}_4 \cdot 2(\text{NEt}_3)$ (**1.26**) ($d(\text{Ga-Ga}) = 2.4467(4) \text{ \AA}$), and the anion in the salt $[\text{Ga}(\text{DMF})_6]^+]_2[\text{Ga}_2\text{Br}_6]^{-2} \cdot 4(\text{DMF})$ (**1.27**) ($d(\text{Ga-Ga}) = 2.420 \text{ \AA}$).^[67] It should, however, be noted that for indium, which has a larger coordination sphere than gallium, it has proven possible to obtain a similar complex in which each indium atom is coordinated by two THF molecules; thus, in $\text{In}_2\text{Cl}_4 \cdot 4(\text{THF})$ (**1.28**) each indium atom has a pseudo trigonal-bipyramidal geometry with the THF ligands located in axial positions.^[68] The use of donors larger than THF produces the more typical $\text{In}_2\text{Cl}_4 \cdot 2\text{D}$ complexes with a pseudo-tetrahedral geometry at each indium center.

It is also worthy of mention that if such complexes are prepared or generated in the presence of donors bearing more than one lone pair of electrons, it is possible to obtain bridged species containing more than one E_2X_4 unit. For example, the treatment of the phosphine-stabilized Ga(+2) iodide $\text{Ga}_2\text{I}_4 \cdot 2\text{PHCy}_2$ (**1.29**) with excess triethylamine resulted in the deprotonation of the secondary phosphine to produce the corresponding phosphide anion. The dimerization of two of the anions with the concomitant elimination of two equivalents of phosphine yielded the salt $[\text{NEt}_3\text{H}][\text{Ga}_2\text{I}_4 \cdot 2\text{PCy}_2]$ (**1.30**), the dianionic portion of which is depicted in Figure 1.9.

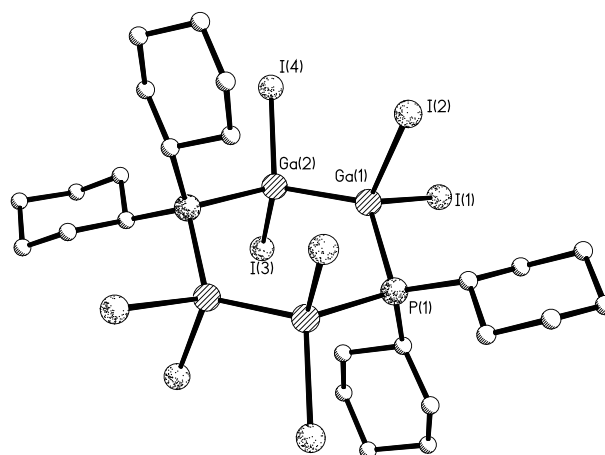


Figure 1.9: Solid state structure of the dianion $[\text{Ga}_2\text{I}_4 \cdot 2\text{PCy}_2]^{2-}$ from **(1.30)**.

On the basis of the general description of $\text{E}_2\text{X}_2 \cdot \text{D}_2$ compounds in Figure 1.8, it should also be emphasized that two different donors may be coordinated simultaneously to a single E_2X_2 acceptor, including mixtures of neutral and anionic donors. For example, the anion in the salt $[\text{H}^{\text{Dipp}}\text{NHC}][\text{I}_3\text{Ga}-\text{GaI}_2(\text{DippNHC})]$ (**1.31**) may be readily rationalized as being a complex of Ga_2I_4 with one neutral DippNHC ligand and one iodide anion.^[69]

As with some of the lighter congeners, in several instances, $\text{In}(+2)$ species that conform to the general type illustrated in Figure 1.8 are generated by way of the oxidation of lower oxidation state precursors, including species that are not typically considered meta-stable. For example, the reaction of ${}^n\text{Pr}_3\text{PI}_2$ with indium metal affords the complex $\text{In}_2\text{I}_4 \cdot 2(\text{P}^n\text{Pr}_3)$ (**1.32**) with an indium-indium bond distance of $2.745(3) \text{ \AA}$,^[70] while the reaction of ${}^{\text{Mes}}\text{NHC}$ with InBr results in the disproportionation of the indium reagent to produce indium metal and the carbene stabilized $\text{In}_2\text{Br}_4 \cdot 2({}^{\text{Mes}}\text{NHC})$ (**1.33**) shown in Figure 1.10 with an indium-indium bond length of $2.7436(7) \text{ \AA}$.^[22]

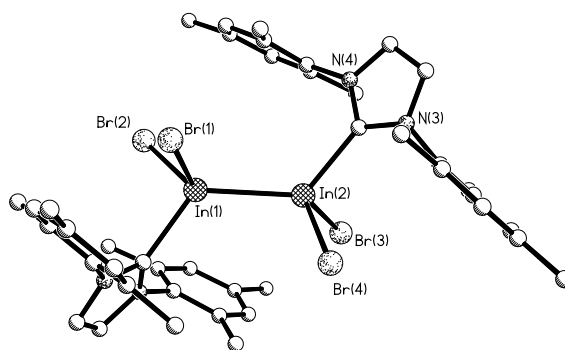


Figure 1.10: ^{Mes}NHC-stabilized In₂Br₄ (**1.33**).

The change from a monodentate to bidentate donors sometimes maintains the overall structural description from Figure 1.8, as Tuck and co-workers demonstrated when they reported the crystal structure of the donor stabilized indium (+2) halide In₂Br₃I·2(TMEDA) (**1.34**) with an indium-indium bond length of 2.775(2) Å.^[71] More recently, this work has been extended by Jones and coworkers, who found that the use of TMEDA as the donor can generate other forms of mixed valent halides of indium. In particular, the reaction of In(+1)I with TMEDA results in the isolation of the neutral compound In₆I₈·4(TMEDA) (**1.35**, Figure 1.11), which contains indium atoms bound to zero, one, or two iodide ligands and features bond distances ranging from 2.7557(9) to 2.8353(10).^[37]

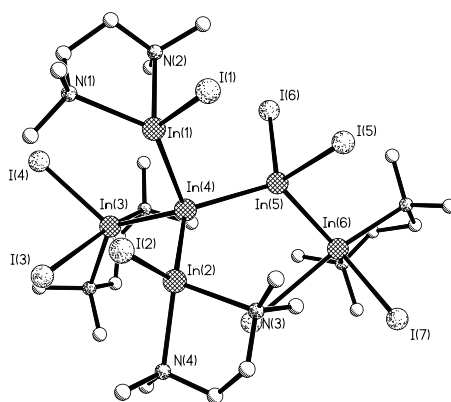


Figure 1.11: Solid state structure of $\text{In}_6\text{I}_8 \cdot 4(\text{TMEDA})$ (**1.35**).

It is worth noting that the reaction of TMEDA with InBr at low temperature results in the formation of the simple Lewis acid-base adduct, which disproportionates upon warming to give the per-brominated analogue of **1.35**. It should also be noted that the similar reaction of the monodentate base quinuclidine with InBr provided a salt containing the mixed-valent anion $[\text{In}_5\text{Br}_8 \cdot 4(\text{quin})]^-$ (**1.36**, Figure 1.12), whose structure is clearly related to that of the neutral iodide in that it contains a central indium atom bonded only to other indium atoms and terminal indium atoms that are ligated by halides and nitrogen bases.^[37, 72] Given the clearly different nature of the products obtained from similar reactions employing the identical bidentate donor (TMEDA) under slightly different conditions, and the perhaps unexpected similarity of the products obtained with both monodentate and bidentate donors, it appears as if there is no definitive general rule as to the type of structure that will be obtained. However, for the case of monodentate donors, it appears as if the product will most likely contain a bond between the donor and a *trivalent* (E^{III}) center.

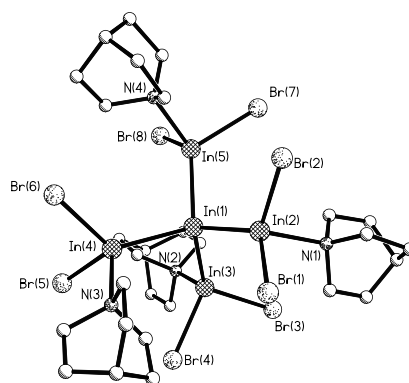


Figure 1.12: Solid State structure of the anion $[\text{In}_5\text{Br}_8(\text{quin})_4]^-$ (**1.36**).

In particular regard to compounds **1.35** and **1.36**, on the basis of counting rules, the average oxidation state of the In atoms in $\text{In}_6\text{I}_8 \cdot 4(\text{TMEDA})$ is +1.33 and that in the anion **1.36** is +1.4, although each of the indium atoms in each species is tetracoordinate and *trivalent* according to the system espoused by Parkin and others.^[2] Many other examples of compounds that are conceptually related to **1.35** and **1.36** have been prepared and these are examined in more detail in the section about discretely-bonded systems (*vide infra*).

In terms of how the nature of donor ligands can influence the type of structure adopted by the E(+2) halides, the special case of the cyclic-poly-ethers known as “crown ethers” must be examined.^[73] In the 1980's, Tuck and associates investigated the reaction in indium(+2) halides with crown ethers and concluded on the basis of elemental analyses and vibrational spectroscopy that mixed valent salts of the form $[\text{In}(\text{crown})][\text{InX}_4]$ were the product.^[74] In 2005, Mudrig et al. showed the mixed valent nature of the related thallium salt, $[\text{Tl}([18]\text{crown-6})][\text{TlI}_4]$, in the solid state.^[75] More recently in the

Macdonald group, the crystal structure of the compound obtained from the reaction of "InCl₂" with dibenzo[18]crown-6 showed that the product, (**1.37**), is actually a neutral compound that has the structure illustrated in Figure 1.13.^[76]

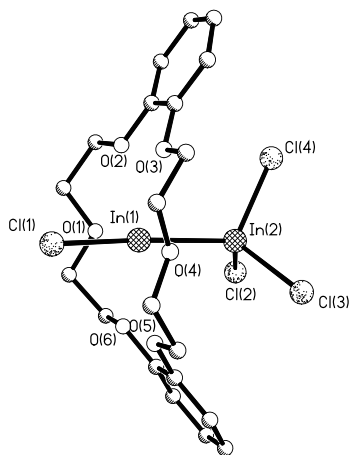


Figure 1.13: Solid state structure of In₂Cl₄(dibenzo[18]crown-6) (**1.37**).

The compound has a structure in which one indium atom has a pseudo-linear arrangement (ignoring the crown ether), linked to one chlorine atom and the other indium atom, whereas the second indium atom has a tetrahedral arrangement involving three chlorine atoms and the first indium atom. This arrangement has been described as a "donor-acceptor" isomer (for reasons described below in the section bearing that name) and it illustrates the third structural alternative for compounds containing the E₂X₄ moiety (Figure 1.14).

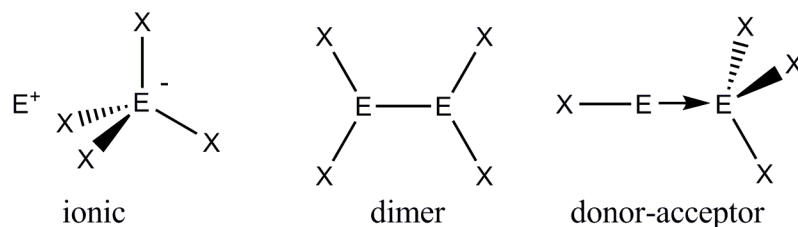


Figure 1.14: Three structural isomers of E_2X_4 .

A computational investigation by Timoshkin and Frenking showed that various R_2E-ER_2 and $RE \rightarrow ER_3$ isomers ($E = B, Al, Ga, In, Tl$; $R = H, Me, Cl$) are relatively close in energy in many instances and that changing the substituent attached to the group 13 element can change which structural isomer is favoured thermodynamically.^[77] In spite of this, until recently, there had been no examples of any kind of mixed valent donor-acceptor complexes. Furthermore, because the treatment of $E(+1)$ halides with neutral donors typically results in disproportionation at ambient temperature to provide the $E(+2)-E(+2)$ adducts described above, it appeared as if donor-acceptor halides may remain elusive. However, examination of the available orbitals for ligation (Figure 1.15) in a putative donor-acceptor isomer reveals how an appropriately-sized cyclic donor has the ideal shape to stabilize the $E(+1)$ centre.

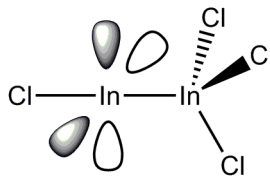


Figure 1.15: Formally vacant orbitals on the E(+1) centre in the donor-acceptor isomer of In_2Cl_4 .

In light of the shape requirements, it is not surprising that the addition of dibenzo[18]crown-6 to In_2Cl_4 afforded the crown ether stabilized indium(+1)-indium(+3) complex $[\text{ClIn}(\text{dibenzo}[18]\text{crown-6})\text{InCl}_3]$, with an In-In bond length of 2.702 Å and a nearly linear Cl-In-In angle of 177.1° .^[78] Several other examples of related donor-acceptor halides have been prepared and these compounds are considered in more detail in the following section.

1.5 Group 13 Donor-Acceptor Compounds

While many cases of neutral and ionic mixed valent species have been discussed, a different class of compounds involves discrete donor-acceptor bonds between group 13 elements that are formally in the E(+1) and E(+3) oxidation states. As illustrated in Figure 1.1, the description of a compound as containing a “donor-acceptor” bond instead of a typical “covalent” bond can appear to be (and actually be) arbitrary; thus, it is worth examining some of the considerations that may render one or the other description more appropriate. One may wish to distinguish between donor-acceptor bonds and typical covalent bonds on the basis of the origin of the electrons in the bond. For example, both electrons in the dative bond of a typical Lewis acid-base complex such as $\text{Me}_3\text{N} \rightarrow \text{BH}_3$

clearly originate from the Lewis basic Me_3N fragment when the components are mixed together. However, the identical argument about the origin of the electrons in a bond can be made when, for example, H_3CLi is mixed with ClCR_3 to produce $\text{H}_3\text{C-CR}_3$, which would always be described as having a typical covalent bond. In a similar vein, the treatment of the Lewis base Me_3P with BrCR_3 produces the phosphonium bromide $[\text{Me}_3\text{P-CR}_3][\text{Br}]$, containing a P-C bond that is considered to be covalent. The origin of the electrons in a bond does not appear to be sufficient for the unambiguous assignment of a bond as being covalent versus donor-acceptor in nature. Thus, as argued by Haaland,^[79] it is more enlightening to consider how a given bond will tend to break. In particular, if it is energetically more favorable for the bond to be cleaved in a heterolytic manner, then the bond is best described as “donor-acceptor”, whereas a bond that is more readily broken in a homolytic fashion is described as “covalent”. It should be noted, however, that it is not always clear how a bond *should* cleave or even *which* bond will cleave in a given compound. Computational investigations can be used to make such assessments, however, most of the compounds described herein have not been subjected to such treatment. As with some of the other concepts described in this chapter, it is always wise to remember that the description one assigns to a bond is simply a model that may (or may not) be appropriate to assist in the rationalization of the structure or behavior of a compound (such as donor exchange chemistry); such models should not necessarily be assigned too much importance.

As indicated previously, disproportionation is a common outcome of the chemistry of group 13 elements in low oxidation states and renders the isolation of stable E(+1) species relatively difficult for elements other than Tl. It has been discovered, however, that ligands such as pentamethylcyclopentadienyl (Cp^*) and

tris(pyrazolyl)borate^[80] can be used to obtain relatively stable E(+1) species that have allowed for the extensive investigation of the chemistry of such compounds.^[81, 82] Schnöckel's study into the disproportionation of aluminum(+1) species produced the mixed valent compound [Cp*₃Al₅I₆] (**1.38**) via the reaction of [Cp*Al]₄ with Al₂I₆, which has an average oxidation state of 1.8 and Al-Al bonds ranging from 2.52 to 2.54 Å.^[83]

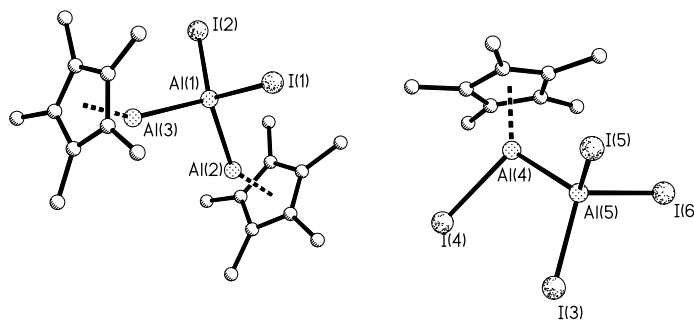


Figure 1.16: Solid state structure of the salt [Cp*₂Al₃I₂][Cp*Al₂I₄] (**1.38**).

As illustrated in Figure 1.16, this compound exists as the salt [Cp*₂Al₃I₂][Cp*Al₂I₄] where the average oxidation states of the atoms in the cation is +5/3 and those in the anion are +2. Computational investigations suggest that the salt is best considered a contact ion pair rather than exclusively ionic in nature. Furthermore, the cation can be considered as consisting of an [Al^{III}I₂⁺] cation that is coordinated by two Cp*Al^I ligands. The slight distortion of the ring-centroid-Al-Al fragment from linearity is likely a consequence of the repulsion between the bulky Cp* ligands. The anion may be rationalized as being derived from the formal insertion (oxidative addition) of a Cp*Al^I ligand into an Al-I bond from a putative tetraiodoaluminate anion. The salt is

only stable below room temperature and further disproportionation into aluminum metal and aluminum(+3) species is observed upon warming to ambient temperature.

It should be re-emphasized that ligands of the general form $\text{Cp}^*\text{E}^{\text{I}}$ are well known and have been used to generate numerous complexes to transition metals,^[29, 32-34, 84-86] and their complexation to main group Lewis acids has provided for a series of interesting mixed-valent compounds. Although it is a common outcome, disproportionation can be prevented by the judicious choice of substituents on both the E(+1) and E(+3) employed in a reaction. For example, whereas reactions involving Cp^*Al and AlX_3 lead to disproportionation and a variety of products, the use of organometallic E(+3) Lewis acids with Cp^*E donors can yield discrete donor-acceptor E(+1)-E(+3) complexes. An example of such a compound is the Al(+1)-Al(+3) species $\text{Cp}^*\text{Al} \rightarrow \text{Al}(\text{C}_6\text{F}_5)_3$ (**1.39**) reported by Cowley synthesized by the reaction of Cp^*Al with $\text{Al}(\text{C}_6\text{F}_5)_3 \cdot \text{toluene}$.^[31] This compound features an Al-Al bond of 2.591 Å and also shows two resonances in the ²⁷Al NMR at -115.7 ppm and 106.9 ppm for the Cp^*Al and $\text{Al}(\text{C}_6\text{F}_5)_3$ centres respectively. Further examples of $\text{Cp}^*\text{E}-\text{E}'(+3)$ donor-acceptor complexes are found in Table 1.2 listed with their E(+1)-E'(+3) bond lengths.^[30, 87, 88]

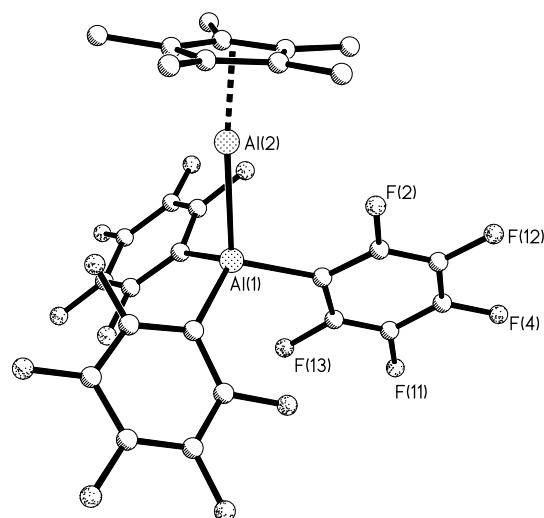


Figure 1.17: Solid state structure of Cp*Al-Al(C₆F₅)₃ (**1.39**).

It is important to note that while the complexes containing different group 13 elements are not "mixed valent" in terms of a single element, they are included to illustrate that this class of mixed-valent compound is actually a subset of a more general type of donor-acceptor complexes. In fact, some related examples of such complexes have also been synthesized using nacnac-substituted E^I donors, however none features the same atom on the donor and acceptor fragments.^[88, 89]

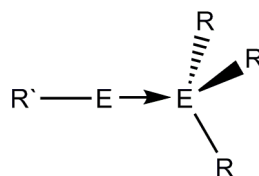


Figure 1.18: General representation of group 13-group13 donor acceptor complexes of Cp*E donors

Table 1.2: Bond distances of E(+1)-E(+3) complexes

E(+3) species	Cp*Al	Cp*Ga	Cp*In
B(C ₆ F ₅) ₃	2.169(3) Å	2.160(2)	/
Al(C ₆ F ₅) ₃	2.591(2) Å	/	/
Al(^t Bu) ₃	2.689(2) Å	2.629(2) Å	2.843(2) Å
Ga(^t Bu) ₃	2.620(2) Å	/	2.845 (2) Å
GaCl ₂ Cp*	/	2.4245(3) Å	/
GaI ₂ Cp*	/	2.437(2) Å	/

As previously discussed, due to periodic trends, in particular the increasing prominence of "inert s-pairs" of electrons, the stability of lower oxidation state species increases as you move down a group in the periodic table. This suggests that for donor-acceptor species the heavier element would prefer to be the E(+1) species and the lighter element would prefer to exist in the E(+3) oxidation state. Consequently, the treatment of Cp*Al with In(C₆F₅)₃ does not result in the isolation of the donor-acceptor complex but rather produces the Al(+3) species Cp*Al(C₆F₅)₂ and an unidentified In-containing by-product. This pattern of reactivity appears to hold true experimentally with the only exception yet reported being Cp*Al→Ga(^tBu)₃ (**1.40**), in which the donor is based on aluminum(+1) and the acceptor is a gallium(+3) moiety. Interestingly, there have been no reports of a structurally characterized Cp*In→In(+3) donor-acceptor complex to date.^[90]

Although the focus of this dissertation is the heavier group 13 elements, it should also be noted that the compound Cp*B→BCl₃ (**1.41**) is an example of a mixed-valence boron donor-acceptor complex that is clearly related to the heavier group 13 analogues described above. However, it should be emphasized that the complex is not obtained from the reaction of BCl₃ and "Cp*B", which, unlike the heavier congeners, is an unknown molecule. Rather, the complex is obtained from the reaction of Cp*Li with B₂Cl₄ followed by a rearrangement from the "covalent" dimeric isomer to the donor-

acceptor. As indicated earlier in this chapter, such a rearrangement is understandable because the energy difference between the covalent and donor-acceptor isomers is relatively small and donors with appropriate geometrical features can alter the relative stabilities of the isomers. In the case above, the Cp* ligand has the appropriate shape to act simultaneously as both a σ -donor and a π -donor, which can stabilize the two vacant p-orbitals on an E^I fragment and renders the donor-acceptor isomer more favourable than the dimer alternative.^[31, 77]

Some other compounds that can be considered as donor-acceptor derived from Cp*Ga are worthy of mention. In terms of the subject of this chapter, perhaps the most interesting of the donor-acceptor complexes with Cp*Ga is a neutral complex isolated as a by-product in one of the reactions reported by Seifert and Linti during the course of their investigation into the protonolysis of Cp*Ga with HOTf; namely, (Cp*Ga)₂(Ga₂OTf₄) (**1.42**), which is depicted in Figure 1.19. The neutral compound is the donor-acceptor complex composed of two Cp*Ga donors and the acceptor is the Ga(+2) triflate salt. Thus, exactly as observed for the E(+2) halides, the presence of monodentate donors favors the dimeric TfO₂Ga-GaOTf₂ isomer of the Ga(+2) compound. The Cp*Ga→Ga distances are reported to be 2.408(2) and 2.435(2) Å for the donor-acceptor bonds and 2.423(2) for the Ga(+2)-Ga(+2) fragment, however the significant positional disorder involving the gallium atoms in the structure makes it unwise to attempt to draw conclusions on the basis of these numbers alone and DFT calculations suggest that the Ga-Ga bond should be only marginally shorter than the Ga→Ga bond.

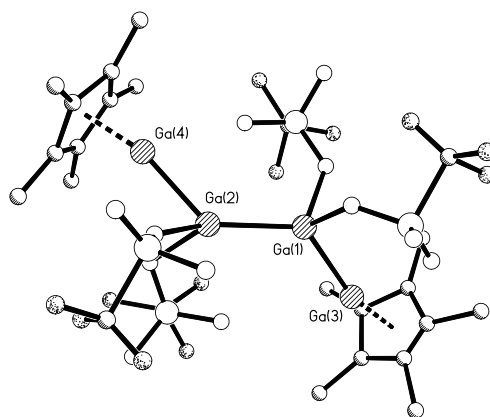


Figure 1.19: Mixed valent donor-acceptor gallium subtriflate (**1.42**).

In that same work Linti and Seifert obtained the salt $[\text{Ga}(\text{toluene})_2][\text{Ga}_5(\text{OTf})_6(\text{Cp}^*)_2]$ (**1.43**),^[91] the anion of which is depicted in Figure 1.20. The anion contains the familiar GaGa_4 core, however in this instance, the compound is probably best understood as being a donor-acceptor complex of two Cp^*Ga donors with a putative $[(\text{TfO})_3\text{Ga}-\text{Ga}-\text{Ga}(\text{OTf})_3]^-$, analogous to $[(\text{Ph}_3\text{Ge})_3\text{Ga}-\text{Ga}-\text{Ga}(\text{GePh}_3)_3]^-$ (**1.44**). The smaller size of the triflate anion, with respect to the triphenylgermyl ligand, certainly allows for the approach of donors, in this instance Cp^*Ga , to ligate the putative dicoordinate cationic gallium center. The Ga-Ga distances of 2.441(1) and 2.458(1) Å for the $\text{Cp}^*\text{Ga} \rightarrow \text{Ga}$ linkages are significantly longer than the distances of 2.425(1) and 2.426(1) Å for the $\text{Ga}-\text{Ga}(\text{OTf})_3$ bonds and are thus consistent with both the donor-acceptor description of the bonding in this anion, and the anticipated changes in atomic radii of $\text{Ga}(+1)$ versus $\text{Ga}(+3)$.

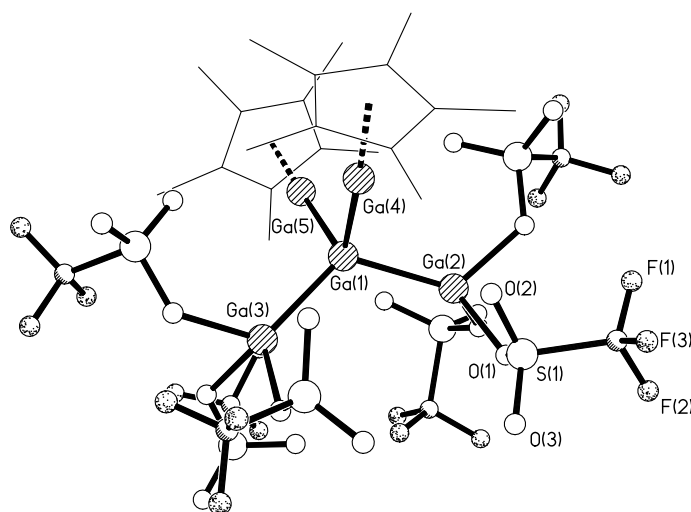


Figure 1.20: Solid state structure of the anion from $[\text{Ga}(\text{toluene})_2][\text{Ga}_5(\text{OTf})_6(\text{Cp}^*)_2]$ (**1.43**).

It should be noted that a related anionic donor-acceptor compound was obtained by Jones and co-workers using the anionic $[(^{\text{Dipp}}\text{DAB})\text{Ga}^-]$ gallium(+1) reagent^[19] In particular, the salt $[\text{K}(\text{TMEDA})_2][((^{\text{Dipp}}\text{DAB})\text{Ga})_2\text{GaH}_2]$ (**1.45**), depicted in Figure 1.21, was obtained through the treatment of two equivalents of $[\text{K}(\text{TMEDA})][(^{\text{Dipp}}\text{DAB})\text{Ga}]$ with $\text{GaH}_3 \cdot \text{quin}$.^[92] The anion is best described as consisting of a donor-acceptor composed of two anionic Ga(+1) donors that stabilize a cationic $[\text{GaH}_2^+]$ fragment. The Ga-Ga distances of 2.4071(9) Å again fall within the predicted range for such linkages. It should also be mentioned that the corresponding donor-acceptor compound to the cationic $[\text{InH}_2^+]$ fragment was prepared in a similar manner, again emphasizing the more general applicability of the donor-acceptor approach for the synthesis of unusual element-element bonds.

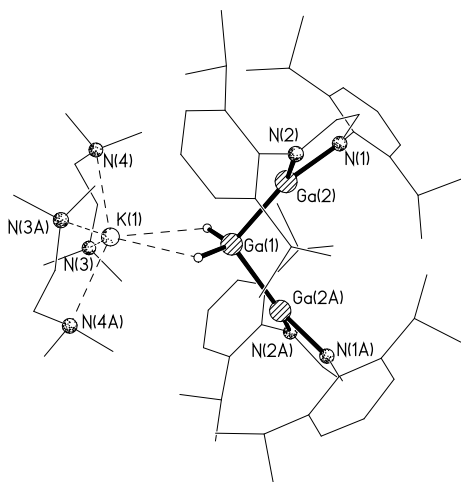


Figure 1.21: state structure of $[K(TMEDA)_2][((^{Dipp}DAB)Ga)_2GaH_2]$ (**1.45**).

Whereas the Cp*E species do not tend to form donor-acceptor complexes with the EX₃ halides because of ligand redistribution, comproportionation or other redox reactions, the change of the supporting ligand on the E(+1) center from Cp* to tris(pyrazolyl)borate alters the reactivity pattern observed (E = Ga, In, Tl).^[17, 93]

In fact, the first monomeric RE^I compound of any sort to be characterized crystallographically was obtained via the reaction of sodium-tris(3,5-di-tert-butylpyrazolyl)hydroborate, [Na][^tBuTpz], with “GaI”^[16, 47, 94, 95] Of importance to the current subject, it was observed, however, that during the reaction some of the “GaI” becomes oxidized to form GaI₃, which is then coordinated by the monomeric gallium(+1) species to provide the donor-acceptor complex ^tBuTpzGa→GaI₃ (**1.46**) featuring a Ga-Ga bond distance is 2.506(3) Å. Furthermore, while the ^tBuTpzGa species is basic enough to coordinate to the GaI₃ acid, the gallium-gallium interaction is not strong enough to preclude displacement by stronger bases such as NEt₃, PMe₃, etc; such behavior is

completely consistent with the donor-acceptor description of the compound ${}^t\text{BuTpzGa} \rightarrow \text{GaI}_3$.

A related In-In donor-acceptor complex (**1.47**) has also been synthesized through the reaction of $[\text{K}][{}^t\text{BuTpz}]$ with InI_3 and involves the *in situ* reduction of indium(+3) to the stabilized indium(+1) species. The indium(+1)-indium(+3) bond distance of 2.747 Å is similar to that recorded for the phosphine stabilized indium(+2) species $\text{In}_2\text{I}_4 \cdot 2\text{P}^n\text{Pr}_3$ (**1.32**), which has an In(+2)-In(+2) distance of 2.745 Å.^[17] In contrast to the structures of the lighter analogues, the indium(+1) center is large enough to accommodate an additional neutral *t*butylpyrazole donor in its coordination sphere.

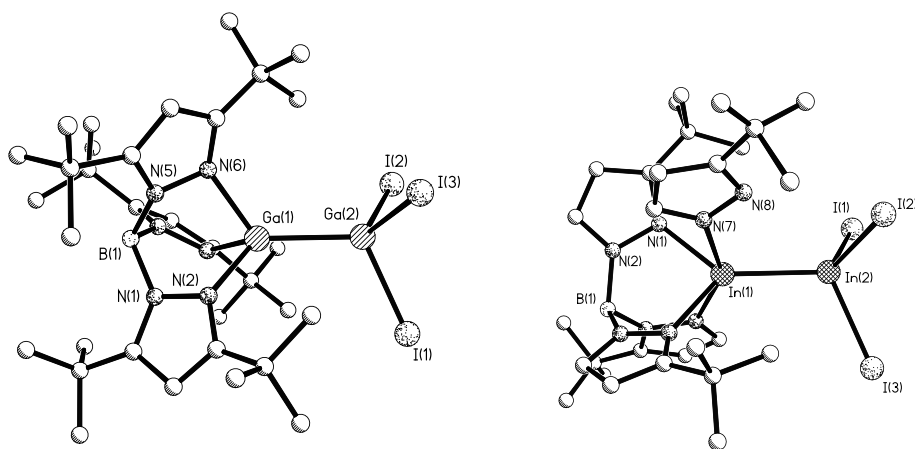


Figure 1.22: Solid state structures of TpzGa-GaI_3 (**1.46**) (left) and an indium analogue ${}^t\text{BuTpz(pz)In-InI}_3$ (**1.47**) (right).

As indicated in several instances in this chapter, the nature of the donor ligands present in a system play a significant role determining the type of structures observed for a given E_2X_4 species. In particular, monodentate σ -donors have been shown to stabilize

the indium(+2) dimer structures while arene ligands tend to result in the adoption of mixed valent ionic structures. In this section, it has been demonstrated that organic substituents with the capacity to act as both σ - and π -donors simultaneously, such as cyclopentadienides and tris-pyrazolylborates, can render the donor-acceptor isomer the most stable alternative. In the section about halides, it was indicated that research showed that appropriately-sized crown ethers can favour the donor-acceptor isomer even for the simple indium(+2) halide, In_2Cl_4 . Specifically, the addition of dibenzo[18]crown-6 to In_2Cl_4 provided the crown ether stabilized indium(+1)-indium(+3) complex $[\text{ClIn}(\text{dibenzo}[18]\text{crown-6})\text{InCl}_3]$ (**1.37**) with an In-In bond length of 2.702 Å and an essentially linear Cl-In-In angle of 177.1°.

1.6 Conclusions

The interesting and often unique chemistry and properties of low oxidation state and mixed valent species has garnered interest from a wide variety of research groups. Low oxidation state triel compounds are usually generated via gas phase reactions, controlled reduction of higher oxidation state materials, or by starting with a cyclopentadienyl (E= Al, Ga, In) or halide (E=Ga, In) starting material. Mixed valent compounds of the heavier group 13 elements are typically generated in a controlled manner either by partial oxidation of low oxidation state starting materials or partial reduction of higher oxidation state materials. In some cases, the comproportionation of, for example, a group 13 metal and a E(+3) compound, has also been used to obtain compounds of oxidation states that intermediate between the two; the donor-acceptor mixed valent compounds derived from the combination of an E^{I} donor and an E^{III} acceptor can similarly be considered as products of comproportionation reactions. In

many instances such compounds are also the products of unintended disproportionation of E(+1) compounds, for E = Al, Ga and In and the structures observed are often a consequence of the substituents or ligands in the system. As indicated several times, the presence of univalent E^I centers is often associated with ionic bonding whereas the presence of the more electronegative trivalent E^{III} center typically results in covalent interactions.

Many organotrirel species form dinuclear, polynuclear or cluster species featuring E-E bonds and extensive or complete delocalization amongst the group 13 elements; the metal-rich core is typically encased in a shell composed of the organic ligands and the steric requirements of the ligands appear to influence the number elements in and structure of the group 13 core. In several instances, polynuclear compounds featuring element-element bonds have been rationalized as being derived from formal oxidative addition/insertion reactions of E^I fragments into E-X or E-R bonds and the compounds are treated as models of intermediates on the reaction pathways between small molecules and nano-scale or bulk materials.

While mixed valent species of the heavier group 13 elements have been studied for more than a century, and have had a classification system for several decades, the insights provided by numerous experimental and theoretical investigations since the 1980's have increased our understanding of such species considerably. Most importantly, recent advances in ligand and reagent design, in conjunction with improved mechanistic understanding, suggest that many more low oxidation state and mixed valent species of the triel elements should become readily accessible using rational and reproducible syntheses. Given their often unique chemical behavior and their relationship to nano-scale and bulk materials containing these important elements, the utility of these species

in terms of their chemical and materials properties will undoubtedly remain an active and growing area of investigation.

Given the unique properties of InOTf, and the synthetic limitations of the indium monohalides, Chapter 2 discusses an improved synthesis approach towards InOTf and related crown-ether ligated salts. Chapter 3 investigates the structural implications of changing the cavity size of the crown-ether ligand; the synthesis of a sandwich complex where the indium center has no interaction with the counter ion, and the interesting solid-state phase properties of the resulting salt. The insertion chemistry of "crowned" InOTf species is presented in Chapter 4, while metathesis reactions are explored in Chapter 5. Chapter 6 discusses the synthesis and solid-state properties of [In][EX₄] species and their "crowned" analogues. The reactivity of InOTf with Lewis bases such as diazabutadienes (DABs) is present in Chapter 7, with Chapter 8 serving as a discussion of the chemical lessons learned throughout the course of the dissertation and the implications on the direction of the project going forward.

References

- [1] J. G. Calvert, *Pure Appl. Chem.* **1990**, *62*, 2167.
- [2] G. Parkin, *Journal of Chemical Education* **2006**, *83*, 791.
- [3] U. W. Martin Jansen, *Angew. Chem., Int. Ed.* **2008**, *47*, 10026.
- [4] A. J. Downs, Ed., *Chemistry of Aluminium, Gallium, Indium, and Thallium*, Chapman and Hall, Glasgow, U.K., **1993**.
- [5] P. Pyykko, *Chem. Rev.* **1988**, *88*, 563.
- [6] T. A. Annan, R. K. Chadha, P. Doan, D. H. Mcconville, B. R. Mcgarvey, A. Ozarowski, D. G. Tuck, *Inorg. Chem.* **1990**, *29*, 3936.
- [7] Z. Y. Yang, E. S. Gould, *Dalton Trans.* **2004**, 1858.
- [8] H. Schnockel, A. Schnepf, *Adv. Organomet. Chem.* **2001**, *47*, 235.
- [9] A. Schnepf, H. Schnockel, *Angew. Chem., Int. Ed.* **2001**, *40*, 712.
- [10] A. Schnepf, R. Koppe, H. Schnockel, *Angew. Chem., Int. Ed.* **2001**, *40*, 1241.
- [11] J. A. J. Pardoe, A. J. Downs, *Chem. Rev.* **2007**, *107*, 2.
- [12] P. Jutzi, N. Burford, *Chem. Rev.* **1999**, *99*, 969.
- [13] N. Wiberg, *Coord. Chem. Rev.* **1997**, *163*, 217.
- [14] M. S. Hill, P. B. Hitchcock, *Chem. Comm.* **2004**, 1818.
- [15] E. S. Schmidt, A. Schier, H. Schmidbaur, *J. Chem. Soc., Dalton Trans.* **2001**, 505.
- [16] D. L. Reger, *Coord. Chem. Rev.* **1996**, *147*, 571.
- [17] A. Frazer, P. Hodge, B. Piggott, *Chem. Comm.* **1996**, 1727.
- [18] B. Twamley, S. T. Haubrich, P. P. Power, *Adv. Organomet. Chem.* **1999**, *44*, 1.
- [19] N. J. Hardman, B. E. Eichler, P. P. Power, *Chem. Comm.* **2000**, 1991.
- [20] A. Kempter, C. Gemel, R. A. Fischer, *Inorg. Chem.* **2005**, *44*, 163.
- [21] R. J. Baker, R. D. Farley, C. Jones, M. Kloth, D. M. Murphy, *J. Chem. Soc., Dalton Trans.* **2002**, 3844.
- [22] R. J. Baker, R. D. Farley, C. Jones, M. Kloth, D. M. Murphy, *Chem. Comm.* **2002**, 1196.
- [23] S. T. Haubrich, P. P. Power, *J. Am. Chem. Soc.* **1998**, *120*, 2202.
- [24] N. J. Hardman, R. J. Wright, A. D. Phillips, P. P. Power, *J. Am. Chem. Soc.* **2003**, *125*, 2667.
- [25] E. S. Schmidt, A. Jockisch, H. Schmidbaur, *J. Am. Chem. Soc.* **1999**, *121*, 9758.
- [26] C. Dohmeier, C. Robl, M. Tacke, H. Schnockel, *Angew. Chem., Int. Ed. Engl.* **1991**, *30*, 564.
- [27] D. Loos, E. Baum, A. Ecker, H. Schnockel, A. J. Downs, *Angew. Chem., Int. Ed. Engl.* **1997**, *36*, 860.
- [28] O. T. Beachley, R. Blom, M. R. Churchill, K. Faegri, J. C. Fettinger, J. C. Pazik, L. Victoriano, *Organometallics* **1989**, *8*, 346.
- [29] P. Jutzi, B. Neumann, G. Reumann, H. G. Stammer, *Organometallics* **1998**, *17*, 1305.
- [30] P. Jutzi, H.-G. Stammer, L. O. Schebaum, G. Reumann, B. Neumann, *Organometallics* **2001**, *20*, 2854.
- [31] J. D. Gorden, C. L. B. Macdonald, A. H. Cowley, *Chem. Comm.* **2001**, 75.
- [32] D. Weiss, T. Steinke, M. Winter, R. A. Fischer, N. Frohlich, J. Uddin, G. Frenking, *Organometallics* **2000**, *19*, 4583.
- [33] Q. Yu, A. Purath, A. Donchev, H. Schnockel, *J. Organomet. Chem.* **1999**, *584*, 94.

- [34] P. Jutzi, B. Neumann, G. Reumann, L. O. Schebaum, H. G. Stammer, *Organometallics* **1999**, *18*, 2550.
- [35] C. L. B. Macdonald, A. M. Corrente, C. G. Andrews, A. Taylor, B. D. Ellis, *Chem. Comm.* **2004**, 250.
- [36] C. G. Andrews, C. L. B. Macdonald, *Angew. Chem., Int. Ed.* **2005**, *44*, 7453.
- [37] S. P. Green, C. Jones, A. Stasch, *Angew. Chem. Int. Ed.* **2007**, *46*, 8618.
- [38] U. Schneider, H. T. Dao, S. Kobayashi, *Organic Letters* **2010**, *12*, 2488.
- [39] H. T. Dao, U. Schneider, S. Kobayashi, *Chem. Comm.* **2011**, *47*, 692.
- [40] M. B. Robin, P. Day, in *Advances in Inorganic Chemistry and Radiochemistry*, Vol. 10, **1967**, pp. 247.
- [41] W. Klemm, W. Tilk, *Z. Anorg. Allg. Chem.* **1932**, *207*, 175.
- [42] L. A. Woodward, G. Garton, H. L. Roberts, *J. Chem. Soc.* **1956**, 3723.
- [43] G. Garton, H. M. Powell, *Journal of Inorganic and Nuclear Chemistry* **1957**, *4*, 84.
- [44] J. W. Akitt, N. N. Greenwood, A. Storr, *J. Chem. Soc.* **1965**, 4410.
- [45] J. D. Corbett, R. K. McMullan, *J. Am. Chem. Soc.* **1956**, 2906.
- [46] J. D. Corbett, R. K. McMullan, *J. Am. Chem. Soc.* **1958**, *80*, 4761.
- [47] R. J. Baker, C. Jones, *Dalton Transactions* **2005**, 1341.
- [48] V. G. Gerlach, W. Honle, A. Simon, *Z. Anorg. Allg. Chem.* **1982**, *486*, 7.
- [49] U. Haussermann, S. I. Simak, R. Ahuja, B. Johansson, *Angewandte Chemie-International Edition* **2000**, *39*, 1246.
- [50] F. A. Cotton, G. Wilkinson, C. A. Murillo, M. Bochmann, *Advanced Inorganic Chemistry*, Sixth Edition ed., John Wiley & Sons, Inc., Chichester, **1999**.
- [51] D. G. Tuck, B. H. Freeland, *Inorg. Chem.* **1976**, *15*, 475.
- [52] D. G. Tuck, M. A. Khan, *Inorganica Chimica Acta* **1985**, *97*, 73.
- [53] T. J. Rowland, J. P. Bromberg, *The Journal of Chemical Physics* **1958**, *29*, 626.
- [54] A. C. Hazell, *J. Chem. Soc.* **1963**, 3459.
- [55] G. Meyer, T. Staffel, *Naturwissenschaften* **1987**, *74*, 491.
- [56] M. Ruck, H. Barnighausen, *Z. Anorg. Allg. Chem.* **1998**, *625*, 577.
- [57] R. Ackermann, C. Hirschle, H. W. Rotter, G. Thiele, *Z. Anorg. Allg. Chem.* **2002**, *628*, 2675.
- [58] R. Bohme, J. Rath, B. Grunwald, G. Thiele, *Z. Naturforsch., B: Chem. Sci.* **1980**, *35*, 1366.
- [59] J. C. Beamish, R. W. H. Small, I. J. Worrall, *Inorg. Chem.* **1979**, *18*.
- [60] L. A. Woodward, N. N. Greenwood, J. R. Hall, I. J. Worrall, *J. Chem. Soc.* **1958**, 1505.
- [61] E. F. Riebling, C. E. Erickson, *J. Phys. Chem.* **1963**, *67*, 307.
- [62] E. F. Riebling, C. E. Erickson, *J. Phys. Chem.* **1963**, *67*, 509.
- [63] M. Mocker, C. Robl, H. Schnockel, *Angew. Chem. Int. Ed. Engl.* **1994**, *33*, 862.
- [64] A. Ecker, E. Baum, M. A. Friesen, M. A. Junker, C. Uffing, R. Koppe, H. Schnockel, *Z. Anorg. Allg. Chem.* **1998**, *624*, 513.
- [65] J. Vollet, R. Burgert, H. Schnockel, *Angew. Chem. Int. Ed.* **2005**, *44*, 6956.
- [66] C. Klemp, G. Stosser, I. Krossing, H. Schnockel, *Angew. Chem. Int. Ed.* **2000**, *39*, 3691.
- [67] H. Schnockel, T. Duan, *Z. Anorg. Allg. Chem.* **2004**, *630*, 2622.
- [68] F. P. Gabbai, A. Schier, J. Riede, H. Schmidbaur, *Inorg. Chem.* **1995**, *34*, 3855.
- [69] R. J. Baker, H. Bettentrup, C. Jones, *Eur. J. Inorg. Chem.* **2003**, 2446.

- [70] S. M. Godfrey, K. Kelly, J., P. Kramkowski, C. A. McAuliffe, R. G. Pritchard, *Chem. Commun.* **1997**, 1001.
- [71] M. A. Khan, C. Peppe, D. G. Tuck, *Can. J. Chem.* **1984**, *62*, 601.
- [72] M. L. Cole, C. Jones, M. Kloth, *Inorg. Chem.* **2005**, *44*, 4909.
- [73] R. D. Rogers, C. B. Bauer, in *Comprehensive Supramolecular Chemistry, Vol. 1* (Eds.: J. L. Atwood, J.-M. Lehn), Pergamon, New York, **1996**, p. 315.
- [74] M. J. Taylor, D. G. Tuck, L. Victoriano, *J. Chem. Soc., Dalton Trans.* **1981**, 928.
- [75] A. V. Mudring, F. Rieger, *Inorg. Chem.* **2005**, *44*, 6240.
- [76] C. G. Andrews, C. L. B. Macdonald, *J. Organomet. Chem.* **2005**, *690*, 5090.
- [77] A. Y. Timoshkin, G. Frenking, *J. Am. Chem. Soc.* **2002**, *124*, 7240.
- [78] C. G. Andrews, C. L. B. Macdonald, *Angew. Chem. Int. Ed.* **2005**, *44*, 7453.
- [79] A. Haaland, *Angew. Chem. Int. Ed. Engl.* **1989**, *28*, 992.
- [80] S. Trofimenko, *Chem. Rev.* **1993**, *93*, 943.
- [81] P. Jutzi, N. Burford, *Chem. Rev.* **1999**, *99*, 969.
- [82] C. L. B. Macdonald, B. D. Ellis, *The Encyclopedia of Inorganic Chemistry*, 2nd ed., John Wiley & Sons, Chichester, U.K., **2005**.
- [83] H. Schnockel, R. Koppe, E. Baum, C. Uffing, *Angew. Chem. Int. Ed.* **1998**, *37*, 2397.
- [84] C. L. B. Macdonald, A. H. Cowley, *J. Am. Chem. Soc.* **1999**, *121*, 12113.
- [85] J. Weiss, D. Stetzkamp, B. Nuber, R. A. Fischer, C. Boehme, G. Frenking, *Angew. Chem. Int. Ed. Engl.* **1997**, *36*, 70.
- [86] R. A. Fischer, J. Weiss, *Angew. Chem. Int. Ed.* **1999**, *38*, 2831.
- [87] S. Schulz, A. Kuczkowski, D. Schuchmann, U. Florke, M. Nieger, *Organometallics* **2006**, *25*, 5487.
- [88] N. J. Hardman, P. P. Power, J. D. Gorden, C. L. B. Macdonald, A. H. Cowley, *Chem. Comm.* **2001**, 1866.
- [89] Z. Yang, X. L. Ma, R. B. Oswald, H. W. Roesky, H. P. Zhu, C. Schulzke, K. Starke, M. Baldus, H. G. Schmidt, M. Noltemeyer, *Angew. Chem., Int. Ed.* **2005**, *44*, 7072.
- [90] A. H. Cowley, *Chem. Commun.* **2004**, 2369.
- [91] G. Linti, A. Seifert, *Z. Anorg. Allg. Chem.* **2008**, *634*, 1312.
- [92] R. J. Baker, C. Jones, M. Kloth, J. A. Platts, *Angew. Chem. Int. Ed.* **2003**, *42*, 2660.
- [93] H. V. R. Dias, W. Jin, *Inorg. Chem.* **2000**, *39*, 815.
- [94] J. C. Green, J. L. Suter, *J. Chem. Soc., Dalton Trans.* **1999**, 4087.
- [95] M. C. Kuchta, J. B. Bonanno, G. Parkin, *J. Am. Chem. Soc.* **1996**, *118*, 10914.

Chapter 2: Improved Synthesis of Indium (I) Starting Materials

2.1 Introduction

Low valent, low oxidation state^[1] indium species have received increased attention in recent years in terms of their fundamental chemistry^[2, 3] and for their use as stoichiometric reagents and catalysts.^[4-9] In 2004, the Macdonald group described the preparation and isolation of a new source of monovalent indium in the form of a trifluoromethane (triflate) salt: InOTf, **2.1**.^[10] This triflate salt is considerably more soluble and more stable at ambient temperature in a variety of organic solvents than are the comparable halide salts and thus allows for its reactions to be conducted under homogeneous conditions. A selection of the reactions that have been reported employing this reagent are illustrated in Figure 2.1. While some of the reactivity of **2.1** clearly mimics that of the related halide salts, such as its use in the metathetical preparation of In^I clusters,^[11] its ability to function as a catalyst for organic allylation reactions^[8] and its use as a reagent for the generation of mixed-valent species,^[12] other chemical behaviour of the triflate reagent is distinct. For example, indium(I) halide salts typically disproportionate rapidly in the presence of coordinating solvents or other Lewis bases^[2, 3] and structural analyses of preparations that have been employed synthetically as soluble indium(I) halide sources reveal that they do not have the proposed composition^[13]; the isolation of a genuine example of a Lewis base adduct of an In^I halide has only proven possible through careful handling at low temperature.^[14] In sharp contrast to the halides, the treatment of **2.1** with crown ethers^[15, 16] or bis(iminopyridyl) ligands^[17] produce stable, monomeric adducts that are even more soluble than the parent salt, as also illustrated in Figure 2.1.

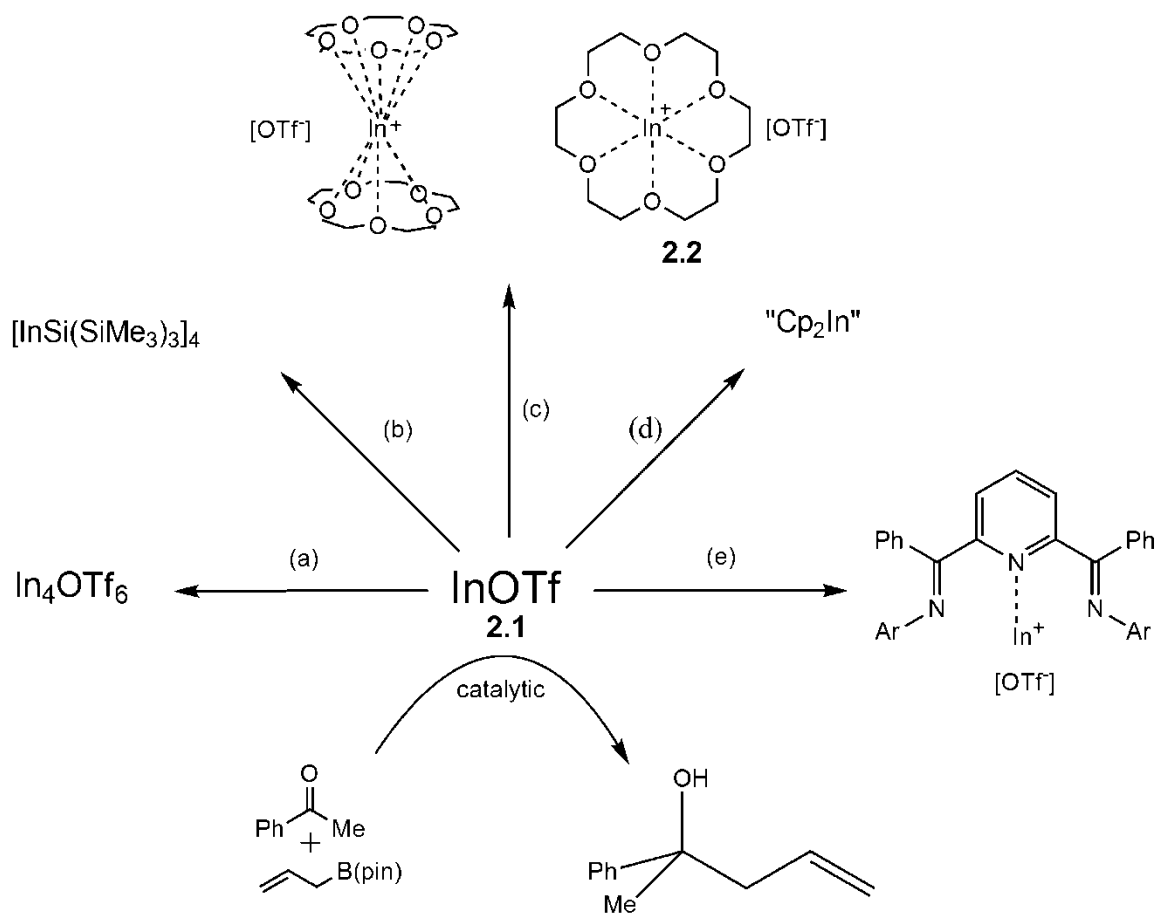


Figure 2.1: Some examples of indium(+1) triflate, **2.1** as a reagent. (a) $[\text{Cp}_2\text{Fe}][\text{PF}_6]$, by products;^[12] (b) $\text{LiSi}(\text{SiMe}_3)_3 \cdot 3\text{thf}$, by products;^[18] (c) $L = 2$ [15]crown-5 or [18]crown-6;^[15, 16] (d) Cp_2Mn , by products;^[12] (e) $[\{2,4\text{-tBu}_2\text{C}_6\text{H}_3\text{NCPH}\}_2(\text{NC}_5\text{H}_3)]$ ^[17]

In the case of the ligand [18]crown-6, it was found that there are significant changes in the behaviour of **2.1** in the presence or absence of the ligand. For example, while **2.1** decomposes upon prolonged exposure to THF, the “crowned” salt $[\text{In}([\text{18}]\text{crown-6})[\text{OTf}]$, **2.2** appears to be stable indefinitely in that solvent. Furthermore, whereas **2.1** does not appear to react with chlorinated solvents at an appreciable rate, the “crowned” indium (I) salt **2.2** rapidly inserts into the carbon-chlorine bonds of dichloromethane and chloroform.^[15, 19] The differing reactivity of the ligated species as

compared to its parent salt, **2.1**, illustrates the potential versatility and tunability of these monovalent indium reagents.



Scheme 2.1: Preparation of InOTf via protonolysis of In^I-containing precursors.

As illustrated in Scheme 2.1, the preparative routes to **2.1** that were reported previously involve the protonolytic removal of C₅Me₅H (Cp*H) or HCl from the corresponding indium(+1) starting materials C₅Me₅In (Cp*In)^[20] or InCl with the strong non-oxidizing triflic acid. In both cases, the resultant protonated by-product is readily removed under reduced pressure and with washing; the use of indium(I) chloride is somewhat more convenient given the commercial availability and lower cost of the reagent; however, subsequent reactivity studies reveal that the salt prepared in this manner contains minor amounts of chloride ion contamination. In this work, a new synthetic approach to **2.1**, **2.2** and related species, is presented that eliminates the possibility of chloride ion contamination and, more importantly, eliminates the need for a pre-existing indium(+1) reagent.

Before describing the new synthetic protocol, it is worth noting that a perhaps predictable modification of the synthetic approach outlined in Scheme 2.1 has also been discovered that can be used to generate **2.2** in a “one-pot” reaction. Given that it was already found that protonated diethylether (present in the ethereal solution of HBF₄) is sufficiently acidic to effect such protonolysis reactions,^[10] it was reasoned that a

protonated crown ether may also be a suitable acid for the reaction. As anticipated, the treatment of either InCl or Cp*In with an equimolar solution of [18]crown-6 and HOTf in toluene results in the formation of **2.2** in essentially quantitative yield. As one might anticipate, it is also possible to treat [18]crown-6 with HOTf prior to the reaction in order to obtain a “crowned-acid” reagent of the form [H([18]crown-6)][OTf] *in situ* that may be more convenient for some applications; the treatment of either of the indium(I) reagents in Scheme 2.1 with toluene solutions of this acid complex also produces **2.2**.

While the one-pot “crowned-acid” approach may appear to be a trivial development, it is worth noting that this protocol can be employed with acids other than triflic acid to generate and isolate stable crown ether adducts of salts that are *not stable in the absence of the crown ether*. For example, whereas the protonolysis of InCl or Cp*In with trifluoroacetic acid results in the formation of a material that rapidly decomposes, if the same reactions are conducted in the presence of [18]crown-6, one is able to isolate a stable, colorless, crystalline material characterized as [In([18]crown-6)][TFA], **2.3** (TFA = trifluoroacetate) on the basis of spectroscopic methods and X-ray diffraction. While the reaction appears to be quantitative, the isolated yield is reduced to 58% due to product loss during work up.

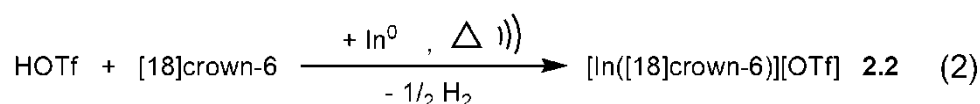
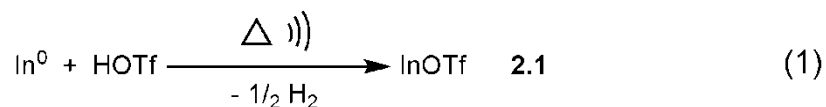
The salt **2.3** crystallizes in the space group $P2_1/m$ with the molecule bisected by a mirror plane; the molecular structure is illustrated in Figure 2.2 and some relevant metrical parameters are included in the figure caption. The In-O(1) distance of 2.272(5)Å is considerably shorter than the corresponding In-OTf distance of 2.370(2)Å found in **2.2**,^[21] which is described as a contact ion pair, and is well within the sum of the ionic radii for In(+1) and O(-2) ($1.04\text{Å} + 1.40\text{Å} = 2.44\text{Å}$).^[22] The shorter In-O distance may suggest a stronger interaction between the indium(I) center and the anion however the C-

indium(I). Given the potential of these and related salts as reagents, an alternative synthetic route to such compounds appeared desirable. Herein, a facile, clean synthetic approach to making univalent salts starting from indium metal is reported.

The ability to synthesize indium(I) species starting from metallic indium has been reported previously. For example, the electrochemical oxidation of indium metal has been used to prepare some monovalent indium species^[23, 24] and, in a related fashion, the redox reaction of silver(I) salts with metallic indium has been used to generate solutions of In^I that were used *in situ*.^[25] More pertinently to the present work, the reaction of indium with boron trifluoride in anhydrous HF generates InBF₄,^[26] whereas attempts to prepare InPnF₆ (Pn = P, As, Sb) using a similar approach employing PnF₅ in HF only worked partially in the case of Pn = P. InF₃ derivatives were generated for reactions where Pn = As and Sb.^[27] In spite of the last observation and in light of the preparation of monovalent indium compounds from phenolic quinone derivatives and indium metal reported by Tuck and co-workers^[28, 29] (and the well-known behaviour of indium's group 14 neighbour tin^[30]), it was reasoned that it might be possible to obtain indium(I) salts by the treatment of indium metal with a stoichiometric quantity of an appropriate acid. The discoveries in this regard are presented below.

The reaction of equimolar amounts of triflic acid and metallic indium in toluene in a heated ultrasonic bath affords **2.1** in high yields (Scheme 2.2) after prolonged treatment (in some cases reactions took months). The progress of the reaction can be followed using ¹¹⁵In NMR spectroscopy. Aliquots of the reaction mixture were taken at several intervals, all volatile components were removed and the remaining solid was dissolved in MeCN. Analysis of the resultant spectra suggests that the reaction proceeds through the initial formation of InOTf₃ ($\delta = -188$ ppm), which subsequently reacts with the remaining

indium metal to provide the stoichiometric product, InOTf ($\delta = -1053$ ppm); signals for each of these species are the only resonances present in the ^{115}In NMR spectra of incomplete reaction mixtures. It should be noted that test reactions starting with commercial InOTf₃ and two equivalents of indium metal in toluene do indeed produce **2.1** and thus corroborate the NMR spectroscopy observations. The amount of time required for completion of the reaction can vary considerably (up to a month in certain instances) and the progress of the reaction can be conveniently estimated visually on the basis of the amount of metal remaining in the flask. It should be emphasized that the solvent employed in this reaction appears to be of critical importance: test reactions reveal that the use of acetonitrile appears to block the reaction of InOTf₃ with In⁰ (perhaps by filling the vacant coordination site(s) on the In^{III} center) and, although it is the solvent used for the preparation, the very low solubility of InOTf₃ in toluene may be responsible for the slow rate of the reaction.



Scheme 2.2: Metal-acid syntheses of indium(+1) salts **2.1** and **2.2**.

Perhaps not surprisingly, the presence of a crown ether ligand in the metal-acid synthesis alters the reaction dramatically and also decreases the time for the reaction to proceed to completion from weeks/months to days. The reaction of triflic acid with [18]crown-6 and indium metal shows no evidence of the formation of InOTf₃ at any point

in the reaction and ^{115}In NMR studies of samples of the incomplete reaction feature only the signal at ca. -1050 ppm attributable to the In^{I} cation. This observation suggests the presence of the crown ether hinders the complete oxidation to In^{III} , either by trapping the In^{I} center and/or by rendering the trivalent alternative relatively unfavourable. The purity of the bulk sample of **2.2** produced by using this method was confirmed by powder X-ray diffraction studies. Figure 2.3 shows the agreement between the predicted pXRD pattern and the experimentally obtained pattern for the metal synthesized product, and confirms that the only observable crystalline material is the desired product. It should be noted that similar pXRD studies of **2.1** are hindered by significant absorption of the Cu $K\alpha$ radiation by the salt.

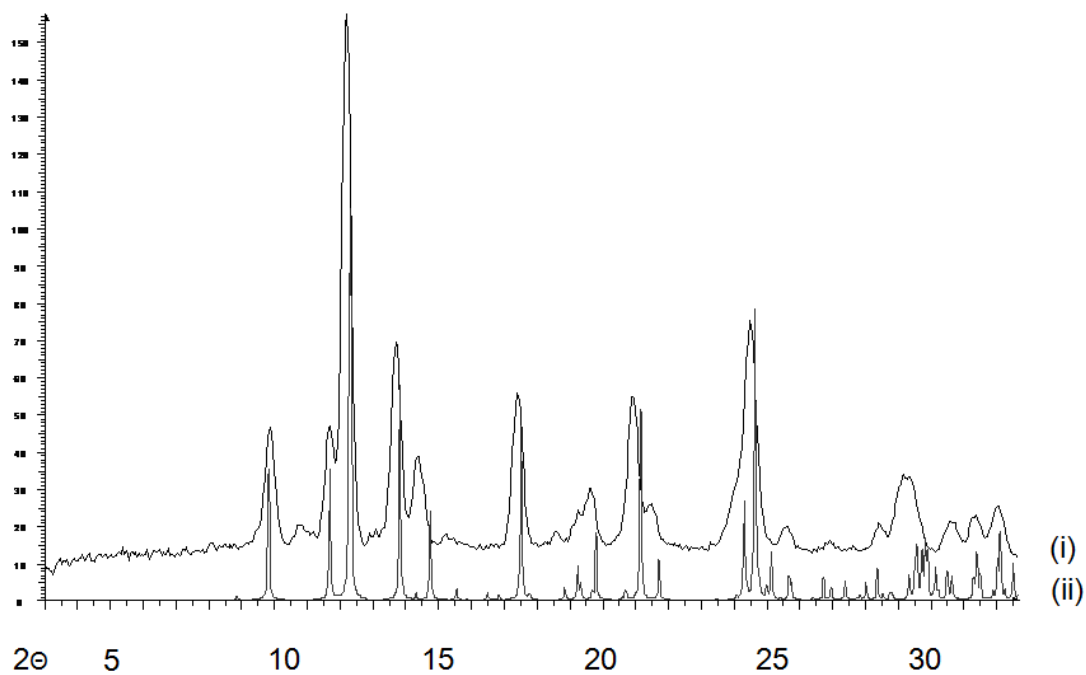


Figure 2.3: (i) experimentally observed pattern for **2.2** prepared by the metal-“crowned-acid” protocol; (ii) calculated powder pattern for **2.2** on the basis of the single crystal structure.^[15]

Given that triflic acid in the presence of [18]crown-6 can successfully oxidize indium metal to produce monovalent indium salts, and the ability of that same crown ether to stabilize In^{I} salts that are otherwise unstable, the reaction of indium metal with other “crowned” acids was investigated. Thus, the reactions of metallic indium with *p*-toluenesulfonic acid, methanesulfonic acid, and trifluoroacetic acid were conducted under conditions identical to those employed for triflic acid. In each case, the reactions featured the characteristic In^{I} resonances in the ^{115}In NMR spectra at -1062, -1070, and -1085 ppm, respectively. However, it must be emphasized that, in contrast to the reaction

employing triflic acid, these reactions were not complete even after 2 months of reaction time, and the low intensities of the signals in their ^{115}In NMR spectra suggest only limited product formation. Attempts to optimize the reaction conditions for these experiments are ongoing.

In closing, it should be emphasized that reaction of a mixture of acid and [18]crown-6 can be employed to synthesize unusually-stable complexed In^{I} salts and, more generally, that the direct reaction of triflic acid with indium metal, either in the presence or absence of [18]crown-6, provides a reliable method for the generation of soluble monovalent indium reagents.

2.2 Experimental

General methods

All work was carried out using standard inert-atmosphere techniques as indium(I) compounds tend to be air- or moisture-sensitive. All reagents and solvents were obtained from Aldrich and were used without further purification. Solvents were dried on a series of Grubbs'-type columns and were degassed prior to use.^[31] Unless otherwise noted in the text, NMR spectra were recorded at room temperature on a Bruker Avance 300 MHz spectrometer. Chemical shifts are reported in ppm, relative to external standards (SiMe_4 for ^1H and ^{13}C , $\text{In}^{+3}(\text{OH}_2)_6$ for ^{115}In , CFCl_3 for ^{19}F), please note that the ^{115}In spectra were referenced using a solution of $[\text{NEt}_4][\text{InCl}_4]$ ($\delta = 365$ ppm) as a secondary standard, because it has a much smaller line-width than the indium(III) hexahydrate standard. Melting points were obtained using an Electrothermal® melting point apparatus on samples sealed in glass capillaries under dry nitrogen. Each of the reactions reported

below appears to occur in a nearly quantitative fashion; the somewhat smaller isolated yields are attributable to mechanical losses during the workup.

X-ray Crystallography

The subject crystal was covered in Nujol®, mounted on a goniometer head and rapidly placed in the dry N₂ cold-stream of the low-temperature apparatus (Kryoflex) attached to the diffractometer. The data were collected using the SMART^[32] software on a Bruker APEX CCD diffractometer using a graphite monochromator with MoK α radiation ($\lambda = 0.71073 \text{ \AA}$). A hemisphere of data was collected using a counting time of 10 seconds per frame at -100 °C. Data reduction was performed using the SAINT-Plus^[33] software and the data were corrected for absorption using SADABS^[34]. The structure was solved by direct methods using SIR97^[35] and refined by full-matrix least-squares on F^2 with anisotropic displacement parameters for the non-disordered heavy atoms using SHELXL-97^[36] and the WinGX^[37] software package and thermal ellipsoid plots were produced using SHELXTL^[38]. Please note that the use of alternative models to describe the disorder of the fluorine atoms did not improve the solution significantly and attempts to solve the crystal in the space group $P2_1$ produce a model containing numerous non-positive definite thermal ellipsoids.

Powder X-ray diffraction experiments were performed with a Bruker D8 Discover diffractometer equipped with a Hi-Star area detector using Cu K α radiation ($\lambda = 1.54186 \text{ \AA}$). Powder XRD pattern simulations were performed using Mercury CSD 2.2.^[39] For

known compounds, these patterns were simulated on the basis of relevant data contained in the Cambridge Structural Database (CSD).^[40]

Table 2.1: Crystal data and structure refinement for [In([18]crown-6)][TFA].

Compound	[In([18]crown-6)][TFA]
Empirical formula	C ₁₄ H ₂₄ F ₃ InO ₈
Formula weight	492.15
Temperature (K)	173(2)
Wavelength (Å)	0.71073
Crystal system	Monoclinic
Space group	<i>P2(1)/m</i>
Unit cell dimensions	<i>a</i> = 9.100(3) Å ; α = 90° <i>b</i> = 11.571(3) Å ; β = 105.692(3)°. <i>c</i> = 9.634(3) Å ; γ = 90°.
Volume (Å ³)	976.7(5)
Z	2
Density (calculated) (g cm ⁻³)	1.674
Absorption coefficient (mm ⁻¹)	1.274
F(000)	496
Crystal size (mm ³)	0.20 x 0.10 x 0.10
θ range for data collection	2.20 to 27.50°.
Index ranges	-11 ≤ <i>h</i> ≤ 11, -14 ≤ <i>k</i> ≤ 14, -12 ≤ <i>l</i> ≤ 12
Reflections collected	10655
Independent reflections	2303
R(int)	0.1133
Absorption correction	Semi-empirical from equivalents
Max. and min. transmission	0.880 and 0.702
Refinement method	Full-matrix least-squares on F ²
Data / restraints / parameters	2303 / 0 / 130
Goodness-of-fit on F ²	0.989
Final R indices [<i>I</i> > 2σ(<i>I</i>)] ^a	R1 = 0.0552 wR2 = 0.0917
R indices (all data)	R1 = 0.1060 wR2 = 0.1040
Largest diff. peak and hole (e Å ⁻³)	1.130 and -1.214

^aR1(*F*): $\sum(|F_o| - |F_c|)/\sum|F_o|$ for reflections with $F_o > 4(\sum(F_o))$. wR2(*F*²): $\{\sum w(|F_o|^2 - |F_c|^2)^2/\sum w(|F_o|^2)^2\}^{1/2}$ where *w* is the weight given each reflection.

Protonolysis synthesis of [In([18]crown-6)][OTf], 2.2

Cp*In (88 mg, 0.333 mmol) was added to a solution of triflic acid (50 mg, 0.333 mmol) and [18]crown-6 (83 mg, 0.333 mmol) in toluene (25 mL). The reaction mixture was then allowed to stir for 12 h. Volatile components were then removed under reduced pressure and the product was obtained as a colorless powder (137 mg, 78% yield).

Protonolysis synthesis of [In([18]crown-6)][TFA], 2.3

InCl (150 mg, 0.995 mmol) was added to a solution of trifluoroacetic acid (113 mg, 0.995 mmol) and [18]crown-6 (263 mg, 0.995 mmol) in toluene (25 mL). The reaction was stirred at ambient conditions for 12 h and then volatile components were then removed under reduced pressure, and the product was obtained as a colorless powder. While the reaction yield appears quantitative, actual yield is diminished by loss of product during work up. (285 mg, 58% yield). mp 96-103°C; ¹H NMR (MeCN-d₃): δ= 3.607 (CH₂); ¹³C NMR (MeCN-d₃): δ= 70.917 (CH₂); ¹¹⁵In NMR (MeCN): δ= -1085 ppm; ¹⁹F NMR (MeCN): δ= -75.3 ppm

Metal-acid synthesis of InOTf, 2.1

Indium metal (1.00 g, 8.71 mmol) was added to a solution of triflic acid (1.31 g, 8.71 mmol) in toluene (25 mL). The reaction mixture was then allowed to sonicate at 40 °C until no traces of indium metal remained in the reaction vessel (this can take up to one month). Volatile components were then removed under reduced pressure, the resultant solid was washed with pentane and the product was obtained as a colorless powder (2.12 g, 92% yield). ¹¹⁵In NMR (MeCN): δ= -1053 ppm. All other physical and spectroscopic

features of the product are identical to those of material obtained using the Cp* protonolysis approach.

Metal-acid synthesis of [In([18]crown-6)][OTf], 2.2

Indium metal (1.00 g, 8.71 mmol) was added to a solution of triflic acid (1.31 g, 8.71 mmol) and [18]crown-6 (2.30 g, 8.71 mmol) in toluene (25 mL). The reaction mixture was then allowed to sonicate at 40 °C for two weeks, or until no traces of indium metal remained in the reaction vessel. Volatile components were then removed under reduced pressure, the resultant solid was washed with pentane and the product was obtained as a colorless powder (4.360 g, 95% yield). ¹¹⁵In NMR (MeCN): δ= -1054 ppm. All other physical and spectroscopic features of the product are identical to those of material obtained using the Cp* protonolysis approach.

References

- [1] G. Parkin, *J. Chem. Educ.* **2006**, *83*, 791.
- [2] J. A. J. Pardoe, A. J. Downs, *Chem. Rev.* **2007**, *107*, 2.
- [3] D. G. Tuck, *Chem. Soc. Rev.* **1993**, *22*, 269.
- [4] J. Podlech, T. C. Maier, *Synthesis* **2003**, 633.
- [5] V. Nair, S. Ros, C. N. Jayan, B. S. Pillai, *Tetrahedron* **2004**, *60*, 1959.
- [6] C. Cesario, M. J. Miller, *Org. Lett.* **2009**, *11*, 1293.
- [7] G. Hilt, K. I. Smolko, *Angew. Chem. Int. Ed.* **2001**, *40*, 3399.
- [8] U. Schneider, S. Kobayashi, *Angew. Chem. Int. Ed.* **2007**, *46*, 5909.
- [9] W. J. Yoo, C. J. Li, *Chemsuschem* **2009**, *2*, 205.
- [10] C. L. B. Macdonald, A. M. Corrente, C. G. Andrews, A. Taylor, B. D. Ellis, *Chem. Commun.* **2004**, 250.
- [11] M. Buhler, G. Linti, *Z. Anorg. Allg. Chem.* **2006**, *632*, 2453.
- [12] C. G. Andrews, C. L. B. Macdonald, *J. Organomet. Chem.* **2005**, *690*, 5090.
- [13] S. P. Green, C. Jones, A. Stasch, *Angew. Chem. Int. Ed.* **2007**, *46*, 8618.
- [14] S. P. Green, C. Jones, A. Stasch, *Chem. Commun.* **2008**, 6285.
- [15] C. G. Andrews, C. L. B. Macdonald, *Angew. Chem., Int. Ed.* **2005**, *44*, 7453.
- [16] B. F. T. Cooper, C. L. B. Macdonald, *J. Organomet. Chem.* **2008**, *693*, 1707.
- [17] T. Jurca, J. Lummiss, T. J. Burchell, S. I. Gorelsky, D. S. Richeson, *J. Am. Chem. Soc.* **2009**, *131*, 4608.
- [18] M. Buhler, G. Linti, *Z. Anorg. Allg. Chem.* **2006**, *632*, 2453.

- [19] B. F. T. Cooper, C. G. Andrews, C. L. B. Macdonald, *J. Organomet. Chem.* **2007**, 692, 2843.
- [20] O. T. Beachley, R. Blom, M. R. Churchill, K. Faegri, J. C. Fettinger, J. C. Pazik, L. Victoriano, *Organometallics* **1989**, 8, 346.
- [21] C. G. Andrews, C. L. B. Macdonald, *Angew. Chem. Int. Ed.* **2005**, 44, 7453.
- [22]
- [23] C. Geloso, H. E. Mabrouk, D. G. Tuck, *J. Chem. Soc., Dalton Trans.* **1989**, 1759.
- [24] J. H. Green, R. Kumar, N. Seudeal, D. G. Tuck, *Inorg. Chem.* **1989**, 28, 123.
- [25] S. K. Chandra, E. S. Gould, *Inorg. Chem.* **1996**, 35, 3881.
- [26] H. Fitz, B. G. Muller, *Z. Anorg. Allg. Chem.* **1997**, 623, 579.
- [27] Z. Mazej, *Eur. J. Inorg. Chem.* **2005**, 3983.
- [28] T. A. Annan, D. H. McConville, B. R. McGarvey, A. Ozarowski, D. G. Tuck, *Inorg. Chem.* **1989**, 28, 1644.
- [29] H. E. Mabrouk, D. G. Tuck, *Can. J. Chem.* **1989**, 67, 746.
- [30] F. A. Cotton, G. Wilkinson, C. A. Murillo, M. Bochmann, *Advanced Inorganic Chemistry*, Sixth Edition ed., John Wiley & Sons, Inc., Chichester, **1999**.
- [31] A. B. Pangborn, M. A. Giardello, R. H. Grubbs, R. K. Rosen, F. J. Timmers, *Organometallics* **1996**, 15, 1518.
- [32] SMART, Bruker AXS Inc., Madison, WI, **2001**.
- [33] SAINTPlus, Bruker AXS Inc., Madison, WI, **2001**.
- [34] SADABS, Bruker AXS Inc., Madison, WI, **2001**.
- [35] SIR97, A. Altomare, M. C. Burla, M. Camalli, G. L. Cascarano, C. Giacovazzo, A. Guagliardi, A. G. G. Moliterni, G. Polidori, R. Spagna, *J. Appl. Crystallogr.* **1999**, 32, 115.
- [36] SHELXL-97, G. M. Sheldrick, Universitat Gottingen, Gottingen, **1997**.
- [37] L. J. Farrugia, *J. Appl. Crystallogr.* **1999**, 32, 837.
- [38] SHELXTL, G. M. Sheldrick, Bruker AXS Inc., Madison, WI, **2001**.
- [39] C. F. Macrae, I. J. Bruno, J. A. Chisholm, P. R. Edgington, P. McCabe, E. Pidcock, L. Rodriguez-Monge, R. Taylor, J. van de Streek, P. A. Wood, *J. Appl. Crystallogr.* **2008**, 41, 466.
- [40] F. H. Allen, *Acta Crystallogr., Sect. B: Struct. Crystallogr. and Cryst. Sci.* **2002**, 58, 380.

Chapter 3: Structural Dependency on Crown Ether Cavity Sizes

3.1 Introduction

The idea of an element existing in a particular oxidation state (or, perhaps more appropriately, valence state)^[1] is one of the most simple and ubiquitous models employed by chemists to explain the structural characteristics and chemical behavior of a molecule containing that element. An element in a lower oxidation state is, by definition, more electron-rich than it would be in a higher oxidation state and the presence of these additional electrons can alter dramatically the chemistry of compounds containing such centers.^[2, 3] For this reason, the investigation of main group elements in unusually low oxidation states has been a very active area of research since the 1990's. For example, for the group 13 elements other than thallium, the +3 oxidation state (E(+3), E = B, Al, Ga, In) is the most stable which explains the Lewis-acidic behavior of the electron-deficient neutral molecules containing these elements. Conversely, the considerably less common compounds that contain a group 13 element in the +1 oxidation state (E(+1)) can behave either as Lewis bases or Lewis acids, as illustrated in Figure 3.1. Because of the presence of the "lone-pair" of electrons in E(+1) compounds, such reagents, especially cyclopentadienyl (C₅R₅, Cp') compounds of the type Cp'E^[4] and, more recently, *N*-heterocyclic E(+1) compounds bearing ligands such as α -dimimines, amidines, guanidines and β -diketimines,^[5] have been employed as donors for transition metal and main group acceptors to generate new types of catalysts or materials precursors.^[5-9] It should be emphasized that R-E compounds most obviously exhibit acceptor behavior in situations where the substituent R is not a π -donor, which can partially populate the formally vacant orbitals on the E(+1) center.^[10] In a similar vein, the R-E ligands in the numerous reported transition metal complexes can act as acceptors, for electrons from the

transition metal center or from an external donor, when R is a hydrocarbyl group or a halogen.^[11-16]

For indium in particular, it is also worth noting that the unique behavior and redox properties of In(+1) compounds (sometimes generated *in situ*) render such species useful as either reagents or catalysts used to effect several types of organic transformations; such reactions almost always proceed through the formation of organoindium intermediates or by-products.^[17-24] In a similar vein, inorganic and organometallic In(+1) reagents have been shown to insert into reactive carbon-element bonds to generate new In(+3) species.^[2, 3]

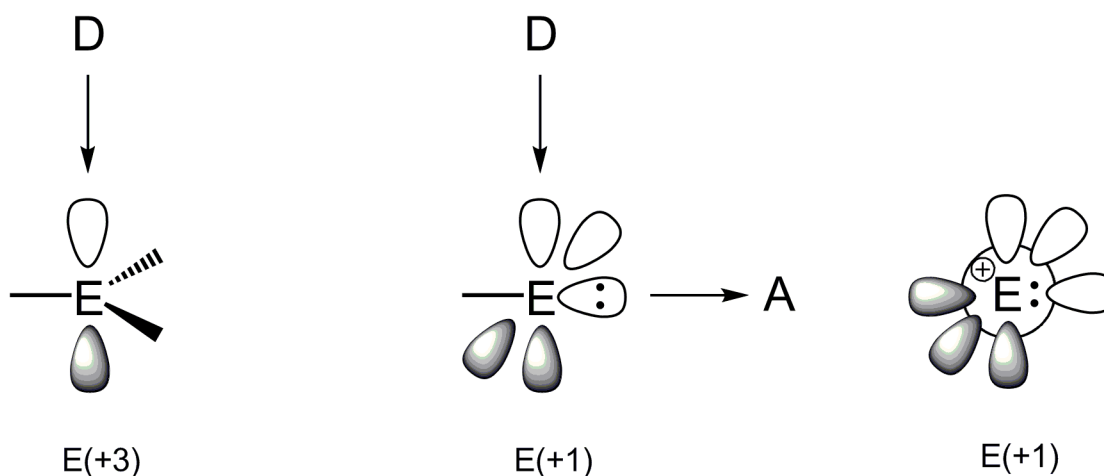


Figure 3.1: Drawings depicting the differing behavior of compounds containing group 13 elements (E) in the +3 and +1 oxidation states with electron donors (D) or acceptors (A).

For indium, a major obstacle to research and development of the chemistry of +1 oxidation state has been the paucity of convenient starting materials.^[2, 25] For while the simple halide salts of both +1 and +3 oxidation states are commercially available, the In(+1) salts are either insoluble or decompose in most common organic solvents.^[2, 25] In

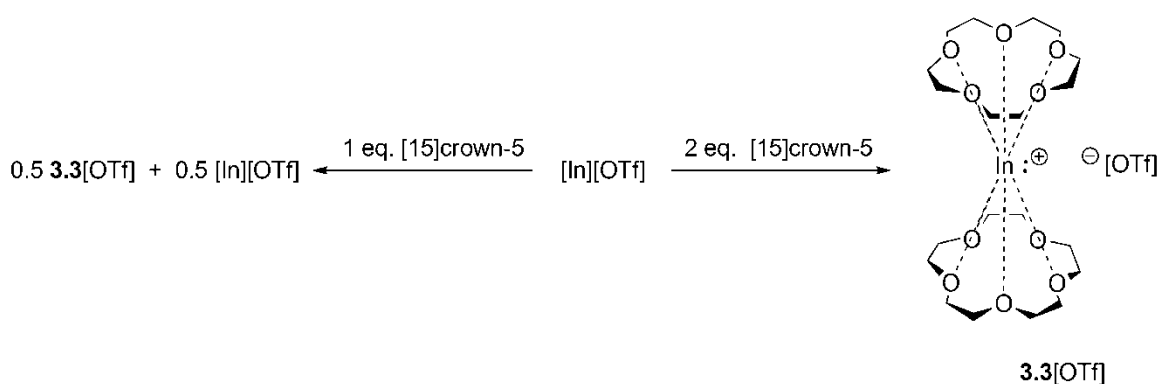
this context, several research groups have pursued a protonolytic approach to sources of In(+1) with improved stabilities and/or solubilities.^[9] Over the course of this work there has been the discovery of several routes to the unusually soluble indium(+1) trifluoromethanesulfonate salt (indium(+1) triflate, InOSO₂CF₃, InOTf, **3.1**); the most effective synthesis of **3.1** involves the oxidation of indium metal and has been discussed previously in Chapter 2.^[26, 27] As discussed in Chapter 2, this In(+1) reagent has already exhibited interesting and sometimes unique chemistry, including the formation of new In-carbon and In-element bonds.^[24, 28-32]

Of particular import to the work reported herein, it has been previously reported that the ligation of **3.1** with cyclic polyethers 1,4,7,10,13,16-hexaoxacyclooctadecane ([18]crown-6) or 2,3,11,12-dibenzo-1,4,7,10,13,16-hexaoxacyclooctadecane (dibenzo[18]crown-6) generates unambiguously monomeric In(+1) compounds [In([18]crown-6)][OTf] (**3.2a**[OTf]) and [In(dibenzo[18]crown-6)][OTf] (**3.2b**[OTf]).^[28] In contrast to most other donors, the ligation of the In(+1) center by the crown ethers occurs without any evidence of disproportionation^[33, 34] and it also changes the reactivity of the In(+1) reagent dramatically.^[31] In this chapter, I discuss the results of some of the investigations concerning the ligation of InOTf with the smaller crown ether 1,4,7,10,13-pentaoxacyclopentadecane ([15]crown-5) that results in the formation of a new, and potentially more reactive, In(+1) reagent. This reactivity will be discussed in later chapters.

3.2. Results and Discussion

Whereas the treatment of a toluene solution of the indium(+1) reagent InOTf with a solution containing an equimolar amount of the crown ether [18]crown-6 (or

dibenzo[18]crown-6) results in the quantitative formation of the complexes **3.2a**[OTf] (or **3.2b**[OTf])^[28], the corresponding reaction of **3.1** with [15]crown-5 does not form a similar 1:1 complex. Instead, the resultant solid was characterized using physical methods and X-ray crystallography as being composed of a 1:1 mixture of the starting material **3.1** and the new complex [In([15]crown-5)₂][OTf], **3.3**[OTf] as illustrated in Scheme 3.1. Predictably, the production of **3.3**[OTf] is quantitative when two equivalents of [15]crown-5 per indium atom are used in the preparation.



Scheme 3.1: Reaction of InOTf with [15]crown-5

The salt **3.3**[OTf] is very soluble in toluene and the slow concentration of a toluene solution of the material yields colorless crystals suitable for examination by single-crystal X-ray diffraction experiments. Details of the data collection, solution and refinement of the crystal structure are listed in Table 3.1, the structures of the cation and anion are depicted in Figure 3.2, and the values of selected metrical parameters are listed in the figure caption. The salt crystallizes in the centrosymmetric space group *P*-1 with a total of one cation and anion in the unit cell. The indium atom resides on an inversion center thus the [In([15]crown-5)₂] cation complex is rendered perfectly centrosymmetric. The In-O distances in the cation range from 2.9802(19) to 3.0954(18) Å with an average of

3.031 Å; these values fall well within the sum of the van der Waals radii for In (1.93 Å) and O (1.52 Å).^[35] Finally, it must be noted that the triflate anion is disordered about one of the inversion centers (located roughly between the S and C atoms) and does not appear to have any unusually short contacts with the cation.

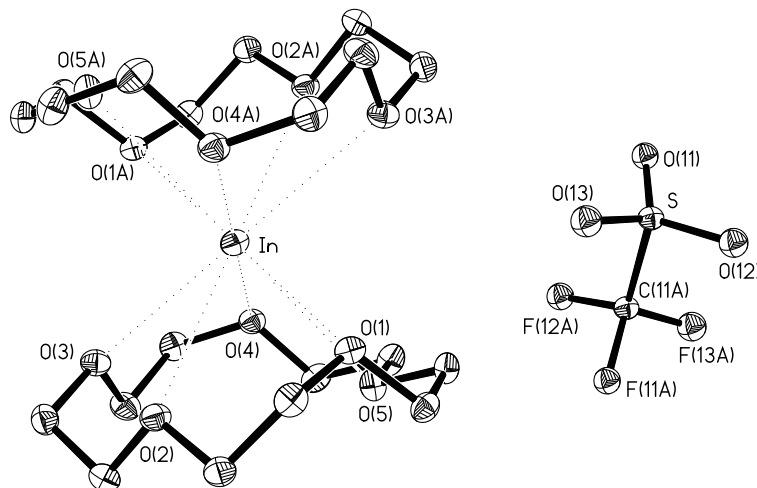


Figure 3.2: Thermal ellipsoid plot (30% probability surface) of the molecular structure of the salt **3.3**[OTf]. Important bond distances (Å): In-O(1) 2.9819(18), In-O(2) 3.0954(18), In-O(3) 3.0103(19), In-O(4) 2.9802(19), In-O(5) 3.0857(19).

Interestingly, **3.3**[OTf] is the first compound reported containing a bond between indium and [15]crown-5 as confirmed by a search of the Cambridge Structural Database (CSD);^[36] thus, structural comparisons must be made to other, potentially related complexes. Given the superficially similar appearance of the structures of In(+1) ligated by [18]crown-6 and the corresponding potassium [18]crown-6 complexes, it is not surprising that the structure of the cation **3.3** is almost indistinguishable from the [K([15]crown-5)₂]⁺ cations in the more than 30 salts containing such ions in the CSD.

The average K-O distances in these cations is 2.906 Å, which is only marginally shorter than the average In-O distance found in **3.3** and thus emphasizes the similarity of the sizes of K^+ and In(+1).

In a somewhat different vein, the "sandwich"-like appearance of $[In([15]crown-5)_2]^+$ is also reminiscent of the structures observed for certain organometallic arene complexes of In(+1) (and some other E(+1) cations).^[37] It should be noted, however, than in complexes such as Schmidbaur's salt $[In(mesitylene)_2][InBr_4]$, **3.4** $[InBr_4]$, the bent geometry of the cation is consistent with the presence of a stereochemically-active "lone pair" of electrons on the In(+1) center.^[38] In contrast, the centrosymmetric nature of the cation **3.3** does not so obviously emphasize the presence of the two remaining valence electrons on the indium atom.

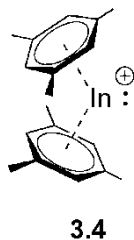


Figure 3.3: Cation of mesitylene stabilized indium salt, **3.4**

Due to the inversion symmetry present at the indium center in the solid state structure, **3.3**[OTf] was thought to be an ideal candidate for solution and solid-state ^{115}In NMR studies. During the course of investigating improved synthetic methods for the synthesis of both "free" InOTf and ligated $[In([18]crown-6)][OTf]$ the ^{115}In chemical shifts of these salts in MeCN were discussed (see Chapter 2). The related salt **3.3**[OTf] was found to

have a chemical shift of -990 ppm. Thus, for a series of triflate salts, ^{115}In NMR studies have been shown to identify the presence of an $[\text{In}^+]$ cation in solution.

While a full analysis of solid-state NMR parameters is beyond the scope of this dissertation, the resulting solid-state analyses provided some very interesting information regarding this compound. During the acquisition of a magic angle spinning spectrum, it was noted that spinning the sample at high speeds resulted in disappearance of the ^{115}In signal. While spinning the sample at high speeds causes an increase in temperature, the melting point of this compound was found to be above 100°C , and therefore loss of signal cannot be attributed to the sample melting. This interesting feature of the compound led to initial microscopy studies where two phase changes were originally observed and the sample was further analyzed by differential scanning calorimetry and variable temperature powder X-ray diffraction studies.

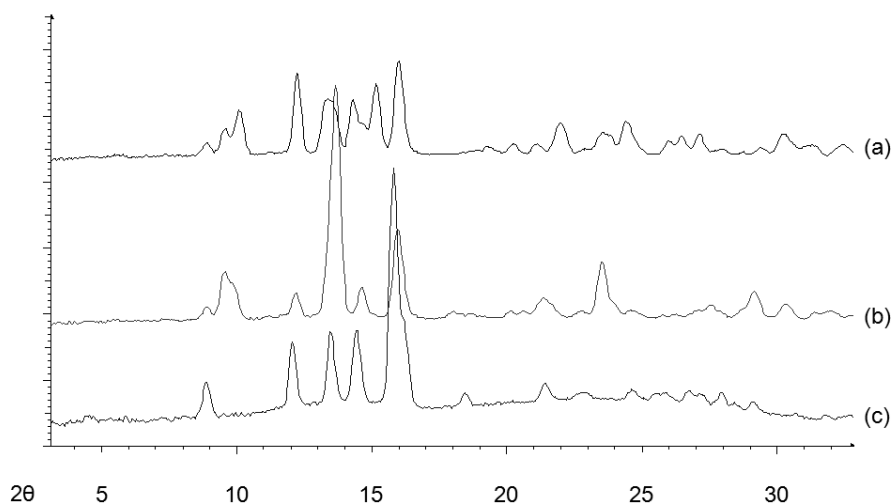


Figure 3.4: Original VT pXRD Experiments of **3.3[OTf]**; (a) ambient temperature, (b) 40 °C, (c) 100 °C.

An initial sample of **3.3[OTf]** was analyzed by VT pXRD and the resulting patterns are shown in Figure 3.4. The data suggest three unique phases in the solid state, the top pattern (Figure 3.4a) was obtained at ambient temperature, the middle pattern (Figure 3.4b) was obtained at 40°C and represents an “intermediate phase”, and the bottom pattern (Figure 3.4c) represents a “high temperature” phase obtained above 100°C. Given this structural data, the initial observation that the ^{115}In NMR spectrum changes upon spinning the sample at high velocities becomes trivial to explain. The increased temperature results in a phase change that alters the crystallinity of the solid, thus changing the environment at the indium center and the observed NMR spectrum. With solid-state structural evidence obtained, the phase changes were then analyzed by

DSC which confirmed two phase changes, one near 40°C and a higher temperature phase change near 100°C (Figure 3.5).

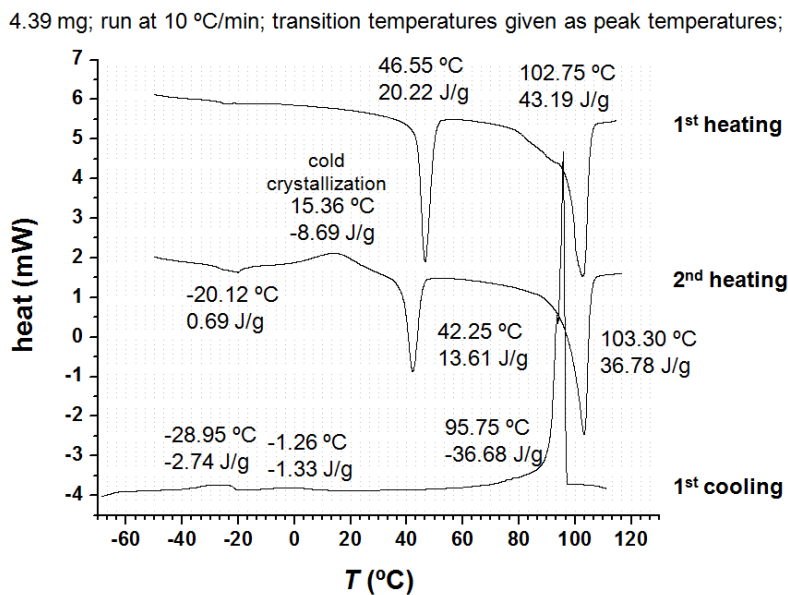


Figure 3.5: DSC data of original sample of **3.3**[OTf]

Having discovered three distinct phases of this solid, further solid-state NMR investigation was required. However, as discussed in Chapter 2, original samples of InOTf were found to contain impurities and as such the synthesis of this salt was improved. Using the improved synthesis for InOTf, and the same reaction conditions previously discussed, the resulting **3.3**[OTf] was found to have a slightly different pXRD pattern than the original sample. In addition, neither sample matched the pattern obtained from calculations using the single crystal structure obtained at -100°C, suggesting a low temperature phase transition is also present for this species. Thus, the single crystal structure of **3.3**[OTf] was obtained at ambient temperature (Figure 3.6) and was found to have unit cell parameters very similar to those obtained at -100°C (see Table 3.1). The

unit cell dimensions at room temperature were found to be slightly larger than the original structure obtained at -100°C , which is consistent with the expected expansion of a lattice with increased temperatures.

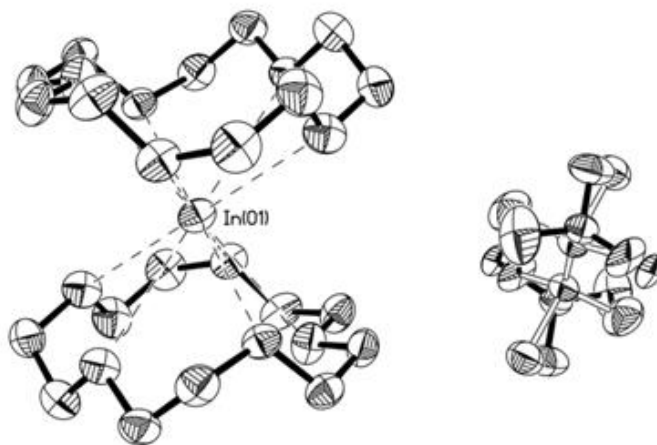


Figure 3.6: Thermal ellipsoid plot (30% probability surface) of the molecular structure of the salt **3.3**[OTf] at room temperature.

As illustrated in Figure 3.7 , a comparison of the simulated pXRD pattern obtained from the room temperature crystal structure and the experimental patterns obtained from **3.3**[OTf] showed the presence of an impurity in the original sample and further illustrates the benefit of the improved synthesis of InOTf obtained directly from indium metal.

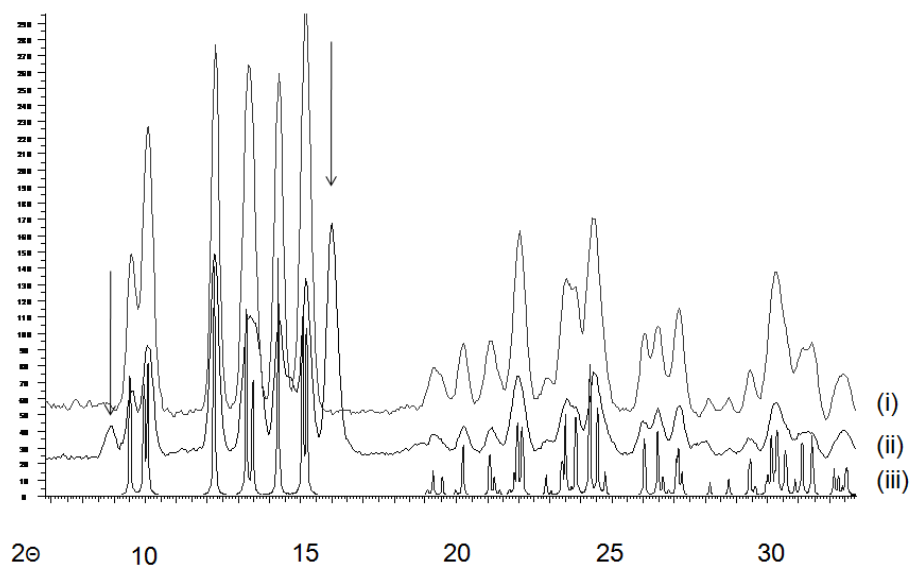


Figure 3.7: Powder XRD patterns of **3.3**[OTf]: Experimental (a); (i) InOTf synthesized directly from indium metal, (ii) InOTf synthesized from InCl₃; (arrows indicate presence of impurity) (iii) Simulated pattern from **3.3**[OTf] at room temperature.

Having obtained pure **3.3**[OTf], it was then necessary to obtain new VT pXRD patterns in order to ascertain whether the unique physical properties were a consequence of the sample itself, or some potential reactivity with the impurity. As observed in Figure 3.8, the pure sample of **3.3**[OTf] shows a reversible phase change near 40°C (Figure 3.8b), where the original powder pattern is obtained upon returning the sample back to ambient conditions (Figure 3.8c). Interestingly, the data collected above 100°C showed no retention of crystalline material. This suggests that the original “high temperature” phase observed in the pXRD and DSC experiments, is actually a result of **3.3**[OTf] melting, with the remaining impurities maintaining their crystallinity, appearing to result

in a second solid-state phase change. While no single crystal experiments have been conducted on **3.3**[OTf] at 40°C, the optimized crystal structure was found to have unit cell parameters of $a=b=c$ 9.3 Å and $\alpha=\beta=\gamma=90^\circ$.

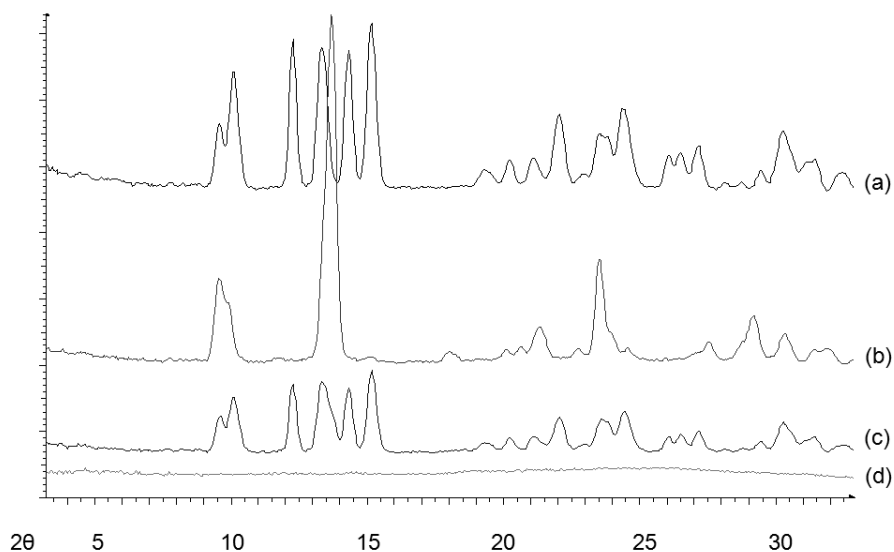


Figure 3.8: VT pXRD patterns of **3.3**[OTf]: (a) ambient conditions; (b) 40°C; (c) after cooling from 40°C to ambient conditions; (d) above 100°C

The interesting phase properties attributed by this salt are in all likelihood the result of the flexible nature of the ligation of the [15]crown-5 ligands, and the ability of disordered triflate anions (and the roughly spherical and unconstrained cation) to occupy positions of higher symmetry within the lattice. Both of these structural features would be accentuated with an increase of temperature and the increased thermal motions and energy would allow for structural changes within the lattice. Figure 3.9 depicts the results of VT ^{115}In NMR studies on **3.3**[OTf] and the increased symmetry of the solid at 40°C is observable by the sharpening of the signal.

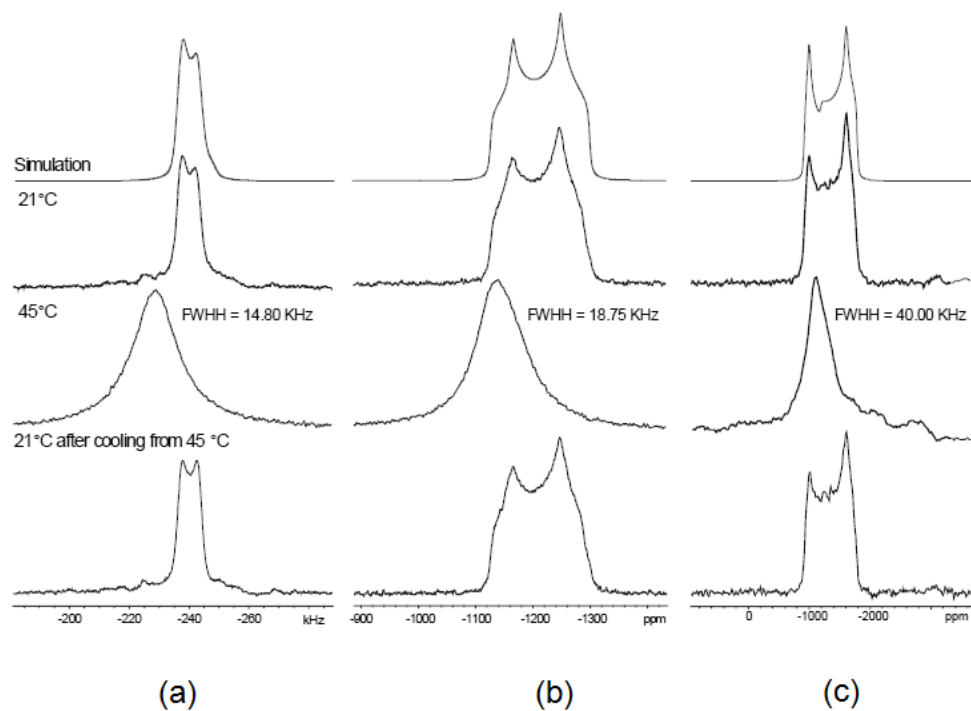


Figure 3.9: Variable temperature ^{115}In NMR spectra of **3.3**[OTf]. (a) MAS at 21.1 T; (b) Static at 21.1 T; (c) Static at 9.4 T.

While the solid-state structure of **3.3**[OTf] at 40°C remains unknown, the sharpening of the ^{115}In NMR can be explained by two possible mechanisms. As previously discussed, the presence of weak anion-cation interactions and the nearly-spherical arrangement of the bis [15]crown-5 sandwich structure could allow for the free rotation of the cation about all 3 axes (as is already evident for the anions at RT) thus producing roughly spherical electron distributions for both the cations and the anions and facilitating the adoption of a cubic structure. Alternatively, the elevated temperature could increase the indium positional disorder within the solid. Both situations would allow for the higher

symmetry spacegroup estimated for the solid at 40°C and explain the sharpening of the ^{115}In resonance.

In conclusion, the first coordination complex of indium with the crown ether [15]crown-5 has been prepared. Like the comparably-sized potassium cation, $\text{In}(+1)$ is too large for the cavity of [15]crown-5 and is preferentially ligated by two crown ethers in a centrosymmetric "sandwich"-like manner. This complex has displayed interesting solid-state properties, not only being a low oxidation state indium species amenable to solid-state ^{115}In NMR studies, but was also found to have a reversible solid-state phase transition near 40°C. Given the interesting chemistry already demonstrated by the InOTf [18]crown-6 derivatives,^[28, 31] the chemistry of this new stable, soluble, monomeric $\text{In}(+1)$ reagent will be explored in the future.

3.3. Experimental

3.3.1 General Methods

All work was carried out using standard inert atmosphere techniques. All reagents and solvents were obtained from Aldrich and were used without further purification. Preparative methods for **3.1** are described in a preliminary communication.^[26] Solvents were dried on a series of Grubbs'-type columns and were degassed prior to use.^[39] Unless otherwise noted in the text, NMR spectra were recorded at room temperature on a Bruker Avance 300 MHz spectrometer. Solid-state NMR spectra were obtained through collaboration with Hiyam Hamaed and the results are discussed in detail in her thesis. Chemical shifts are reported in ppm, relative to external standards (SiMe_4 for ^1H and ^{13}C ; CFCl_3 for ^{19}F). Melting points were obtained using an Electrothermal[®] melting point apparatus on samples sealed in glass capillaries under dry nitrogen.

Synthesis of 3.3[OTf]

A toluene (25 mL) [15]crown-5 (0.167 g, 0.758 mmol) solution was added to a toluene solution of InOTf (0.100 g, 0.379 mmol) in a 100 mL Schlenk flask and stirred overnight. After addition, an orange color was observed initially, however, after completion of the reaction, all volatile components were removed under reduced pressure and the product was obtained as a white powder. (0.21 g, 78%) m.p. 104-107 °C; ¹H NMR (C₆D₆) : δ= 3.48 (s; CH₂); ¹³C NMR (C₆D₆) : δ= 70.76 (s; CH₂); ¹⁹F NMR (C₆D₆) δ= -76.5 (s), ¹¹⁵In NMR (MeCN) δ= -990. The pXRD pattern of the solid is consistent with 3.3[OTf] being the only crystalline material present.

3.3.2 Crystallography

The subject crystal was covered in Nujol[®], mounted on a goniometer head and rapidly placed in the dry N₂ cold-stream of the low-temperature apparatus (Kryoflex) attached to the diffractometer. The data were collected using the SMART^[40] software on a Bruker APEX CCD diffractometer using a graphite monochromator with MoK α radiation ($\lambda = 0.71073 \text{ \AA}$). A hemisphere of data was collected using a counting time of 10 seconds per frame at -100 or 25 °C. Details of crystal data, data collection and structure refinement are listed in Table 3.1. Data reduction was performed using the SAINT-Plus^[41] software and the data were corrected for absorption using SADABS^[42]. The structure was solved by direct methods using SIR97^[43] and refined by full-matrix least-squares on F^2 with anisotropic displacement parameters for the non-disordered heavy atoms using SHELXL-97^[44] and the WinGX^[45] software package and thermal ellipsoid plots were produced using SHELXTL^[46]. The trifluoromethanesulfonate anion resides on a crystallographic

inversion center and is disordered; the bond distances in the anion were restrained to be similar and appropriate thermal parameters in the anion were constrained to be equal in the solution.

pXRD experiments were performed with a Bruker D8 Discover diffractometer equipped with a Hi-Star area detector using Cu K α radiation ($\lambda = 1.54186 \text{ \AA}$).

Table 3.1: Summary of collection and refinement data for the X-ray diffraction investigation of **3.3**[OTf].

Compound	[In([15]cr-5) ₂][OTf], 3.3 [OTf]	[In([15]cr-5) ₂][OTf], 3.3 [OTf] – RT
CCDC code	661703	n/a
Empirical formula	C ₂₁ H ₄₀ F ₃ InO ₁₃ S	C ₂₁ H ₄₀ F ₃ InO ₁₃ S
Formula weight	704.41	704.41
Temperature (K)	173(2)	293(2)
Wavelength (Å)	0.71073	0.71073
Crystal system	Triclinic	Triclinic
Space group	<i>P</i> -1	<i>P</i> -1
<i>Unit cell dimensions:</i>		
<i>a</i> (Å)	8.7238(10)	8.857(3)
<i>b</i> (Å)	9.0650(10)	9.158(3)
<i>c</i> (Å)	9.4298(10)	9.526(3)
α (°)	102.375(1)	102.030(4)
β (°)	91.359(1)	91.875(4)
γ (°)	97.681(1)	96.737(4)
Volume (Å ³)	720.80(14)	749.3(4)
<i>Z</i>	1	1
Density (calculated) (g cm ⁻³)	1.623	1.561
Absorption coefficient (mm ⁻¹)	0.972	0.935
<i>F</i> (000)	362	362
θ range for data collection (°)	2.32 to 27.49	2.19 to 27.50
Limiting indices	-11 ≤ <i>h</i> ≤ 11, -11 ≤ <i>k</i> ≤ 11, -12 ≤ <i>l</i> ≤ 12	-11 ≤ <i>h</i> ≤ 11, -11 ≤ <i>k</i> ≤ 11, -12 ≤ <i>l</i> ≤ 12
Reflections collected	7926	8458
Independent reflections	3184	3325
<i>R</i> _{int}	0.0199	0.0569
Data / restraints / parameters	3184 / 6 / 175	3325 / 31 / 215
Final <i>R</i> indices [<i>I</i> > 2σ(<i>I</i>)] ^a	<i>R</i> 1 = 0.0329, <i>wR</i> 2 = 0.0778	<i>R</i> 1 = 0.0541, <i>wR</i> 2 = 0.0801
<i>R</i> indices (all data)	<i>R</i> 1 = 0.0340, <i>wR</i> 2 = 0.0785	<i>R</i> 1 = 0.1156, <i>wR</i> 2 = 0.0951
Goodness-of-fit (<i>S</i>) ^b on <i>F</i> ²	1.128	0.983
Largest diff. peak and hole (e Å ⁻³)	1.005 and -0.386	0.447 and -0.287

^a $R1(F) = \frac{\sum(|F_o| - |F_c|)}{\sum|F_o|}$ for reflections with $F_o > 4(\sigma(F_o))$. $wR2(F^2) = \frac{\{\sum w(|F_o|^2 - |F_c|^2)^2 / \sum w(|F_o|^2)^2\}^{1/2}}$, where *w* is the weight given each reflection. ^b $S = \frac{[\sum w(|F_o|^2 - |F_c|^2)^2] / (n-p)}{1/2}$, where *n* is the number of reflections and *p* is the number of parameters used.

3.4. Supplementary Material

CCDC 661703 contains the supplementary crystallographic data for this paper. These data can be obtained free of charge from The Cambridge Crystallographic Data Centre via www.ccdc.cam.ac.uk/data_request/cif.

References

- [1] G. Parkin, *J. Chem. Educ.* **2006**, *83*, 791.
- [2] D. G. Tuck, *Chem. Soc. Rev.* **1993**, *22*, 269.
- [3] C. L. B. Macdonald, B. D. Ellis, *The Encyclopedia of Inorganic Chemistry*, 2nd ed., John Wiley & Sons, Chichester, U.K., **2005**.
- [4] P. Jutzi, N. Burford, *Chem. Rev.* **1999**, *99*, 969.
- [5] R. J. Baker, C. Jones, *Coord. Chem. Rev.* **2005**, *249*, 1857.
- [6] R. A. Fischer, J. Weiss, *Angew. Chem., Int. Ed.* **1999**, *38*, 2831.
- [7] G. Linti, H. Schnockel, *Coord. Chem. Rev.* **2000**, *206*, 285.
- [8] C. Gemel, T. Steinke, M. Cokoja, A. Kemper, R. A. Fischer, *Eur. J. Inorg. Chem.* **2004**, 4161.
- [9] S. Aldridge, C. Jones, T. Gans-Eichler, A. Stasch, D. L. Kays, N. D. Coombs, D. J. Willock, *Angew. Chem., Int. Ed.* **2006**, *45*, 6118.
- [10] C. L. B. Macdonald, A. H. Cowley, *J. Am. Chem. Soc.* **1999**, *121*, 12113.
- [11] C. Boehme, J. Uddin, G. Frenking, *Coord. Chem. Rev.* **2000**, *197*, 249.
- [12] J. Uddin, G. Frenking, *J. Am. Chem. Soc.* **2001**, *123*, 1683.
- [13] H. Behrens, M. Moll, E. Sixtus, G. Thiele, *Z. Naturforsch., B: Chem. Sci.* **1977**, *32*, 1109.
- [14] M. M. Schulte, E. Herdtweck, G. RaudaschlSieber, R. A. Fischer, *Angew. Chem., Int. Ed. Engl.* **1996**, *35*, 424.
- [15] G. N. Harakas, B. R. Whittlesey, *Inorg. Chem.* **1997**, *36*, 2704.
- [16] R. A. Fischer, M. M. Schulte, J. Weiss, L. Zsolnai, A. Jacobi, G. Huttner, G. Frenking, C. Boehme, S. F. Vyboishchikov, *J. Am. Chem. Soc.* **1998**, *120*, 1237.
- [17] P. Cintas, *Synlett* **1995**, 1087.
- [18] C. J. Li, T. H. Chan, *Tetrahedron* **1999**, *55*, 11149.
- [19] B. C. Ranu, *Eur. J. Org. Chem.* **2000**, 2347.
- [20] J. Podlech, T. C. Maier, *Synthesis-Stuttgart* **2003**, 633.
- [21] K. K. Chauhan, C. G. Frost, *J. Chem. Soc., Perkin Trans. 1.* **2000**, 3015.
- [22] V. Nair, S. Ros, C. N. Jayan, B. S. Pillai, *Tetrahedron* **2005**, *61*, 2725.
- [23] T. P. Loh, G. L. Chua, *Chem. Comm.* **2006**, 2739.
- [24] U. Schneider, S. Kobayashi, *Angew. Chem., Int. Ed.* **2007**, *46*, 5909.
- [25] J. A. J. Pardoe, A. J. Downs, *Chem. Rev.* **2007**, *107*, 2.
- [26] C. L. B. Macdonald, A. M. Corrente, C. G. Andrews, A. Taylor, B. D. Ellis, *Chem. Comm.* **2004**, 250.

- [27] B. F. T. Cooper, C. L. B. Macdonald, *New J. Chem.* **2010**, *34*, 1551.
- [28] C. G. Andrews, C. L. B. Macdonald, *Angew. Chem., Int. Ed.* **2005**, *44*, 7453.
- [29] C. G. Andrews, C. L. B. Macdonald, *J. Organomet. Chem.* **2005**, *690*, 5090.
- [30] M. Buhler, G. Linti, *Z. Anorg. Allg. Chem.* **2006**, *632*, 2453.
- [31] B. F. T. Cooper, C. G. Andrews, C. L. B. Macdonald, *J. Organomet. Chem.* **2007**, *692*, 2843.
- [32] H. T. Dao, U. Schneider, S. Kobayashi, *Chem. Comm.* **2011**, *47*, 692.
- [33] R. J. Baker, H. Bettentrup, C. Jones, *Eur. J. Inorg. Chem.* **2003**, 2446.
- [34] R. J. Baker, C. Jones, M. Kloth, D. P. Mills, *New J. Chem.* **2004**, *28*, 207.
- [35] www.webelements.com.
- [36] F. H. Allen, *Acta Crystallogr., Sect. B: Struct. Sci.* **2002**, *58*, 380.
- [37] H. Schmidbaur, *Angew. Chem., Int. Ed. Engl.* **1985**, *24*, 893.
- [38] J. Ebenhoch, G. Muller, J. Riede, H. Schmidbaur, *Angew. Chem., Int. Ed. Engl.* **1984**, *23*, 386.
- [39] A. B. Pangborn, M. A. Giardello, R. H. Grubbs, R. K. Rosen, F. J. Timmers, *Organometallics* **1996**, *15*, 1518.
- [40] SMART, Bruker AXS Inc., Madison, WI, **2001**.
- [41] SAINTplus, Bruker AXS Inc., Madison, WI, **2001**.
- [42] SADABS, Bruker AXS Inc., Madison, WI, **2001**.
- [43] WINGX, A. Altomare, M. C. Burla, M. Camalli, G. Cascarano, C. Giacovazzo, A. Guagliardi, M. A. G. G., G. Polidori, R. Spagna, CNR-IRMEC, Bari, **1997**.
- [44] SHELXL-97, G. M. Sheldrick, Universitat Gottingen, Gottingen, **1997**.
- [45] L. J. Farrugia, *J. Appl. Crystallogr.* **1999**, *32*, 837.
- [46] SHELXTL, G. M. Sheldrick, Bruker AXS Inc., Madison, WI, **2001**.

Chapter 4: Insertion Chemistry of "Crowned" Indium Triflate

4.1. Introduction

As previously discussed, the presence of additional electron density of E(+1) species has the potential to drastically alter the chemistry of compounds containing such centers.^[1] Group 13 elements in the +1 oxidation state (E(+1)) can behave either as Lewis bases or Lewis acids. Given their electron-rich nature, the use of E^I compounds, particularly cyclopentadienyl (C₅R₅, Cp') compounds of the type Cp'E,^[2] as ligands for transition metal and main group acceptors has been exploited significantly since the late 1990's for the synthesis of new catalysts or materials precursors.^[3, 4] For indium, the unique behavior and redox properties of In^I compounds (often generated *in situ*) have proven to be particularly useful for the catalysis of several types of organic transformations.^[5-9]

One significant drawback to the exploitation of the chemistry of +1 oxidation state group 13 chemistry has been the lack of convenient starting materials.^[10] For example, whereas well-characterized oligomeric E^I halides for E = B, Al and Ga are known, these materials have only been prepared in gas-phase reactions using special equipment that is not readily available. Furthermore, the meta-stable materials obtained using that protocol tend to decompose or disproportionate at ambient temperature.^[11, 12] The gallium reagent known as "Ga^I",^[13] which is often used as source of Ga^I centers, has neither the structure nor the composition suggested by the indicated formula.^[14, 15] In contrast to the lighter congeners, thallium(I) salts are often more stable than the corresponding thallium(III) analogues because of inert pair effects. For indium, simple halide salts of both +1 and +3 oxidation states are well-known and commercially available, however such In^I salts are

insoluble in most common organic solvents.^[10] To allay the situation, the unusually soluble indium(I) trifluoromethanesulfonate salt (indium(I) triflate, $\text{InOSO}_2\text{CF}_3$, **4.1**) was synthesized as an improved starting material for the study of low oxidation state group 13 chemistry.^[16]

Because of their electron-rich nature, it is not surprising that oxidative addition chemistry is typical of In^{I} reagents.^[10] Several research groups have reported that In^{I} halides will readily insert into, e.g., elemental halogens; the C-H bonds in some peroxy-acids (C = O), organodithiolates (C = S), or organodiselenides (C = Se); and certain other reactive heteronuclear bonds.^[10] Of particular import to the work presented herein, is the reported insertion of In^{I} halides into dihalomethanes (CH_2X_2 ; X = Br, I) to yield In^{III} compounds of the type $\text{X}_2\text{InCH}_2\text{X}$ ^[17, 18] or into haloforms (CHX_3 ; X = Cl, Br, I) to provide In^{III} compounds of the form X_2InCHX_2 .^[19, 20] These products were generally isolated as Lewis base adducts or as phosphonium ylides.

Recently, it has been shown that the ligation of **4.1** with cyclic polyethers 1,4,7,10,13,16-hexaoxacyclooctadecane ([18]crown-6, indicated by the label "a" in the text) or 2,3,11,12-dibenzo-1,4,7,10,13,16-hexaoxacyclooctadecane (dibenzo[18]crown-6, indicated by the label "b" in the text) allows for the isolation of unambiguously monomeric indium(I) compounds and alters the reactivity of the reagent significantly.^[21] In this chapter, findings regarding the reaction of $[\text{In}([\text{18}]\text{crown-6})][\text{OTf}]$ (**4.2a**[OTf]) and $[\text{In}(\text{dibenzo}[18]\text{crown-6})][\text{OTf}]$ (**4.2b**[OTf]) with solvents containing carbon-chlorine bonds is presented.

4.2 Results and Discussion

Given that insertion chemistry is typical of In^I halides and is employed for many organic transformations, it was surprising that the uncomplexed indium(+1) reagent InOTf^[16] appears to be stable and unreactive toward chlorinated solvents, as evidenced by multinuclear NMR experiments, IR spectroscopy, physical characteristics (appearance, melting point) and X-ray crystallography studies of the solids obtained after exposure to these solvents.. In contrast, when the crown ether ligated complexes of InOTf, **4.2a**[OTf] or **4.2b**[OTf], are subjected to chlorinated solvents, it was noticed that the reagent behaves quite differently. It was observed that whereas the dissolution of **4.1** in chlorinated solvents appears to occur slowly, samples of **4.2a**[OTf] or **4.2b**[OTf] are taken up rapidly in either dichloromethane or chloroform. More importantly, multinuclear NMR spectroscopic investigations and other characterization techniques reveal that the crowned indium triflate compound is not simply dissolved in the process but that the reagent actually reacts with the solvent. The results of the experiments with dichloromethane and chloroform (illustrated in Scheme 4.1) are summarized in the following sections.

possible to obtain some extremely-low-quality crystals of a related by-product of **4.3b** containing a different anion.^[22] The crystallographic data were of such poor quality that the investigation of the sample (space group *P-1*: a 10.837(5), b 13.422(6), c 14.783(7), α 110.829(5), β 97.986(6), γ 109.970(5)) is only able to establish the connectivity of the cation, which is depicted in Figure 4.1. Although the values of the metrical parameters in this model are not reliable, the presence of the observed C-Cl moiety and the Cl atom attached to the indium atom are consistent with the insertion of the In^I center into a carbon-chlorine bond of dichloromethane.

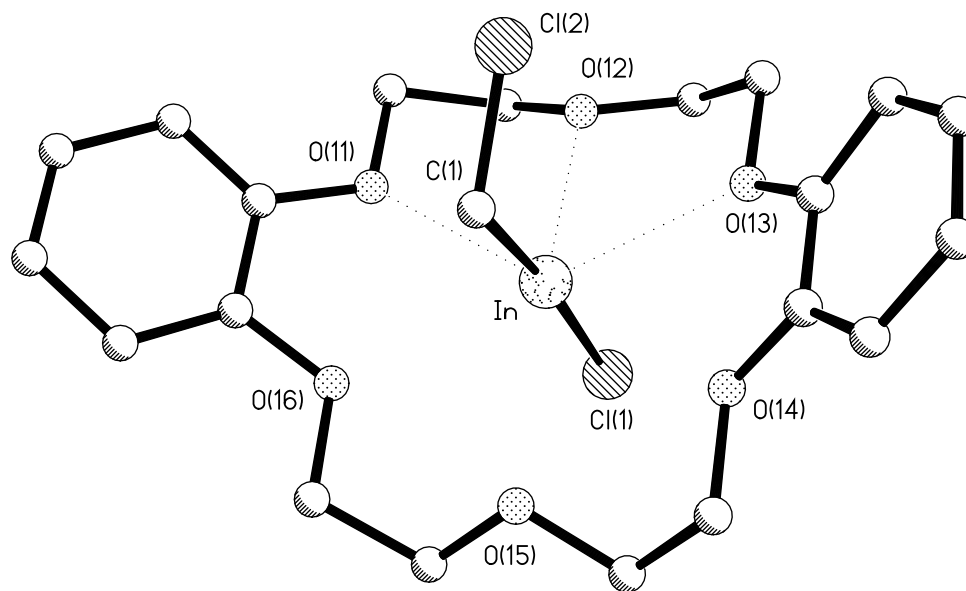


Figure 4.1: Ball and stick representation of the connectivity in the cation **4.3b** from a diffraction experiment on a crystal of very poor quality.

It is perhaps interesting to note that whereas the attempted reaction of InCl with CH₂Cl₂ did not provide for the isolation of the expected C-Cl insertion product in almost every instance because of a competing disproportionation process,^[17, 18] in the cases of the crowned In^I reagents, the insertion reaction occurs as anticipated and no comparable disproportionation reactions are evident.

Chloroform

The reaction of **4.2a**[OTf] (or **4.2b**[OTf]) with chloroform proceeds in a similar manner to that with dichloromethane. Thus the immersion of solid **4.2a**[OTf] (or **4.2b**[OTf]) with chloroform results in the rapid disappearance of the solid and does not produce any obvious color changes. Removal of volatile materials under reduced pressure provides a colorless solid characterized as **4.4a**[OTf] (or **4.4b**[OTf]) in very high yield. In one NMR scale reaction, large crystals rapidly precipitated from the as-prepared reaction mixture, however this behavior appears to have been a fortuitous consequence of the particular concentration; in most instances, crystalline material is obtained by the slow concentration of a solution of the salt in chloroform. As with the insertion products described above, every manner of characterization that was employed indicates the formation of the insertion products. For example, the melting point of ca. 194°C for **4.4a**[OTf] is clearly different than that of ca. 137°C for **4.2a**[OTf]; the difference in temperatures between the melting points of 135°C for **4.4b**[OTf] and 128°C for **4.2b**[OTf] is considerably smaller, but the behavior is quite distinctive. Similarly, the new signals in the multinuclear NMR spectra are suggestive of the presence of the dichloromethyl substituent in **4.4a**[OTf] and **4.4b**[OTf] and the isotope ratios in mass

spectrometric investigations are consistent with the presence of three chlorine atoms in the cations of the salts.

For **4.4a**[OTf], the slow evaporation of a chloroform solution of the material yielded crystals suitable for examination by single-crystal X-ray diffraction. Details of the structure solution and refinement are located in the Experimental section and in Table 4.1; a rendering of the salt components is provided in Figure 4.2 and the values for important metrical parameters are listed in the figure caption. The salt crystallizes in the space group $P2_1/m$ with half a cation and half an anion in the asymmetric unit. There are no unusually short contacts between the cation and the anion and the triflate anion is (as is commonly observed) very disordered; only the arrangement with the highest occupancy is shown in the figure. Of most import is the structure of the cation, which clearly shows the presence of a dichloromethyl fragment and a chloride substituent directly attached to the In center. The bond distances for the In-C bond (2.182(15) Å) and the In-Cl bond (2.329(4) Å) are consistent with the values that have been reported previously for the anion in the related salt [NEt₄][Cl₃In-CHCl₂] (In-C, 2.17(1) Å; In-Cl range from 2.366(4) to 2.376(4) Å).^[20] Consequently, the observed values fall within the range of values for such bonds^[23] that have been collected in the Cambridge Structural Database (CSD).^[24] The most interesting features of the structure involve the arrangement of the crown ether about the cationic indium fragment. The [18]crown-6 ligand in **4.4a** adopts a conformation that allows for five close "equatorial" contacts (In-O distances range from 2.409(9) to 2.531(8) Å) between oxygen atoms on crown ether. The five-fold-coordination is in stark contrast to the symmetric six-fold coordinated structure (with In-O distances from 2.8299(18) to 2.9292(18) Å) observed for the identical crown ether in **4.2a**[OTf] and emphasizes the difference in the sizes of In(+3) and In(+1) centers, as

univalent indium will have a larger radius due to having more electron density associated with them.

A final observation concerning the conformation of the [18]crown-6 ligand in **4.4a** is that the five-coordinate ligation of the indium center leaves one oxygen atom available to form a hydrogen bond to the hydrogen atom situated on the dichloromethyl substituent.^{[25,}

^{26]} In fact, the importance of the putative hydrogen bonding interaction in determining the conformation adopted by the crown ether is illustrated by the structure of $[\text{InI}_2([\text{18}]\text{crown-6})][\text{InI}_4]$, in which none of the oxygen atoms in the crown ether is distorted significantly away from the equatorial plane of the In atom.^[27]

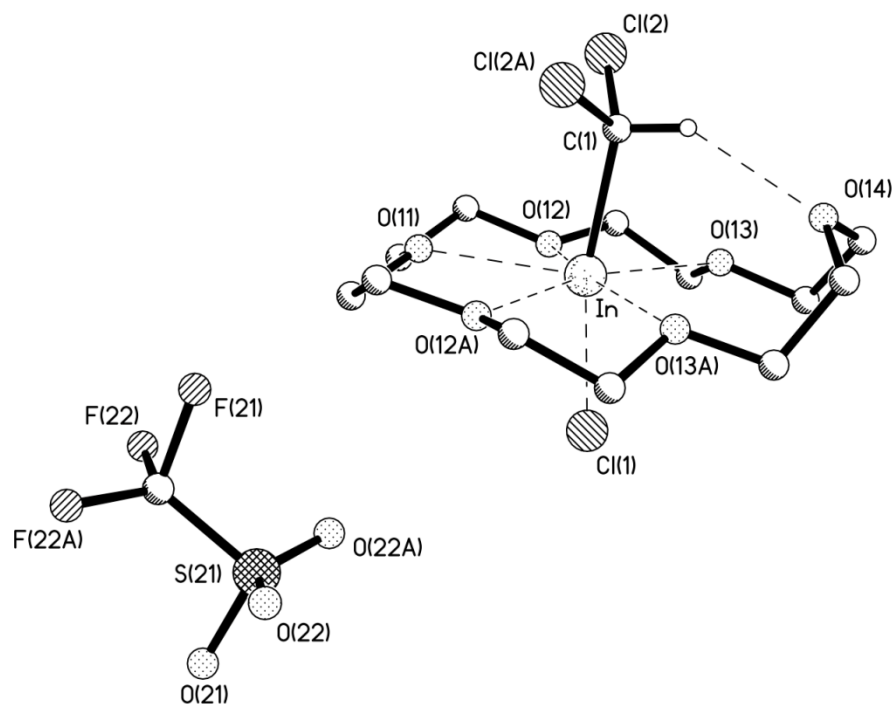


Figure 4.2: Ball and stick representation of the salt **4.4a**[OTf] from a crystal with disordered refinement; most of the hydrogen atoms have been omitted. Important bond distances (Å) and angles (°): In-C(1) 2.182(15), In-Cl(1) 2.329(4), In-O(11) 2.492(12), In-O(12) 2.409(9), In-O(13) 2.531(8), H(1)⋯O(14) 2.25(2), C(1)⋯O(14) 3.13(2), C(1)-In-Cl(1) 167.8(4), O(14)-H(1)-C(1) 146.0(9).

In the case of **4.4b**[OTf], colorless crystals suitable for examination by single crystal X-ray diffraction experiments were obtained by the slow concentration of a solution of the salt in chloroform. Details regarding the solution and refinement of the structure are located in the Experimental section and in Table 4.1. The molecular structures of the

cation and anion in the asymmetric unit are depicted in Figure 4.3 (two molecules of chloroform that are also located in the asymmetric unit are not shown) and the values of important metrical parameters for the cation are listed in the figure caption. The bond distances and angle for the Cl-In-CHCl₂ fragment in **4.4b**[OTf] (In-C 2.174(7) Å; In-Cl 2.304(2) Å; C-In-Cl 171.81(19)°) are very similar to those described above for **4.4a**[OTf] and do not warrant further discussion. The indium atom in the cation **4.4b** is offset from the centroid of the six oxygen atoms in the ring toward one of the arene rings such that there are four close contacts (In-O from 2.517(5) to 2.550(5) Å) and two significantly longer contacts (2.738(5) and 2.756(5) Å).

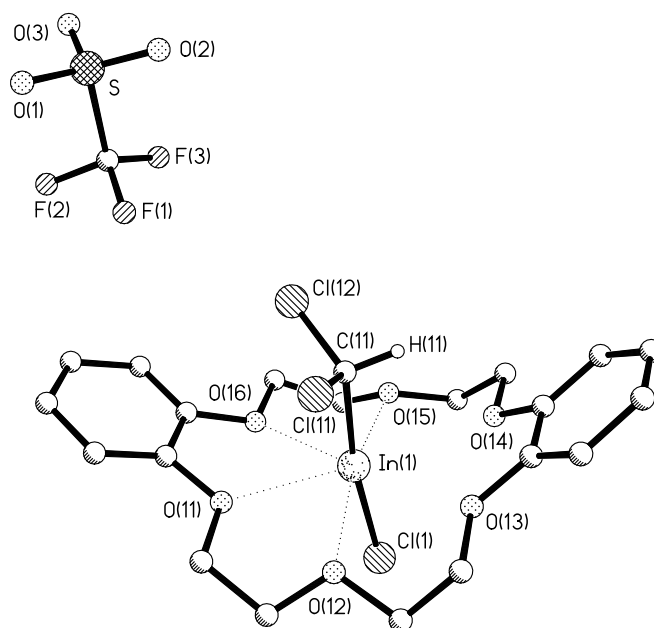


Figure 4.3: Ball and stick representation of the salt **4.4b**[OTf] from crystal with disordered refinement; most of the hydrogen atoms have been omitted for clarity. Important bond distances (Å) and angles (°) C(11)-In(1) 2.174(7), Cl(1)-In(1) 2.304(2), O(11)-In(1) 2.528(5), O(12)-In(1) 2.517(5), O(13)-In(1) 2.738(5), O(14)-In(1) 2.756(5), O(15)-In(1) 2.533(5), O(16)-In(1) 2.550(5), C(11)-In(1)-Cl(1) 171.81(19).

Perhaps the most interesting difference between the structures of **4.4a**[OTf] and **4.4b**[OTf] is the conformations adopted by the parent and benzannelated crown ethers. Whereas the parent [18]crown-6 polyether ligates the indium cation using five oxygen atoms at roughly similar distances and is contorted to engage in hydrogen bonding, the benzannelated analogue exhibits a structure that is virtually identical in conformation to that which is adopted in most of the structures in which the ligand is found in the CSD. It

appears as if the rigidity imposed by the presence of the aromatic rings in dibenzo[18]crown-6 prevents the contortions that are possible for the more flexible polyether. In both cases, however, it is clear that the reduction in the size of the indium cation upon oxidation of the In^I centers (ionic radius 1.04 Å^{[28][27]}) in the starting materials to In^{III} (ionic radius 0.81 Å) requires an alteration in the arrangement of the crown ether to maximize the ligation of the metal.^[28]

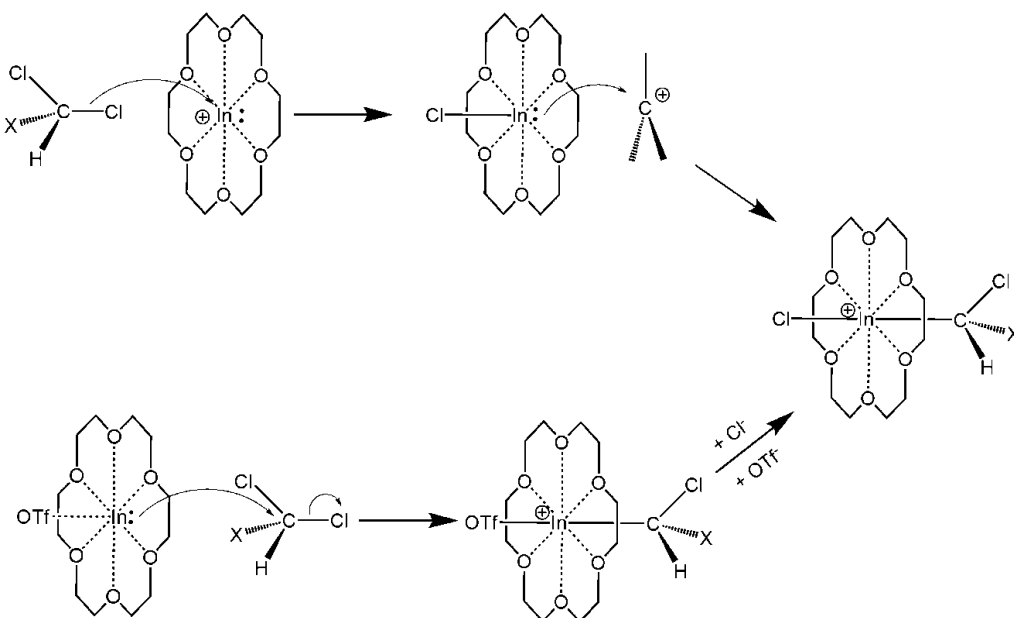
Commentary

The reaction of the crown-ether-ligated In^I salts **4.2a**[OTf] and **4.2b**[OTf] with dichloromethane and chloroform proceed rapidly to yield products derived from the formal insertion of the In^I center into a C-Cl bond of the solvent molecule. The observed reactivity is in contrast to the relatively inert behavior observed for the unligated salt InOTf, which does not appear to react with chlorocarbons at an appreciable rate. It was initially surmised that the apparent non-reactivity of **4.1** was a kinetic effect that is likely attributable the agglomeration of the salt into clusters containing numerous In-O contacts, as observed in the crystal structure of **4.1**,^[16] however a better understanding of the nature of crown ether ligation on the reactivity of such species is present in Chapter 6. In any case, the ligation of **4.1** by the appropriately-sized crown ethers results in the formation of monomeric species, and the increased reactivity of salts **4.2a**[OTf] and **4.2b**[OTf] is indisputable.

It should be noted that the preliminary investigations of the interaction of salts **4.2a**[OTf] and **4.2b**[OTf] with carbon tetrachloride suggest that, while a reaction certainly occurs, the nature of the resultant products is ambiguous; mass spectrometric data suggest the major cationic components are the chlorination products [InCl₂([18]crown-6)⁺] and

[InCl₂(dibenzo[18]crown-6)⁺], respectively. More detailed studies of this system and studies of the insertion chemistry of **4.2a**[OTf] and **4.2b**[OTf] with more complex organochlorine compounds are currently underway.

Finally, it should be noted that, while the In^{III} products obtained from the reactions described above appear to be completely analogous to those that one would obtain from a traditional oxidative addition of a transition metal fragment, the mechanism for the actual process is unclear. If the crown ether remains attached to the In center during the reaction, it would seem unlikely that the reaction could occur by way of a concerted addition into the bond given that the Cl atom and CHClX fragments are *trans* to one another in the products. A more likely scenario would likely involve a step-wise addition similar to one of the routes shown in Scheme 4.2. It should be noted that in addition to the routes illustrated in Scheme 4.2, the insertion could also proceed through a radical mechanism.



Scheme 4.2: Potential stepwise reaction pathways for C-Cl bond insertion.

4.3 Experimental

4.3.1 General Methods

All work was carried out using standard inert-atmosphere techniques as In^I compounds tend to be air- or moisture-sensitive. All reagents and solvents were obtained from Aldrich and were used without further purification. Preparative methods for **4.2a**[OTf] and **4.2b**[OTf] are described in a preliminary communication by Andrews and Macdonald.^[21] Solvents were dried on a series of Grubbs'-type columns and were degassed prior to use.^[29] Unless otherwise noted in the text, NMR spectra were recorded at room temperature on a Bruker Avance 300 MHz spectrometer. Chemical shifts are reported in ppm, relative to external standards (SiMe₄ for ¹H and ¹³C). Melting points were obtained using an Electrothermal[®] melting point apparatus on samples sealed in glass capillaries under dry nitrogen. The low and high resolution mass spectra were recorded either in house or at the McMaster Regional Mass Spectrometry Facility. FT-IR spectra were obtained as Nujol mulls on KBr plates using a Bruker Vector22 spectrometer.

4.3.2 Specific procedures

Synthesis of 4.3a[OTf]

Dichloromethane (20 mL) was added to InOTf·C₁₂H₂₄O₆ (105 mg, 0.198 mmol) in a 100 mL Schlenk flask and stirred overnight. Volatiles were removed *in vacuo* and the product was obtained as a white powder (60 mg, 0.097 mmol) in 49 % yield. m.p. 220-225 °C; ¹H NMR (CD₂Cl₂) : δ= 3.84 (s; 24H; CH₂), 3.47 (s; 2H; CH₂Cl) ppm; ¹³C NMR (CD₂Cl₂) : δ=70.5 (s; CH₂) ppm. HRMS (ESI-TOF): *m/z* calculated for InC₁₃H₂₆O₆Cl₂: 463.0145, found: 463.0166 (4.5 ppm).

Synthesis of 4.3b[OTf]

Dichloromethane (20 mL) was added to InOTf·C₂₀H₂₄O₆ (101 mg, 0.162 mmol) in a 100 mL Schlenk flask and stirred overnight. Volatiles were removed *in vacuo* and the product was obtained as a white powder (72 mg, 0.102 mmol) in 63 % yield. m.p. 140 – 144 °C; ¹H NMR (CD₂Cl₂) : δ= 4.03 (s; 8H; CH₂), 4.13 (s; 8H; CH₂), 6.91 (m; 8H; Ar-H), 4.37 (m; 2H; CH₂Cl) ppm; ¹³C NMR (CD₂Cl₂) δ= 67.7 (s, CH₂), 69.6 (s, CH₂), 112.7 (s; β-Ar), 122.2 (s; α-Ar), 147.2 (s, O-C_{Ar}) ppm. HRMS (ESI-TOF): *m/z* calculated for InC₂₁H₂₆O₆Cl₂: 559.0145, found: 559.0153 (1.4 ppm).

Synthesis of 4.4a[OTf]

Chloroform (20 mL) was added to InOTf·C₁₂H₂₄O₆ (104 mg, 0.196 mmol) in a 100 mL Schlenk flask and stirred overnight. Volatiles were removed *in vacuo* and the product was obtained as a white powder (72 mg, 0.112 mmol) in 57 % yield. m.p. 193 – 198 °C; ¹H NMR (CDCl₃) : δ= 3.89 (s; 24H; CH₂), 5.87 (s; 1H; CHCl₂) ppm; ¹³C NMR (CDCl₃) : δ=70.2 (s; CH₂) ppm. HRMS (ESI-TOF): *m/z* calculated for InC₁₃H₂₅O₆Cl₃: 496.9755, found: 496.9743 (-2.5 ppm).

Synthesis of 4.4b[OTf]

Chloroform (20 mL) was added to InOTf·C₂₀H₂₄O₆ (103 mg, 0.165 mmol) in a 100 mL Schlenk flask and stirred overnight. Volatiles were removed *in vacuo* and the product was obtained as a white powder (75 mg, 0.100 mmol) in 61 % yield. m.p. 129 - 135°C; ¹H NMR (CDCl₃) : δ= 4.12 (m; 16H; CH₂), δ= 7.06 (m; 8H; Ar-H), δ=5.65 (m; 1H; CHCl₂) ppm; ¹³C NMR (CDCl₃) : δ= 67.9 (s; CH₂) , 69.0 (s; CH₂), 111.7 (s; β-Ar), 123.8 (s; α-Ar), 149.0 (s; O-C_{Ar}) ppm. HRMS (ESI-TOF): *m/z* calculated for InC₂₁H₂₅O₆Cl₃: 592.9755, found: 592.9745 (-1.8 ppm).

4.3.3 Crystallography

In the dry N₂ atmosphere of a VAC glovebox, each crystal was selected and mounted in thin-walled glass capillary tubes. These were subsequently flame-sealed and glued to brass pins suitable for attachment to a goniometer head. The data were collected using the SMART^[30] software on a Bruker APEX CCD diffractometer using a graphite monochromator with MoK α radiation ($\lambda = 0.71073 \text{ \AA}$). A hemisphere of data was collected using a counting time of 10 seconds per frame at -100 °C. Details of crystal data, data collection and structure refinement are listed in Table 4.1. Data reductions were performed using the SAINT^[31] software and the data were corrected for absorption using SADABS.^[32] The structures were solved by direct methods using SIR97^[33] and refined by full-matrix least-squares on F^2 with anisotropic displacement parameters for the non-disordered heavy atoms using SHELXL-97^[34] and the WinGX^[35] software package and thermal ellipsoid plots were produced using SHELXTL.^[36] Considerable disorder in either anions or solvent molecules was manifested in each of the structures reported below; various restraints, constraints and partial occupancy models were employed in the solutions.

Table 4.1: Summary of collection and refinement data for the X-ray diffraction investigations of **4.4a** and **4.4b**.

Compound	[Cl-In-CHCl ₂ ·[18]crown-6][OTf], 4.4a [OTf]	[Cl-In-CHCl ₂ ·db[18]crown-6][OTf], 4.4b [OTf]
Empirical formula	C ₁₄ H ₂₅ Cl ₃ F ₃ InO ₉ S	C ₂₄ H ₂₇ Cl ₉ F ₃ InO ₉ S · 2CHCl ₃
Formula weight	647.57	982.39
Temperature (K)	173(2)	173(2)
Wavelength (Å)	0.71073	0.71073
Crystal system	Monoclinic	Monoclinic
Space group	<i>P2₁/m</i>	<i>P2₁/n</i>
<i>Unit cell dimensions:</i>		
<i>a</i> (Å)	8.209(2)	8.8651(13)
<i>b</i> (Å)	11.010(3)	17.844(3)
<i>c</i> (Å)	13.018(3)	23.039(3)
α (°)	90	90
β (°)	101.763(3)	90.327(2)
γ (°)	90	90
Volume (Å ³)	1151.9(5)	3644.5(9)
<i>Z</i>	2	4
Density (calculated) (g cm ⁻³)	1.867	1.790
Absorption coefficient (mm ⁻¹)	1.531	1.427
<i>F</i> (000)	648	1952
θ range for data collection (°)	1.60 to 25.00	1.44 to 25.00
Limiting indices	-9 ≤ <i>h</i> ≤ 9, -13 ≤ <i>k</i> ≤ 13, -15 ≤ <i>l</i> ≤ 15	-10 ≤ <i>h</i> ≤ 10, -21 ≤ <i>k</i> ≤ 21, -27 ≤ <i>l</i> ≤ 27
Reflections collected	10622	33811
Independent reflections	2136	6424
<i>R</i> _{int}	0.0609	0.0808
Data / restraints / parameters	2136 / 24 / 151	6424 / 6 / 437
Final <i>R</i> indices [<i>I</i> > 2σ(<i>I</i>)] ^a	<i>R</i> 1 = 0.0959, <i>wR</i> 2 = 0.2303	<i>R</i> 1 = 0.0826, <i>wR</i> 2 = 0.1767
<i>R</i> indices (all data)	<i>R</i> 1 = 0.1223, <i>wR</i> 2 = 0.2499	<i>R</i> 1 = 0.1126, <i>wR</i> 2 = 0.1948
Goodness-of-fit (<i>S</i>) ^b on <i>F</i> ²	1.133	1.156
Largest diff. peak and hole (e Å ⁻³)	4.749 and -1.542	1.399 and -0.838

^a $R1(F) = \frac{\sum(|F_o| - |F_c|)}{\sum|F_o|}$ for reflections with $F_o > 4(\sigma(F_o))$. $wR2(F^2) = \frac{\{\sum w(|F_o|^2 - |F_c|^2)^2 / \sum w(|F_o|^2)^2\}^{1/2}}$, where *w* is the weight given each reflection. ^b $S = [\sum w(|F_o|^2 - |F_c|^2)^2 / (n-p)]^{1/2}$, where *n* is the number of reflections and *p* is the number of parameters used.

4.4 Supplementary Material

CCDC 280062 and 623766 contain the supplementary crystallographic data for this paper. These data can be obtained free of charge from The Cambridge Crystallographic Data Centre via www.ccdc.cam.ac.uk/data_request/cif.

References

- [1] C. L. B. Macdonald, B. D. Ellis, *The Encyclopedia of Inorganic Chemistry*, 2nd ed., John Wiley & Sons, Chichester, U.K., **2005**.
- [2] P. Jutzi, N. Burford, *Chem. Rev.* **1999**, 99, 969.
- [3] R. A. Fischer, J. Weiss, *Angew. Chem., Int. Ed.* **1999**, 38, 2831.
- [4] G. Linti, H. Schnockel, *Coord. Chem. Rev.* **2000**, 206, 285.
- [5] P. Cintas, *Synlett* **1995**, 1087.
- [6] C. J. Li, T. H. Chan, *Tetrahedron* **1999**, 55, 11149.
- [7] B. C. Ranu, *Eur. J. Org. Chem.* **2000**, 2347.
- [8] J. Podlech, T. C. Maier, *Synthesis-Stuttgart* **2003**, 633.
- [9] T. P. Loh, G. L. Chua, *Chem. Comm.* **2006**, 2739.
- [10] D. G. Tuck, *Chem. Soc. Rev.* **1993**, 22, 269.
- [11] P. L. Timms, *Acc. Chem. Res.* **1973**, 6, 118.
- [12] C. Dohmeier, D. Loos, H. Schnockel, *Angew. Chem., Int. Ed. Engl.* **1996**, 35, 129.
- [13] M. L. H. Green, P. Mountford, G. J. Smout, S. R. Speel, *Polyhedron* **1990**, 9, 2763.
- [14] M. Kehrwald, W. Kostler, A. Rodig, G. Linti, T. Blank, N. Wiberg, *Organometallics* **2001**, 20, 860.
- [15] R. J. Baker, C. Jones, *Dalton Transactions* **2005**, 1341.
- [16] C. L. B. Macdonald, A. M. Corrente, C. G. Andrews, A. Taylor, B. D. Ellis, *Chem. Comm.* **2004**, 250.
- [17] M. A. Khan, C. Peppe, D. G. Tuck, *Organometallics* **1986**, 5, 525.
- [18] T. A. Annan, D. G. Tuck, M. A. Khan, C. Peppe, *Organometallics* **1991**, 10, 2159.
- [19] J. E. dosSantos, C. Peppe, M. A. Brown, D. G. Tuck, *Organometallics* **1996**, 15, 2201.
- [20] C. Peppe, D. G. Tuck, F. M. de Andrade, J. A. Nobrega, M. A. Brown, R. A. Burrow, *J. Organomet. Chem.* **2005**, 690, 925.
- [21] C. G. Andrews, C. L. B. Macdonald, *Angew. Chem., Int. Ed.* **2005**, 44, 7453.
- [22] The anion is very disordered and sits on an inversion center but appears to be primarily $[\text{In}(\text{OTf})_4\text{Cl}]^{-2}$
- [23] CSD range for non-bridging In-C bonds: 2.044-2.453 Å, average 2.177 Å. CSD range for terminal In-Cl bonds: 2.266-2.893 Å, average 2.428 Å.
- [24] F. H. Allen, *Acta Crystallogr., Sect. B: Struct. Sci.* **2002**, 58, 380.

- [25] P. R. Ashton, P. J. Campbell, E. J. T. Chrystal, P. T. Glink, S. Menzer, D. Philp, N. Spencer, J. F. Stoddart, P. A. Tasker, D. J. Williams, *Angew. Chem., Int. Ed. Engl.* **1995**, *34*, 1865.
- [26] P. R. Ashton, E. J. T. Chrystal, P. T. Glink, S. Menzer, C. Schiavo, N. Spencer, J. F. Stoddart, P. A. Tasker, A. J. P. White, D. J. Williams, *Chem.-Eur. J.* **1996**, *2*, 709.
- [27] L. A. Kloo, M. J. Taylor, *Journal of the Chemical Society-Dalton Transactions* **1997**, 2693.
- [28] *www.webelements.com*.
- [29] A. B. Pangborn, M. A. Giardello, R. H. Grubbs, R. K. Rosen, F. J. Timmers, *Organometallics* **1996**, *15*, 1518.
- [30] SMART, Bruker AXS Inc., Madison, WI, **2001**.
- [31] SAINTPlus, Bruker AXS Inc., Madison, WI, **2001**.
- [32] SADABS, Bruker AXS Inc., Madison, WI, **2001**.
- [33] A. Altomare, M. C. Burla, M. Camalli, G. Cascarano, C. Giacovazzo, A. Guagliardi, M. A. G. G., G. Polidori, R. Spagna, CNR-IRMEC, Bari, **1997**.
- [34] G. M. Sheldrick, Universitat Gottingen, Gottingen, **1997**.
- [35] L. J. Farrugia, *J. Appl. Crystallogr.* **1999**, *32*, 837.
- [36] G. M. Sheldrick, Bruker AXS Inc., Madison, WI, **2001**.

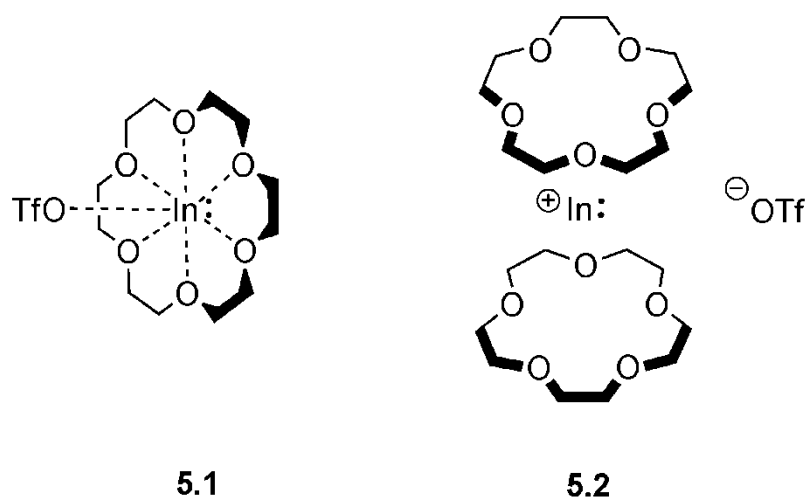
Chapter 5: Metathesis Reactions With “crowned” Indium Salts

5.1 Introduction

The chemistry of compounds containing main group elements in unusually low oxidation or valence states has been an active area of research for several decades. By definition, elements in unusually-low oxidation or valence states are more electron-rich than their more typical oxidation state relatives and the compounds in which they are found often exhibit interesting or unique structural properties, bonding descriptions and reactivity patterns.^[1] Consequently, investigations into the chemistry of compounds containing low oxidation state centers have often been hindered by the relative instability or highly-reactive nature of the compounds and it has been through the groundbreaking efforts of pioneers such as Alan H. Cowley that the field has developed and flourished.^[2-4]

As part of the continuing investigation of compounds containing main group elements in lower-than usual oxidation states, the Macdonald research group has been examining the use of cyclic-polydentate crown ethers^[5] as ligands for the stabilization of low-valent species.^[6-8] For univalent indium,^[9,10] it was discovered that the ligation of the unusually-soluble indium(I) trifluoromethanesulfonate salt (indium(I) triflate, $[\text{In}][\text{SO}_3\text{CF}_3]$, $[\text{In}][\text{OTf}]$)^[11] with (1,4,7,10,13,16)-hexaoxacyclooctadecane ([18]crown-6) provides the 1:1 crown ether complex $[\text{In}([\text{18}]\text{crown-6})][\text{OTf}]$, **5.1**.^[6] The contact ion pair **5.1** is important for several reasons: it was the first stable monomeric acid-base complex of an inorganic indium(I) salt; it has even greater solubility and tolerance to some organic solvents than the uncomplexed salt; and, it exhibits reactivity that is distinct from both the uncomplexed salt and other univalent indium compounds.^[12,13] In light of the apparently good fit of the In^{I} cation within the cavity of the [18]crown-6 ligand, it is perhaps not surprising that similar reactions with the smaller crown ether (1,4,7,10,13)-

pentaoxacyclopentadecane ([15]crown-5) yield instead the salt of 2:1 "crown sandwich" complex $[\text{In}([\text{15crown-5})_2][\text{OTf}]$, **5.2**.^[7]



Scheme 5.1: Crowned complexes of InOTf

In this chapter, I describe an aspect of the reactivity of **5.1** that to this point has yet to be investigated and exploited, namely, the use of potassium cations to remove the In^{I} center from the [18]crown-6 ligand. Given the abundance of structurally characterized $[\text{K}([\text{18crown-6})]$ complexes, and that potassium ions have the highest association constants and thus the greatest affinity for [18]crown-6 ligands of any of the alkali metals,^[5] it was reasoned that potassium ions should displace the indium(I) cation from the ligand in a manner that may be of significant synthetic utility, as it could allow for the isolation of previously unobtainable In^{I} salts. The results of the investigations into the use of potassium salts for the attempted generation of some well-known In^{I} species are described herein.

5.2. Experimental

5.2.1 General Methods

All manipulations were carried out using standard Schlenk techniques and solvents were dried using a series of Grubbs'-type columns and degassed prior to use.^[14] Starting materials were purchased from either Strem or Aldrich and used without further purification. Melting points were obtained using an Electrothermal[®] melting point apparatus on samples sealed in glass capillaries under dry nitrogen. NMR spectra were recorded at room temperature in D₃-acetonitrile solutions on a Bruker Avance 300 MHz spectrometer. Chemical shifts are reported in ppm, relative to external standards (SiMe₄ for ¹H and ¹³C NMR, CCl₃ for ¹⁹F NMR, 85 % H₃PO₄ for ³¹P NMR, In⁺(OH)₂)₆ for ¹¹⁵In NMR). FT-IR spectra were recorded as Nujol[™] mulls on KBr plates using a Bruker Vector 22 spectrometer. InOTf^[11] and [In([18]crown-6)][OTf]^[6] were prepared according to reported procedures; [K([18]crown-6)][OTf] has been observed previously but no synthetic details were provided.^[15]

Please note that each of the salts employed in this proof-of-principle demonstration was chosen in order to generate a well-known and crystallographically-characterized In^I product to allow for identification and characterization by powder X-ray diffraction and/or other physical methods.

5.2.2 General Synthetic Approach

In a typical experiment, a 10 mL solution or suspension of a potassium salt [K][A] (ca. 0.28 mmol) in acetonitrile, thf or toluene was added to a 10 mL solution of [In([18]crown-6)][OTf] (0.150 g, 0.284 mmol) in a 100 mL Schlenk flask and stirred for 2 h after which all volatile components were removed under reduced pressure. Because of the low solubility of the potassium salts in toluene, the reactions in that solvent were refluxed for several hours. In the case of the potassium halides (i.e., A = Cl, Br, I), the

solvent was removed *in vacuo* immediately following the reaction in order to minimize the amount of by-products generated from the disproportionation of resultant In^I halide.

For the purpose of spectroscopic or spectrometric comparisons, some simple potassium salts were prepared. The recrystallization of [K][OTf] from acetonitrile provides a crystalline material with a distinctly different powder X-ray diffraction pattern than the parent salt and is formulated as [K(MeCN)_x][OTf]. Similarly, as assessed by pXRD experiments, the treatment of ether [K][PF₆] or [K][OTf] with one equivalent of [18]crown-6 quantitatively provides [K([18]crown-6)][PF₆] (CSD 231012) or [K([18]crown-6)][OTf] (*vide infra*).

5.2.3 Crystallographic Investigations

The subject crystal was covered in Nujol[®], mounted on a goniometer head and rapidly placed in the dry N₂ cold-stream of the low-temperature apparatus (Kryoflex) attached to the diffractometer. The data were collected using the SMART software^[16] on a Bruker APEX CCD diffractometer using a graphite monochromator with MoK α radiation ($\lambda = 0.71073 \text{ \AA}$). A hemisphere of data was collected using a counting time of 30 seconds per frame at -100 °C. Data reduction was performed using the SAINT-Plus software^[17] and the data were corrected for absorption using SADABS.^[18] The structure was solved by direct methods using SIR97^[19] and refined by full-matrix least-squares on F^2 with anisotropic displacement parameters for the heavy atoms using SHELXL-97^[20] and the WinGX^[21] software package, the solution were assessed using tools in PLATON,^[22] and thermal ellipsoid plots were produced using SHELXTL.^[23] The crown ether in the structure of [K([18]crown-6)][OTf] was modeled as being disordered in two

positions; the thermal parameters for the corresponding atoms on the two rings were constrained to be equivalent and the occupancies of the two components thus defined refined to an approximate ratio of 61:39. CCDC 688042 contains the supplementary crystallographic data for this paper. These data can be obtained free of charge from The Cambridge Crystallographic Data Centre via www.ccdc.cam.ac.uk/data_request/cif.

Powder X-ray diffraction experiments were performed with a Bruker D8 Discover diffractometer equipped with a Hi-Star area detector using Cu K α radiation ($\lambda = 1.54186$ Å). Powder XRD pattern simulations were performed using Mercury CSD 2.2.^[24] For known compounds, these patterns were simulated on the basis of relevant data contained in the Cambridge Structural Database.^[25]

Table 5.1: Summary of X-ray crystallographic data for [K([18]crown-6)][OTf].

Compound	[K([18]crown-6)][OTf]
CSD code	688042
Empirical formula	C ₁₃ H ₂₄ F ₃ KO ₉ S
Formula weight	452.48
Temperature (K)	173(2)
Wavelength (Å)	0.71073
Crystal system	Monoclinic
Space group	<i>P</i> 2 ₁ / <i>n</i>
Unit cell dimensions:	
<i>a</i> (Å)	8.5895(19)
<i>b</i> (Å)	16.489(4)
<i>c</i> (Å)	14.088(3)
β (°)	95.720(3)
Volume (Å ³)	1985.3(8)
<i>Z</i>	4
Density (calculated) (g cm ⁻³)	1.514
Absorption coefficient (mm ⁻¹)	0.442
<i>F</i> (000)	944
θ range for data collection (°)	1.91 to 24.98
Limiting indices	-10 ≤ <i>h</i> ≤ 10, -19 ≤ <i>k</i> ≤ 19, -16 ≤ <i>l</i> ≤ 16
Reflections collected	18651
Independent reflections	3492
Observed reflections	2139
<i>R</i> _{int}	0.0965
Data / restraints / parameters	3492 / 55 / 347
Goodness-of-fit on <i>F</i> ²	1.034
Final <i>R</i> indices [<i>I</i> > 2σ(<i>I</i>)] ^a	<i>R</i> 1: 0.0678, <i>wR</i> 2: 0.1470
<i>R</i> indices (all data)	<i>R</i> 1: 0.1210, <i>wR</i> 2: 0.1745
Largest difference map peak and hole (e Å ⁻³)	0.615 and -0.366

^a $R1(F) = \frac{\sum(|F_o| - |F_c|)/\sum|F_o|}{\sum|F_o|}$ for reflections with $F_o > 4(\sigma(F_o))$. $wR2(F^2) = \{\sum w(|F_o|^2 - |F_c|^2)^2 / \sum w(|F_o|^2)^2\}^{1/2}$, where w is the weight given each reflection. ^b $S = [\sum w(|F_o|^2 - |F_c|^2)^2] / (n-p)^{1/2}$, where n is the number of reflections and p is the number of parameters used.

5.3. Results and Discussion

As one may anticipate on the basis of the strong preference of [18]crown-6 for potassium cations,^[5] the treatment of **5.1** with potassium salts results in the instantaneous liberation of the less-favorable $[\text{In}^{\text{I}}]^+$ cation from the crown ether. The affinity of [18]crown-6 for potassium over indium is perhaps most obviously demonstrated where the two cations are in the presence of identical anions. Thus, the reaction of **5.1** with $[\text{K}][\text{OTf}]$ seemed a logical starting point for this investigation. Analysis of the pXRD pattern following the addition of a substoichiometric amount of $[\text{K}][\text{OTf}]$ to **5.1** in acetonitrile (Figure 5.1(a)) shows the drastic reduction of $[\text{K}][\text{OTf}]$ and the formation of peaks corresponding to $[\text{K}([\text{18}]\text{crown-6})][\text{OTf}]$ (*vide infra*). It should be noted that competition exists between formation of $[\text{K}(\text{MeCN})_x][\text{OTf}]$ and $[\text{K}([\text{18}]\text{crown-6})][\text{OTf}]$, and appears to be dominated by acetonitrile adduct formation presumably due to the vast stoichiometric excess of the solvent. Addition of a greater-than-stoichiometric amount of $[\text{K}][\text{OTf}]$ provides a solid in which all of the pXRD peaks attributable to **5.1** are absent and the peaks present are consistent with those of $[\text{K}([\text{18}]\text{crown-6})][\text{OTf}]$ and the acetonitrile solvate of $[\text{K}][\text{OTf}]$. As illustrated in Figure 5.1(b), the pXRD pattern of the product obtained from a stoichiometric mixture of $[\text{K}][\text{OTf}]$ and **5.1** that was refluxed in toluene contains $[\text{K}([\text{18}]\text{crown-6})][\text{OTf}]$. Regardless of the solvent employed for the exchange reaction, the ^{115}In NMR spectrum in of the isolated product dissolved in acetonitrile features a signal at around -1075 ppm, which is characteristic of the In^{I} cation.^[26] These result illustrate that the addition of the potassium salt does indeed offer a viable method for the removal of the In^{I} center from the crown ether, and, consequently,

suggest that such displacement reactions may provide a viable route for the preparation of "uncrowned" indium(I) species from the crowned starting reagent **5.1**.

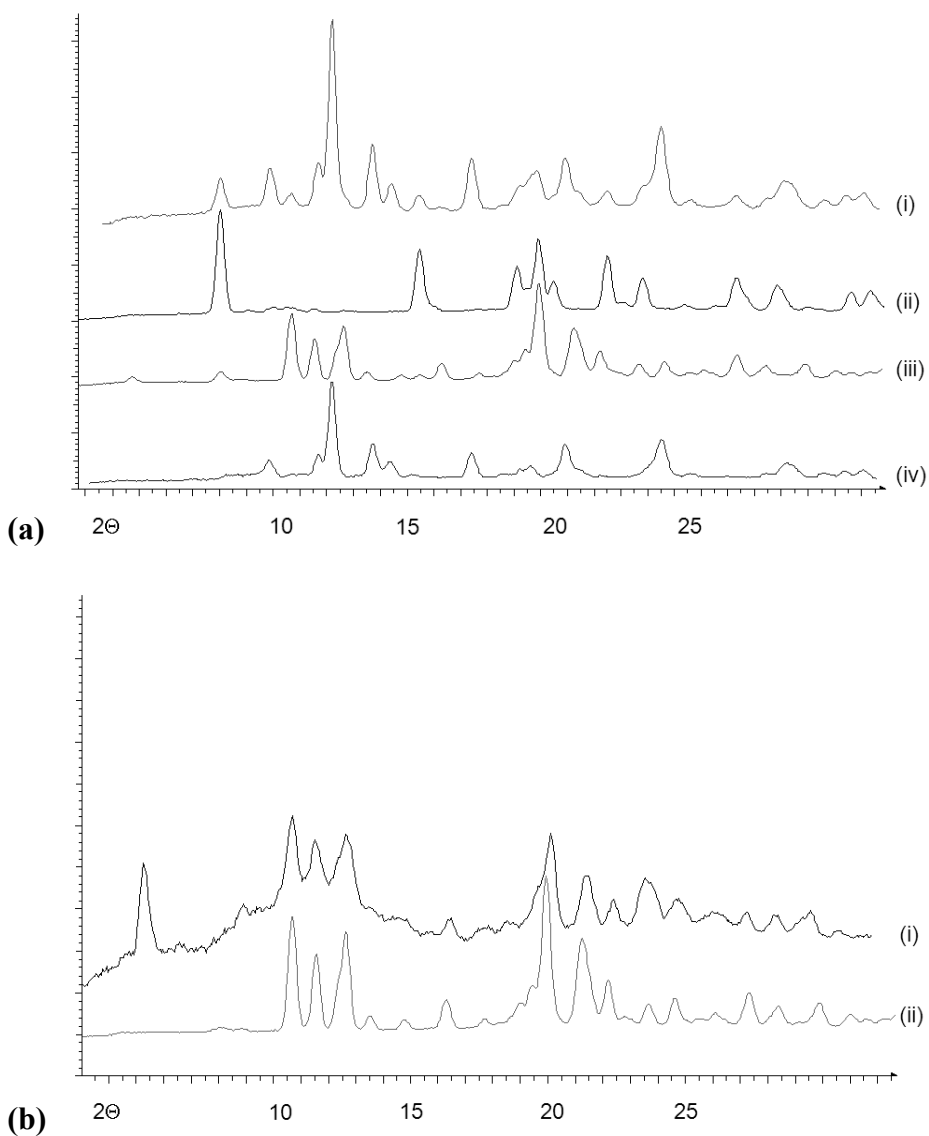


Figure 5.1: pXRD patterns of: (a) (i) excess $[\text{In}([\text{18crown-6})][\text{OTf}] + [\text{K}][\text{OTf}]$ from MeCN, (ii) $[\text{K}][\text{OTf}] + \text{MeCN}$, (iii) $[\text{K}([\text{18crown-6})][\text{OTf}]$, (iv) $[\text{In}([\text{18crown-6})][\text{OTf}]$; (b) (i) $[\text{In}([\text{18crown-6})][\text{OTf}] + [\text{K}][\text{OTf}]$ from toluene (Note the presence of a large d-spacing impurity or layer effect in the solid), (ii) $[\text{K}([\text{18crown-6})][\text{OTf}]$.

Given the promising nature of the cation exchange that was observed with identical anions, the next logical step was to probe how such reactions might occur for potassium salts of anions other than triflate. In the case of the reaction of **5.1** with $[\text{K}][\text{PF}_6]$ in toluene, it was fortunate that crystals were obtained of one of the products that were suitable for analysis by single crystal X-ray diffraction; the salt was identified as $[\text{K}([\text{18}]\text{crown-6})][\text{OTf}]$, the structure of which described below. No evidence of disproportionation was observed during or after the reaction and the signal at -1075 ppm in the ^{115}In NMR spectrum is, again, consistent with the removal of the indium cation from the crown ether. The In^{I} -containing product is likely a mixture of the salts $[\text{In}][\text{OTf}]$ and $[\text{In}][\text{PF}_6]^{[27]}$ as identified by multinuclear NMR of MeCN solutions of the reaction mixture: ^{19}F , δ -72.3 (d, $^1J_{\text{P-F}}$ 706, $[\text{PF}_6]$, 3F) and -78.6 (s, $[\text{OTf}]$, 2F); ^{31}P , δ -143 (sept., $^1J_{\text{P-F}}$ 707). The pXRD pattern of the bulk solid obtained contain signals that are consistent with the presence of $[\text{K}([\text{18}]\text{crown-6})][\text{OTf}]$ and other crystalline materials; unfortunately, the pXRD peaks that are characteristic for $[\text{In}][\text{PF}_6]^{[27]}$ at ca. $2\theta = 19.0$, 22.0 , and 31.3° are masked by peaks for $[\text{K}([\text{18}]\text{crown-6})][\text{OTf}]$. The relative insolubility of $[\text{K}][\text{PF}_6]$ in toluene appears to hinder the progress of the reaction.

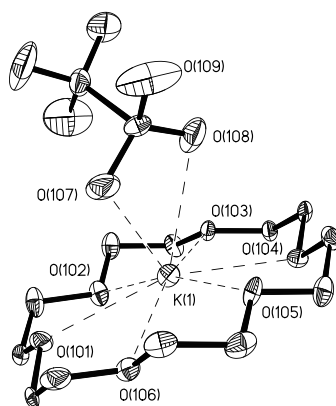


Figure 5.2: Thermal ellipsoid plot (30% probability surface) of the molecular structure of [K([18]crown-6)][OTf]. Important bond distances (Å): K(1)-O(101) 2.948, K(1)-O(102) 2.887(17), K(1)-O(103) 2.768(14), K(1)-O(104) 2.751(15), K(1)-O(105) 2.700(13), K(1)-O(105) 2.700(13), K(1)-O(106) 2.883(13), K(1)-O(107) 2.877(5), K(1)-O(108) 2.984(5).

Regardless of the predictably mixed nature of the salts in solution, as indicated above, it was possible to obtain crystals of one of the possible solids. The potassium salt [K([18]crown-6)][OTf] crystallizes in the monoclinic space group $P2_1/n$ and the molecular structure is depicted in Figure 5.2. Even at -100°C , the crown ether ligand exhibits significant disorder and was modeled in two different positions, only one of which is depicted in the figure. In contrast to the structure of the indium analogue, the potassium salt has two K-O contacts with the triflate anion with bond distances of 2.877(5) and 2.985(5) Å. Depictions of the crystalline packing of the salts [K([18]crown-6)][OTf] and **5.1** (Figure 5.3) highlight the differences between the salts and presents features that may be attributable to the presence of a stereochemically active “lone pair” of electrons on the In^{I} center versus the empty valence shell of potassium. In particular, Figure 5.3(i) shows that there are close contacts between the fluorine atoms of the triflate

anions and adjacent potassium centers (i.e., there are interactions with anions on both available faces of the crowned metal cation). In contrast, the indium salt exhibits no close interactions between the fluorine atoms of the triflate anion and each indium cation features only a single close contact with one oxygen atom; the face opposite the triflate anion has no close contacts with any negatively-charged fragment and is thus consistent with the space being occupied by the two non-bonding valence electrons remaining on the indium(I) center.

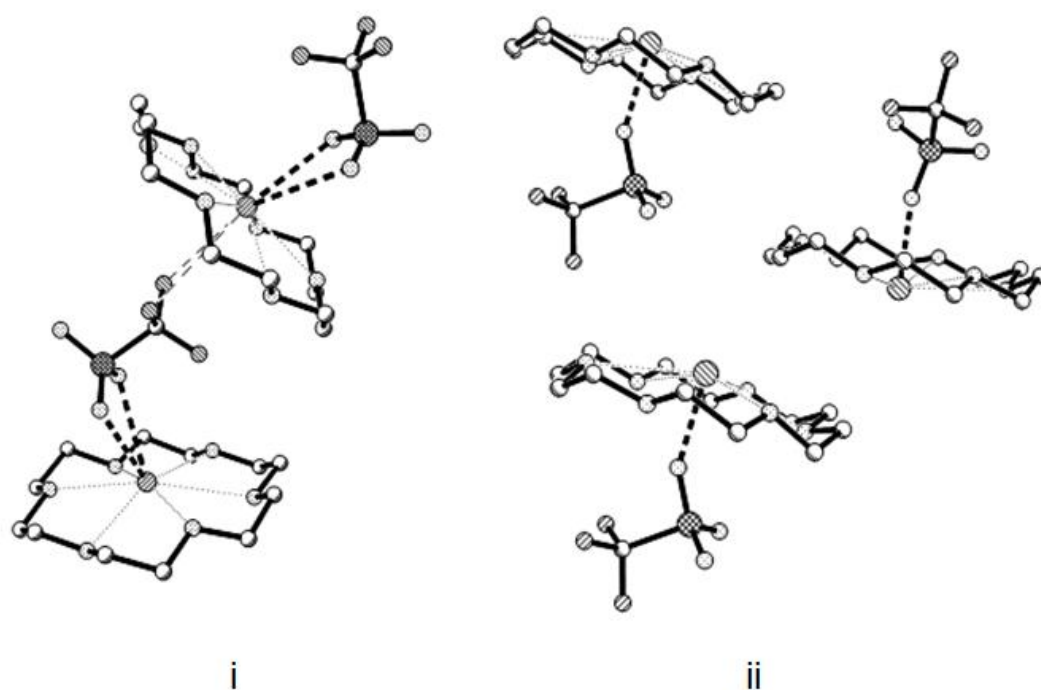


Figure 5.3: Crystal packing diagrams of $[K([18]\text{crown-6})][\text{OTf}]$ (i) and $[\text{In}([18]\text{crown-6})][\text{OTf}]$ (ii); (ii) exhibits features that are consistent with a stereochemically-active "lone pair" of electrons on the InI ion.

When the reaction of **5.1** with $[K][PF_6]$ is performed in acetonitrile, the pXRD pattern of the solid obtained from the reaction (Figure 5.4) suggests that a very different distribution of crystalline products is favored. Instead of $[K([18]crown-6)][OTf]$, the most abundant crystalline product appears to be $[K([18]crown-6)][PF_6]$. Overall for this exchange reaction, it appears as if the subtle differences in either the solvation energies, solubilities or lattice energies between the possible triflate and hexafluorophosphate salts allow the solvent to significantly alter the product distribution and make it highly probable that a mixture is obtained.

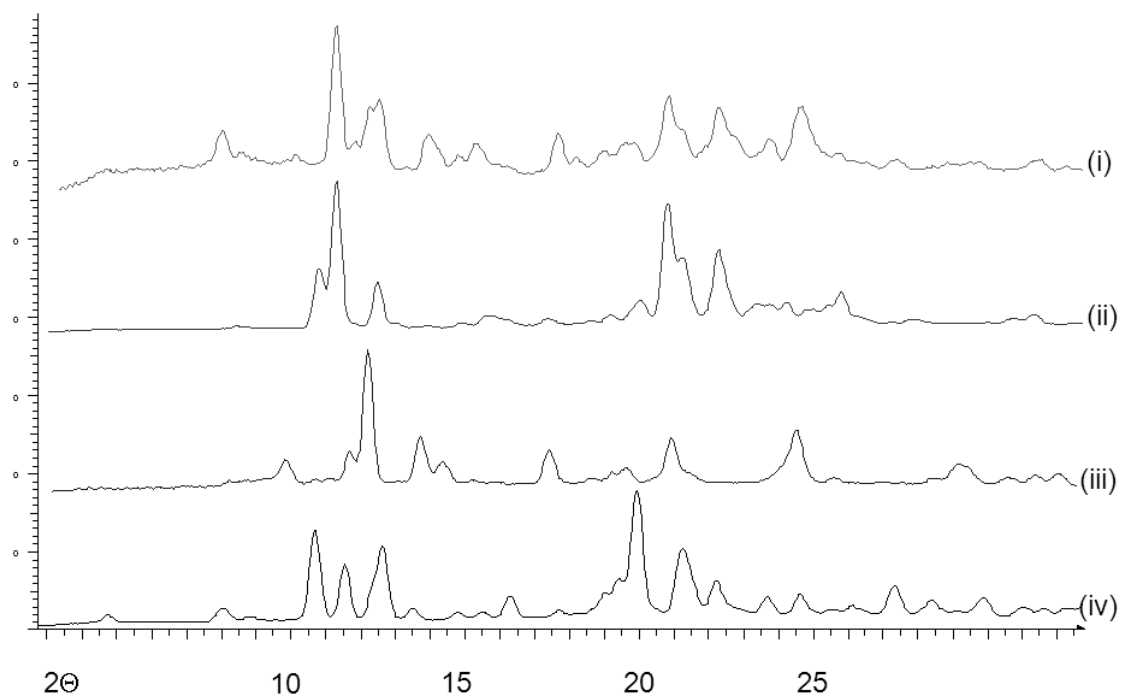


Figure 5.4: pXRD patterns of: (i) $[\text{In}([\text{18}]\text{crown-6})][\text{OTf}] + [\text{K}][\text{PF}_6]$ from MeCN, (ii) $[\text{K}][\text{PF}_6] + [\text{18}]\text{crown-6}$ from MeCN, (iii) $[\text{In}([\text{18}]\text{crown-6})][\text{OTf}]$, (iv) $[\text{K}([\text{18}]\text{crown-6})][\text{OTf}]$.

The indium(I) halides are commercially available and are likely the most commonly-employed starting materials for the preparation low oxidation state compounds of indium; however, these salts have very limited solubility in many organic solvents.^[9,10] Furthermore, the halides tend to disproportionate in donor solvents at ambient temperature and often produce mixed valent species with compositions that differ from the anticipated 1:1 indium:halogen ratio.^[28,29] Given the synthetic importance of these halides, it was desirable to ascertain if the potassium displacement protocol is suitable for the *in situ* generation of indium(I) halides from the readily prepared and

handled compound **5.1**. To this end, it was observed that the dissolution of an equimolar mixture of **5.1** and KCl in acetonitrile immediately yields a yellow solid in the reaction mixture. If it is left in acetonitrile solution, this yellow solid decomposes rapidly with the concomitant formation of indium metal and thus exhibits the reactivity anticipated for $\text{In}^{\text{I}}\text{Cl}$. In spite of the foregoing, it is worth noting that the yellow product can be isolated if the solvent is removed rapidly after the start of the reaction. While the latter protocol does not allow the reaction to go to completion, analysis of the pXRD pattern (Figure 5.5) indicates that the reaction mixture at that point, Figure 5.5(i), consists of a mixture of the starting reagent **5.1**, $[\text{K}([\text{18}]\text{crown-6})][\text{OTf}]$ and at least one other crystalline material. Attempts to collect powder XRD patterns of commercially available $\text{In}^{\text{I}}\text{Cl}$ were hindered by the strong absorption of the Cu K_α radiation by the material and a comparison to the yellow solid of the reaction mixture could not be made unambiguously however the physical properties (color) and chemical behavior (disproportionation in MeCN) of the yellow product strongly suggests that it is $\text{In}^{\text{I}}\text{Cl}$. Unfortunately, the insolubility of KCl in toluene precludes the convenient isolation of pure $\text{In}^{\text{I}}\text{Cl}$ under conditions in which it does not disproportionate.

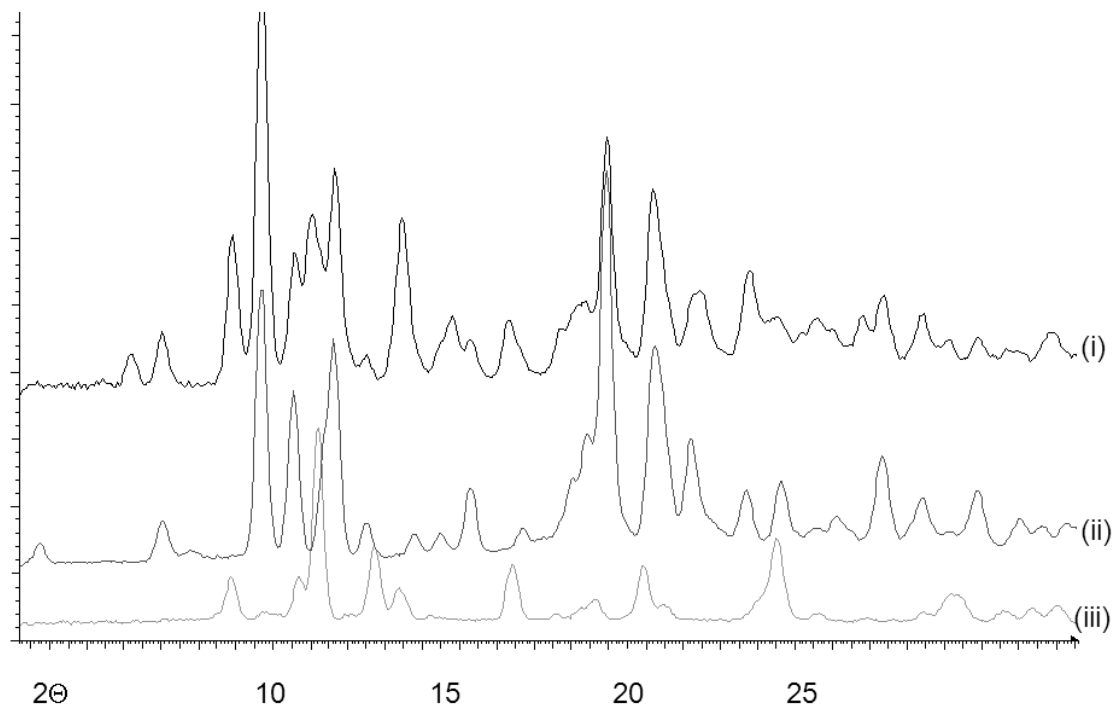


Figure 5.5: pXRD patterns of: (i) $[\text{In}([\text{18}]\text{crown-6})][\text{OTf}] + \text{KCl}$ from MeCN, (ii) $[\text{K}([\text{18}]\text{crown-6})][\text{OTf}]$, (iii) $[\text{In}([\text{18}]\text{crown-6})][\text{OTf}]$.

Along the same lines, the treatment of **5.1** with KBr or KI under similar conditions to those described above generates orange and purple solids, respectively. The orange solid disproportionates rapidly in acetonitrile solution and thus exhibits the reactivity consistent with $\text{In}^{\text{I}}\text{Br}$ while the purple solid appears to be more long lived. It should be noted however that the pXRD pattern of these materials did not provide conclusive evidence for the formation of any identifiable species and further investigations are required. Overall, it appears as if the treatment of **5.1** with potassium halides does result in the formation of the corresponding indium(+1) halide; however, there is an aspect of the chemistry inherent in the system that diminishes the potential utility of the approach: the starting potassium halides have minimal solubility in solvents that do not result in the

rapid disproportionation of the corresponding indium(+1) halides. It is possible that this difficulty may perhaps be surmountable through the use of solubilizing agents such tetramethylethylenediamine for the potassium salt to which some low valent indium species have demonstrated tolerance at low temperature;^[28,29] the investigations to prove this postulate are currently underway.

Given that InOTf has been employed as a reagent for the metathetical preparation of organoindium(+1) compounds (albeit with some disproportionation observed)^[30] the next step was to determine if the crowned salt **5.1** could be used in a similar manner and to assess whether the presence of the crown could alter the propensity for disproportionation during the process. In particular, it was desired to ascertain if the reaction of **5.1** with $K(C_5Me_5)$, KCp^* , is suitable for the preparation of the well-known organoindium(+1) compound Cp^*In .^[31,32] The treatment of **5.1** with KCp^* in toluene results in the formation of a brown solution and immediate precipitate. Removal of the volatile components from the reaction mixture yields a mixture of colorless and brown solids that contains $[K([18]crown-6)][OTf]$ as identified by pXRD (Figure 5.6). More interestingly, the intense signals observed at ca. $2\theta = 8.5, 12.0^\circ$ are indeed at the angles predicted for the most intense peaks for crystalline Cp^*In ^[31], however the insolubility of the brown solid in hydrocarbon solvent is not consistent with behavior of pentamethylcyclopentadienylindium. Furthermore, ^{115}In NMR experiments on the portion of the solid that is soluble in acetonitrile indicate the presence of free In^I cations in the mixture; mixed valent salts of $[In^I]^+$ with OTf and Cp have been observed previously and are a likely possibility given the observed spectroscopic and physical properties.^[12] Thus, while metallic indium was not observed, the reaction did not proceed

smoothly and the overall nature of the final indium-containing products remains ambiguous.

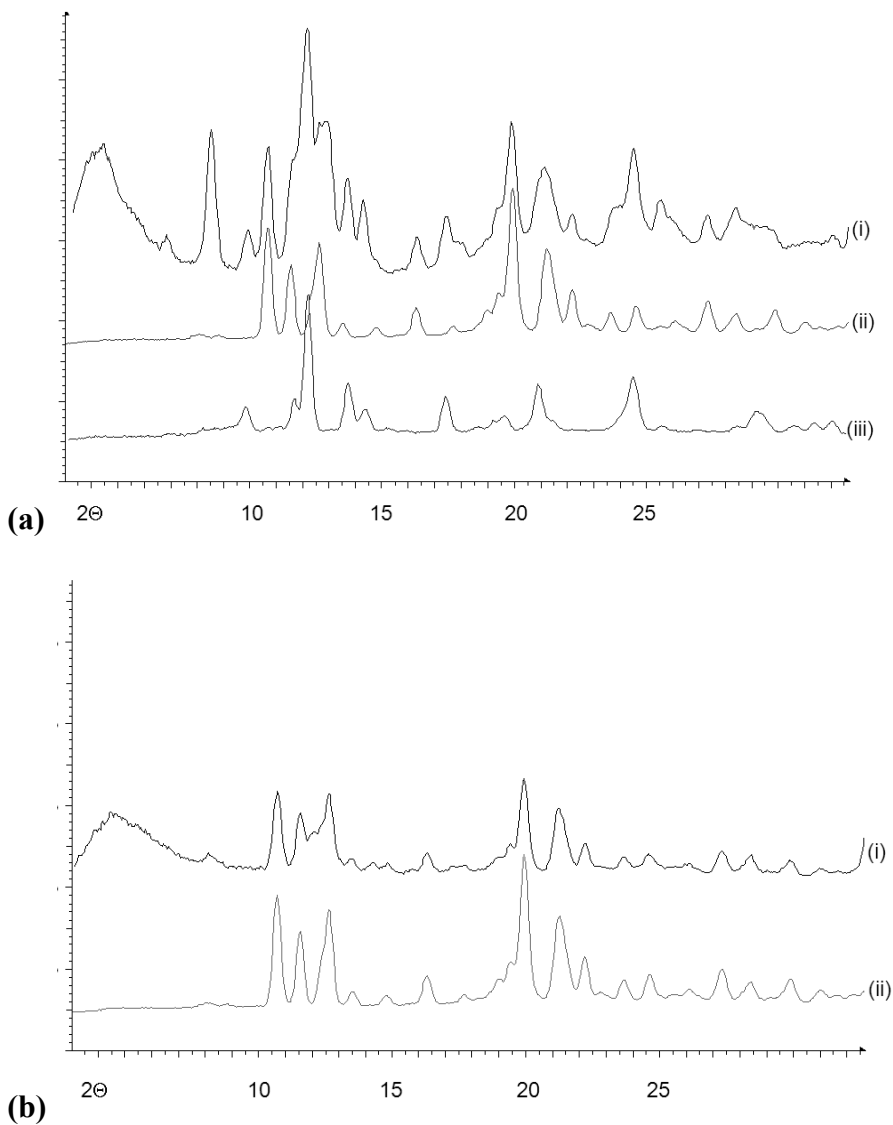
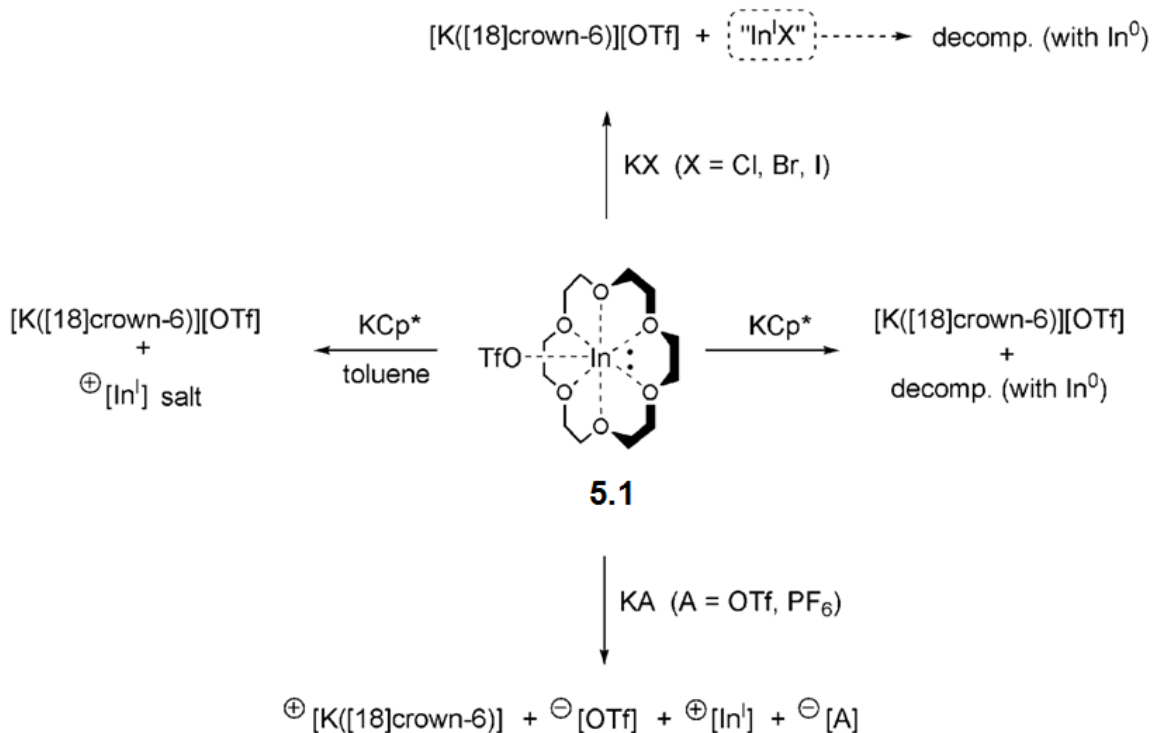


Figure 5.6: pXRD patterns of: (a) (i) $[\text{In}([\text{18}]\text{crown-6})][\text{OTf}] + \text{KCp}^*$ from toluene (Note the presence of a large d-spacing impurity or layer effect in the solid), (ii) $[\text{K}([\text{18}]\text{crown-6})][\text{OTf}]$, (iii) $[\text{In}([\text{18}]\text{crown-6})][\text{OTf}]$; (b) (i) $[\text{In}([\text{18}]\text{crown-6})][\text{OTf}] + \text{KCp}^*$ from thf (Note the presence of a large d-spacing impurity or layer effect in the solid), (ii) $[\text{K}([\text{18}]\text{crown-6})][\text{OTf}]$.

In contrast to the reaction in toluene, in thf, the treatment of **5.1** with KCp^* results in the immediate deposition of metallic indium. Removal of volatiles from the reaction mixture provides a colorless solid in addition to the metal. As illustrated in Figure 5.6, the pXRD pattern of the colorless solid confirms that it is $[\text{K}([\text{18}\text{crown-6})][\text{OTf}]$. Given that **5.1** is stable in thf whereas "uncrowned" InOTf disproportionates rapidly in the solvent, the observation suggests that the potassium ion does indeed displace the In^{I} cation from the crown ether however the indium(+1) cation does not appear to combine rapidly enough with the Cp^* anion to avoid decomposition in this case.



Scheme 5.2: Summary of potassium salt reactions with **5.1**.

Overall, while it is clear that K^+ is able to liberate the In^I cation from the [18]crown-6 cyclic poly-ether in every instance, as illustrated in Scheme 5.2, the method does not necessarily allow for the control which of the anions will crystallize with each of the cations to form a given salt. Thus, while the method would, in theory, appear to be best suited for the generation of *neutral* In^I compounds such as Cp^*In that may be readily removed from the $[K([18]crown-6)][OTf]$ by-product, the presence of the crown ether did not prevent disproportionation from occurring under the condition that were examined. In the cases where both reagents and products are salts, the formation of different combinations of cations and anions is probable. In instances where ion solvation or lattice enthalpy considerations strongly favor the formation of a particular salt, one may be able to separate the salts but, in other instances, mixtures of salts are a distinct possibility and a potential complication.

5.4. Conclusions

The stable, soluble, monomeric salt **5.1** has been shown to readily give up its crown ether to potassium in reactions with a variety of salts. While the nature of the indium containing species is not always apparent by powder XRD, the formation of salts of $[K([18]crown-6)^+]$ and the absence of disproportionation and the results of ^{115}In NMR experiments confirm that the In^I center is maintained during the exchange reaction (so long as the resultant product is not subject to disproportionation under the conditions employed), and suggests that cation exchange may be a viable synthetic approach for In^I species. Further investigations into the use of this protocol for the preparation of new In^I compounds are currently underway.

References

- [1] C. L. B. Macdonald, B. D. Ellis, *The Encyclopedia of Inorganic Chemistry*, 2nd ed., John Wiley & Sons, Chichester, U.K., **2005**.
- [2] R. A. Jones, *J. Organomet. Chem.* **1999**, 582, 1.
- [3] A. H. Cowley, *J. Organomet. Chem.* **2004**, 689, 3866.
- [4] A. H. Cowley, *Modern Aspects of Main Group Chemistry* **2006**, 917, 2.
- [5] G. Gokel, *Crown Ethers & Cryptands*, The Royal Society of Chemistry, Cambridge, **1991**.
- [6] C. G. Andrews, C. L. B. Macdonald, *Angew. Chem., Int. Ed.* **2005**, 44, 7453.
- [7] B. F. T. Cooper, C. L. B. Macdonald, *J. Organomet. Chem.* **2008**, 693, 1707.
- [8] P. A. Rugar, R. Bandyopadhyay, B. F. T. Cooper, M. R. Stinchcombe, P. J. Ragona, C. L. B. Macdonald, K. M. Baines, *Angew. Chem. Int. Ed.* **2009**, 48, 5155.
- [9] D. G. Tuck, *Chem. Soc. Rev.* **1993**, 22, 269.
- [10] J. A. J. Pardoe, A. J. Downs, *Chem. Rev.* **2007**, 107, 2.
- [11] C. L. B. Macdonald, A. M. Corrente, C. G. Andrews, A. Taylor, B. D. Ellis, *Chem. Commun.* **2004**, 250.
- [12] C. G. Andrews, C. L. B. Macdonald, *J. Organomet. Chem.* **2005**, 690, 5090.
- [13] B. F. T. Cooper, C. G. Andrews, C. L. B. Macdonald, *J. Organomet. Chem.* **2007**, 692, 2843.
- [14] A. B. Pangborn, M. A. Giardello, R. H. Grubbs, R. K. Rosen, F. J. Timmers, *Organometallics* **1996**, 15, 1518.
- [15] W. Petz, F. Weller, *Z. Naturforsch., B: Chem. Sci.* **1996**, 51, 715.
- [16] SMART, Bruker AXS Inc., Madison, WI, **2001**.
- [17] SAINTPlus, Bruker AXS Inc., Madison, WI, **2001**.
- [18] SADABS, Bruker AXS Inc., Madison, WI, **2001**.
- [19] WINGX, A. Altomare, M. C. Burla, M. Camalli, G. Cascarano, C. Giacovazzo, A. Guagliardi, M. A. G. G., G. Polidori, R. Spagna, CNR-IRMEC, Bari, **1997**.
- [20] G. M. Sheldrick, *Acta Crystallogr., Sect. A: Found. Crystallogr.* **2008**, 64, 112.
- [21] L. J. Farrugia, *J. Appl. Crystallogr.* **1999**, 32, 837.
- [22] A. L. Spek, *J. Appl. Crystallogr.* **2003**, 36, 7.
- [23] SHELXLTL, G. M. Sheldrick, Bruker AXS Inc., Madison, WI, **2001**.
- [24] C. F. Macrae, I. J. Bruno, J. A. Chisholm, P. R. Edgington, P. McCabe, E. Pidcock, L. Rodriguez-Monge, R. Taylor, J. van de Streek, P. A. Wood, *J. Appl. Crystallogr.* **2008**, 41, 466.
- [25] F. H. Allen, *Acta Crystallogr., Sect. B: Struct. Sci.* **2002**, B58, 380.
- [26] While a complete description of the In-115 NMR investigations of "free" and "crowned" indium(I) species will be reported elsewhere, it should be noted that [In([18]crown-6)] generally resonates at ca. -1080 ppm with relatively broad signals in MeCN whereas the "uncrowned" In(I) cation produces a sharper signal at ca. -1070 ppm; the actual width of any given signal appears to be highly concentration dependent which renders numerical comparisons of peak widths unreliable in situations where the actual concentration is undetermined.
- [27] Z. Mazej, *Eur. J. Inorg. Chem.* **2005**, 3983.
- [28] S. P. Green, C. Jones, A. Stasch, *Angew. Chem., Int. Ed.* **2007**, 46, 8618.
- [29] S. P. Green, C. Jones, A. Stasch, *Chem. Commun.* **2008**, 6285.

- [30] M. Buhler, G. Linti, *Z. Anorg. Allg. Chem.* **2006**, *632*, 2453.
- [31] O. T. Beachley, Jr., M. R. Churchill, J. C. Fettinger, J. C. Pazik, L. Victoriano, *J. Am. Chem. Soc.* **1986**, *108*, 4666.
- [32] O. T. Beachley, R. Blom, M. R. Churchill, K. Faegri, J. C. Fettinger, J. C. Pazik, L. Victoriano, *Organometallics* **1989**, *8*, 346.

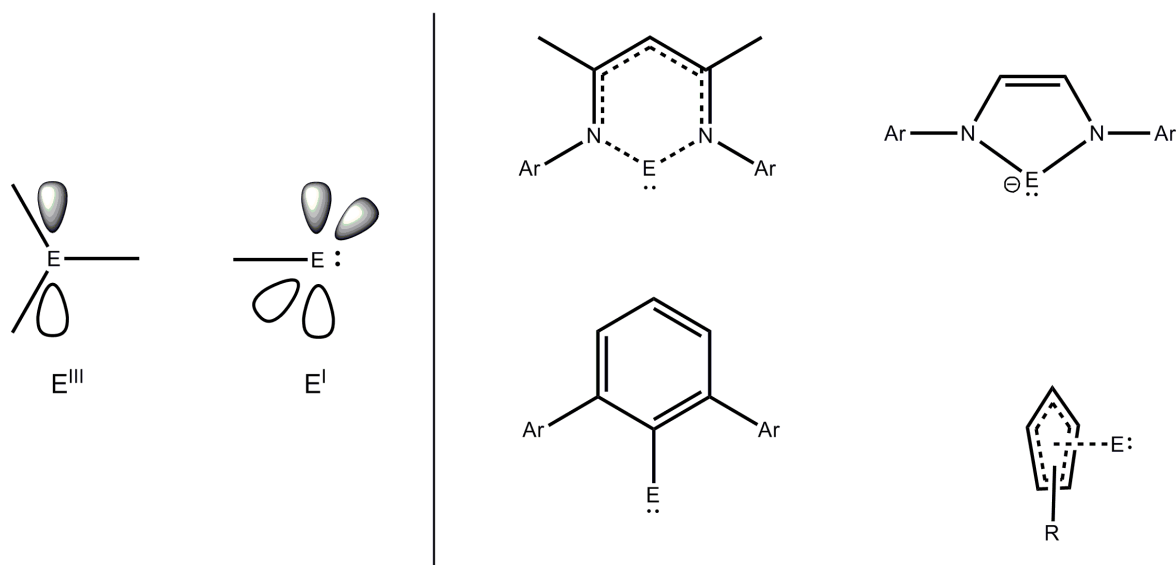
Chapter 6: Experimental and computational insights on the valence isomers of

EE'X₄ species

6.1 Introduction

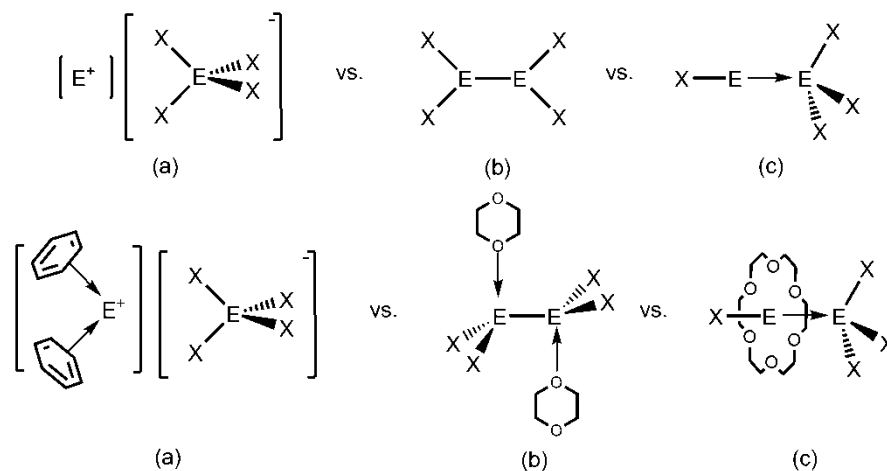
The donor chemistry of compounds containing group 13 elements in the +1 oxidation state (perhaps more appropriately termed univalent elements, E^I, where E = B, Al, Ga, In)^{[1][2]} is an area of inorganic chemistry that has been the subject of a tremendous number of investigations over the last two decades.^[3, 4] While the investigation of such compounds may appear to some as a perhaps esoteric, the chemistry engendered by the electron rich nature of these compounds can allow for unprecedented and useful modes of reactivity. As illustrated in Scheme 6.1, compounds containing E^I centers feature a "lone pair" of electrons on the group 13 element and, therefore, can make elements that are typically associated with Lewis acids behave as Lewis bases instead. Most importantly, the availability of such donors allows them to be used to easily prepare various Lewis acid base complexes, coordination complexes and organometallic (or inorganometallic) compounds. Indeed, numerous research groups have succeeded in preparing donor-acceptor complexes with acceptors that include a variety of main group Lewis acids and transition metal fragments.^[5-15] Certain examples of such molecules have proven to be excellent precursors for the formation of group 13-containing intermetallics and other materials.^[7] Perhaps the most thoroughly investigated family of such group 13 donors are those where the stabilizing ligand is a cyclopentadienyl derivative. Numerous examples of group-13 pentamethylcyclopentadienide complexes, Cp*-E (E = Al, Ga, In), acting as donors to both transition metals and main group Lewis acids have been reported.^[14, 16-19] Similarly, tris(pyrazolyl)borate ligands and a similar tris(2-mercapto-1-tert-

butylimidazolyl) borate have also been shown to ligate group 13 metal centers and obtain complexes with reactive lone pairs of electrons suitable for donation to appropriate acceptors.^[20-22] Another family of donors that has yielded many donor-acceptor complexes are the group 13 analogues of *N*-heterocyclic carbenes. For example, the anionic compounds featuring E^I centers stabilized by α -dimine ligands and the related neutral complexes featuring β -diketiminato ("nacnac") ligands provide group 13 reagents that can be used as donors.^[17, 23, 24] It is perhaps worth noting that such group 13 donors can behave as pure σ -donors in complexes with main group Lewis acids and, depending on the nature of the ligand attached to group 13 element, transition metal complexes of such group 13 donors may exhibit metal to ligand π -backbonding in addition to σ -donation.^[25-28]



Scheme 6.1: Simplified illustration of the different electronic structure for E^{III} vs. E^I valence states and selected examples of univalent group-13 species that have been used as donors ($E = B, Al, Ga, Tl$)

Of somewhat more fundamental interest have been the homonuclear complexes in which both the donor and acceptor atoms are elements in group 13 because these compounds may be considered as valence isomers of dinuclear compounds containing the elements in the +2 oxidation state, $E(+2)$. The mixed-valent nature of " In_2Cl_4 " and other related group 13 halides in the solid state is well documented.^[29-31] The selection of appropriate ligands or solvents allows one the ability to obtain either a mixed-valent indium(+1)/indium(+3) "ionic" isomer or a formally homovalent indium(+2) "covalent" isomer, as illustrated in parts (a) and (b) of Scheme 6.2. For example, the presence of π -donating ligands such as arenes affords the ionic isomer, while σ -donating ligands favor the covalent isomer featuring a metal-metal bond.



Scheme 6.2: Valence isomers of E_2X_4 ($X = \text{Cl}, \text{Br}$ or I) including idealized parent valence isomers (top row) and selected examples observed experimentally (bottom row) for: (a) the ionic isomer; (b) the "covalent" isomer; (c) the donor-acceptor isomer.

In 2005, it was communicated that the treatment of " In_2Cl_4 " with the appropriately sized dibenzo[18]crown-6 cyclic poly-ether ligand yields the species, $\text{Cl}(\text{dibenzo}[18]\text{crown-6})\text{In-InCl}_3$ (**1**), which features an indium-indium bond.^[32] In light of the structures illustrated in Scheme 6.2, it is worth emphasizing that compound **6.1** represented a new and different valence isomeric form that may be adopted by " In_2Cl_4 "; in fact, the isomer depicted in Scheme 6.2(c) is probably the first new isomeric form identified for " ECl_2 " in at least five decades. Given the stereochemically active lone pair that may exist for any In^{I} compound, and that is postulated to be present in the stable salt $[\text{In}([18]\text{crown-6})][\text{O}_3\text{SCF}_3]$ ($[\text{In}([18]\text{crown-6})][\text{OTf}]$, **6.2**),^[32, 33] one description of indium-indium bond observed in **6.1** is that of a donor-acceptor complex.^[34] Such a description is particularly relevant in light of the large number of donor-acceptor complexes that have been prepared using monovalent group 13 donors and trivalent group 13 acceptors described above. In most of these cases, the direct reaction of stable

univalent group 13 reagents such as those supported by Cp* ligands, β -diketiminato ligands, or bulky terphenyl ligands with group 13 Lewis acids provides the anticipated donor-acceptor adducts in quantitative yield.^[14] One final observation about the use of crown-ethers as stabilizing ligands for In^I fragments must be emphasized: whereas the complex of InOTf with [18]crown-6 ligands is stable in the solid-state and in many solvents, all attempts to stabilize indium(+1) halides using crown ethers have resulted in the rapid disproportionation of the compound with the concomitant deposition of indium metal.

In light of the related donor-acceptor complexes, and of the ability to obtain different isomers of E₂X₄ species depending on ligand selection (and especially the previous observations with crown ether ligands), in the present work a detailed report of the results of the investigations into the reactions of **6.2** with indium-containing Lewis acids is presented, along with the discovery of alternative syntheses of In₂X₄ donor-acceptor complexes and enlightening findings regarding the related InEX₄ (E = Al, Ga, In) species and their "crowned" analogues.

6.2 Results and Discussion

6.2.1. [In([18]crown-6)][X] as an In^I-centered donor

The donor properties of "crowned" indium(I) species were initially investigated by the reaction of **6.2** with a series of indium-containing Lewis acids, InCl₃, InBr₃ and InI₃. Thus, the treatment of **6.2** with InX₃ (X = Cl, Br, I) in toluene yields the donor-acceptor complexes X([18]crown-6)In-InX₃ (X = Cl **6.3**, Br **6.4**, I **6.5**) consisting of a "crowned" indium(+1) halide donor fragment and an indium(+3) halide acceptor as the only

identifiable crystalline materials with both indium centers being trivalent. Depictions of the molecular structures exhibited by several examples of the complexes are presented in Figure 6.1 and; important metrical parameters are collected in Table 6.1. It should be emphasized that these crystal structures confirm that the donor-acceptor valence isomeric form illustrated in Scheme 6.2(c) that was initially observed for "InCl₂" is not anomalous and is indeed viable for the heavier dihalides InBr₂ and InI₂. The In-In bond distances are found to range from 2.6726(7) and 2.725(2) Å and are on the shorter end of the values reported (2.654-3.197 Å) in the Cambridge Structural Database.^[34-40] It is worth noting that the In-In distance increases as the halogen atom becomes heavier; such an observation is consistent with the decreasing Lewis acidity of the InX₃ as X is changed from Cl to Br to I. Finally, it is observed that the complexes features a slightly distorted to almost perfectly linear arrangements of the X-In-In moieties with angles ranging from 170.09(4) ° to 179.63(10) °.

In the case of compound **6.3**, it proved possible to crystallize the complex in forms that may be considered as solvates or co-crystals of the donor-acceptor complex. For example, **6.3**·CH₂Cl₂ was readily obtained from the slow concentration of dichloromethane solution of the material; it is worth highlighting that the stability of **6.3** in the chlorinated solvent contrasts sharply with the insertion chemistry observed for the starting material of **6.2**.^[41] The molecular structure of **6.3**·CH₂Cl₂ depicted in Figure 6.1 has one atypical feature when compared to the non-solvated analogues: the In(+1) centre is asymmetrically positioned within the crown ether. Specifically, the indium atom is displaced by around 0.283(3) Å from the centroid of the six crown ether oxygen atoms and the In-O distances range from 2.494(3) to 3.047(3) Å. It is surmised that the presence of a molecule of CH₂Cl₂, which has a relatively short contact (Cl···H 2.722(1) Å, Cl···C

3.623(7) Å) with the Cl(1) atom, is the reason for the somewhat anomalous arrangement; the metrical parameters for the solvent-free complex are consistent with this supposition. It is also noteworthy that complex **6.3** remains intact even when an excess of the [18]crown-6 ligand is present in solution and the crystallization of the compound from such a mixture yields the [18]crown-6 solvate/co-crystal illustrated in Figure 6.1. In contrast to the dichloromethane solvate, the lack of significant Cl···H interactions in this solvate structure affords a more linear In-In-Cl fragment that closely resembles that of the solvent-free complex.

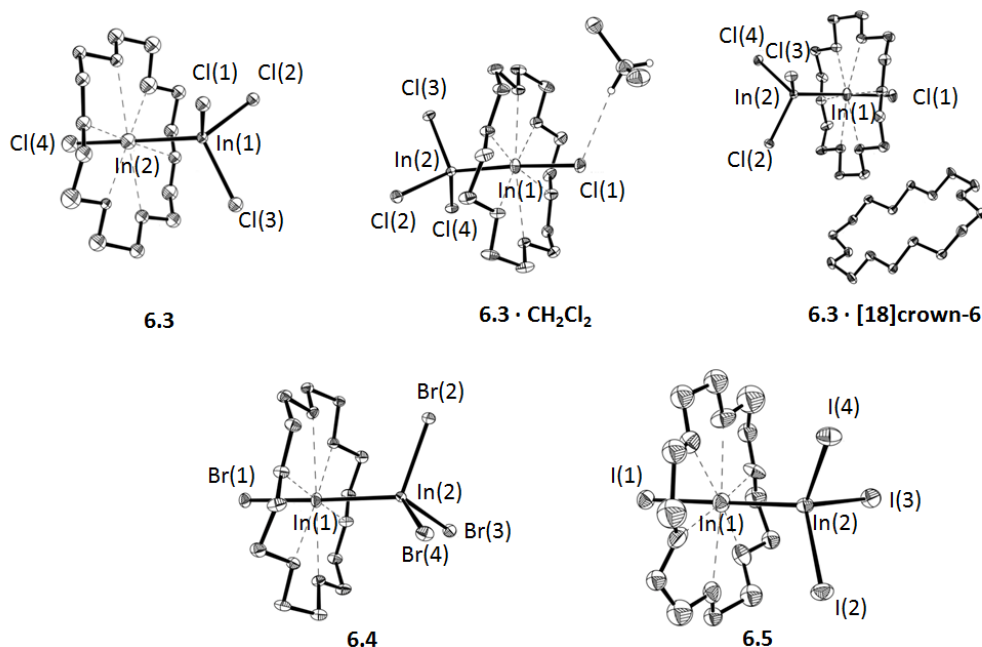


Figure 6.1: Thermal ellipsoid plot (30% probability surface) of the molecular structure of **6.3**, **6.3·CH₂Cl₂**, **6.3·[18]crown-6**, **6.4**, **6.5**. (Most hydrogen atoms have been removed for clarity)

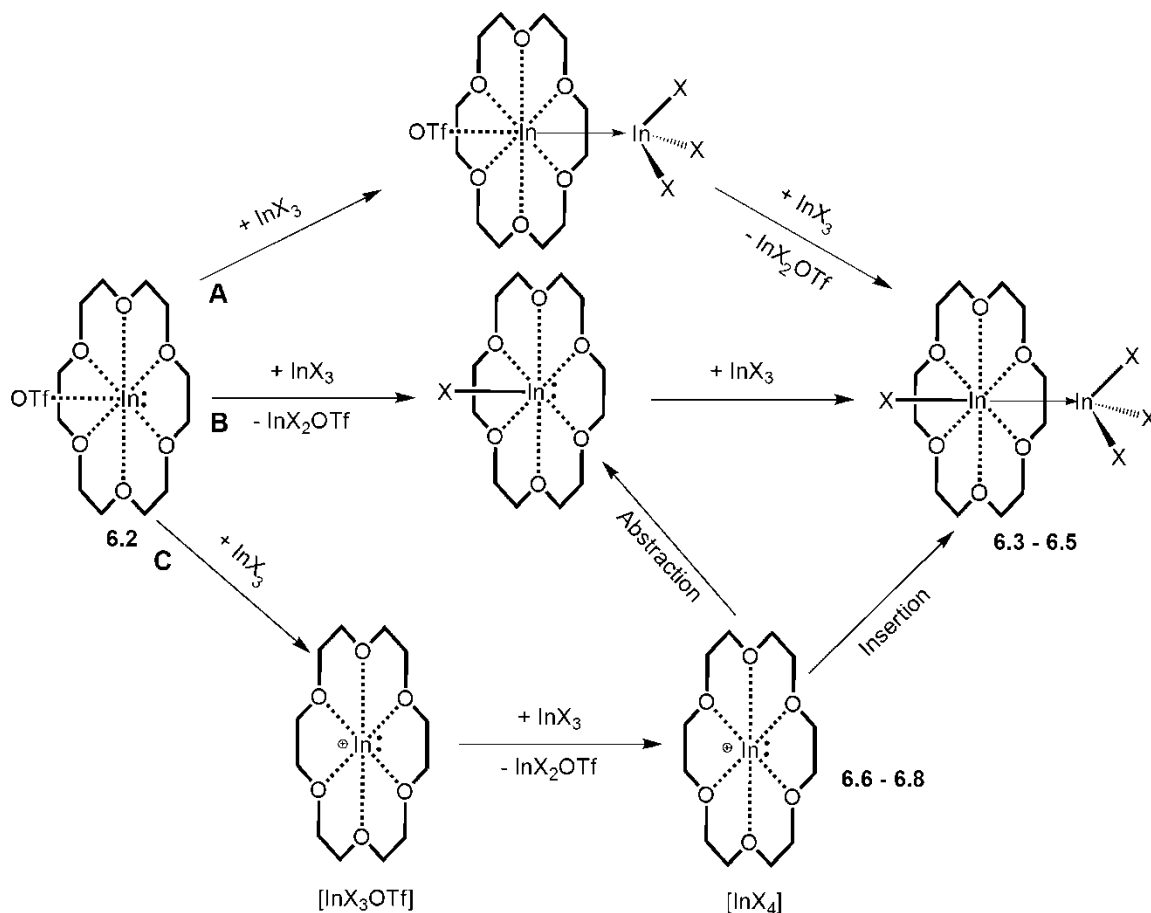
Table 6.1: Selected metrical parameters for compounds **6.3**, **6.3·CH₂Cl₂**, **6.3·[18]crown-6**, **6.4**, and **6.5**.

Compound	X-In(+1) distance (Å)	In-In distance (Å)	X-In-In angle (°)	In-O distance (range)
6.3	2.3149(18)	2.6727(7)	175.39(6)	2.481(5) – 3.081(5)
6.3 · CH₂Cl₂	2.3288(11)	2.6819(5)	170.09(4)	2.494(3) – 3.047(3)
6.3 · [18]crown-6	2.3334(9)	2.6808(4)	173.57(3)	2.548(2) – 2.966(3)
6.4	2.4572(5)	2.7073(4)	176.07(3)	2.630(3) – 2.846(3)
6.5	2.663(3)	2.725(2)	179.63(10)	2.65(3) – 2.75(3)

One obvious and important feature of each of the compounds depicted in Figure 6.1 is the absence of triflate groups. The transfer of the triflate substituent for a halide ion on the indium(+1) center in **6.3** - **6.5** (presumably to an indium(+3) center) may be rationalized in terms of hard and soft acid base theory (HSAB)^[42] given that the harder OTf anion should be more likely to bind with a harder In(+3) ion than a softer In(+1) ion. Alternatively, it is possible that the replacement of the triflate group for a halide might also be anticipated to result in stronger In-In bonding by increasing the donor ability of the putative In^I fragment and may favor the isolation of the observed products rather than any triflate-containing variants (see the Computational Investigations section for more in depth analysis). In terms of the products that were isolated, it is also plausible that only crystalline samples of **6.3** have been obtained because the asymmetric nature of the OTf-containing adducts may render crystallization of such species less favorable; pXRD experiments are always consistent with **6.3** being the only crystalline material present in the bulk product. As a final comment, it is worth noting that, given the instability of free "[In([18]crown-6)][Cl]", such a ligand transfer in the presence of the Lewis acid appears to provide a viable method for the generation of such fragments.

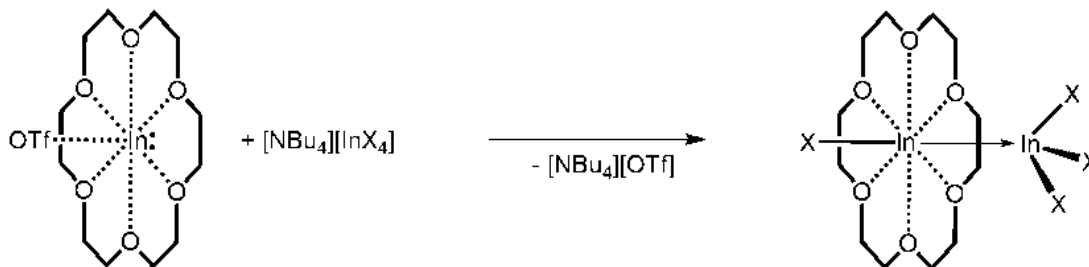
While the molecular structures of **6.3** – **6.5** may suggest that the anticipated donor-acceptor complex was generated in each instance, the details of the formation process are not unambiguous. For example, instead of the simple formation of an In-In bond followed by or preceded by OTf for halide exchange (as illustrated by routes **A** and **B** in Scheme 6.3), it is plausible that the triflate anion may first be abstracted by the InX₃ Lewis acid to generate a salt of the form [In([18]crown-6)][InX₃OTf]. The anion may then symmetrize to produce [In([18]crown-6)][InX₄]; although the thallium analogues of these salts have been characterized,^[43-47] such mixed-valence indium salts had been

posited to exist by Tuck and co-workers as early as 1981 (conclusive evidence has never been produced).^[48] The formal insertion of the In^{I} center into an In-X bond of the tetrahaloindate anion (route **C** in Scheme 6.3) which, because of geometrical considerations, most likely occurs by the step wise abstraction of a halide and formation of the donor-acceptor bond, could then yield the observed product.



Scheme 6.3: Some possible routes from **6.2** to **6.3** ($\text{X} = \text{Cl}$), **6.4** ($\text{X} = \text{Br}$), or **6.5** ($\text{X} = \text{I}$). Route A starts with the formation of the In-In donor-acceptor bond, route B commences with OTf- for Cl- exchange, and route C proceeds via the valence isomeric ionic species **6.6** ($\text{X} = \text{Cl}$), **6.7** ($\text{X} = \text{Br}$), or **6.8** ($\text{X} = \text{I}$) and is completed by the formal insertion of the In^{I} center into an In-X bond.

To assess the plausibility of route **C**, the synthesis of the putative intermediate salt $[\text{In}([\text{18}]\text{crown-6})][\text{InCl}_4]$, **6.5**, was attempted directly by the metathetical reaction of **6.2** with $[\text{NBu}_4][\text{InCl}_4]$ ^[49] in toluene, as outlined in Scheme 6.4. The reaction occurs as anticipated and extraction of the resultant solid mixture of products with toluene yielded crystals of **6.3** in the solvent-free form as depicted previously in Figure 6.1. The reaction of **6.2** with $[\text{NBu}_4][\text{InBr}_4]$ in toluene produces **6.4** in a similar manner. The observation of **6.3** (**6.4**) from this reaction is important for two reasons: firstly, it confirms that anion metathesis is viable for the reagent **6.2**, and secondly, it suggests that the ionic valence isomers of **6.3** (**6.4** or **6.5**) such as **6.6** (**6.7** or **6.8**) are not actually favored under the reaction conditions that were employed.



Scheme 6.4: Metathetical synthesis of In-In donor-acceptor complexes

In order to ensure that the products **6.3** – **6.5** that were obtained were not formed by the decomposition of the starting materials reactions of [18]crown-6 with InCl_3 or InBr_3 were studied. It was confirmed that these reactions result exclusively in the production of ionic compounds of the form $[\text{InX}_2([\text{18}]\text{crown-6})][\text{InX}_4]$ and not of compounds **6.3** – **6.5**. While it has been problematic to grow diffraction-quality crystals of these compounds, the compositions of the materials have been confirmed by high-

resolution electrospray ionization mass spectrometric investigations and the structure of the heavier analogue $[\text{InI}_2(\text{[18]crown-6})][\text{InI}_4]$ is known.^[50]

It is also worth emphasizing again that in contrast to the indium(+3) halides, the reaction of [18]crown-6 with indium(+1) halides always results in the rapid disproportionation of the indium salt. Furthermore, in the context of the present work, it is worth noting that the mixed-valent donor-acceptor adducts are among the resultant products that have been characterized from such disproportionation reactions in the cases of $X = \text{Cl}$ and I . In fact, such donor-acceptor complexes have been obtained as products arising from many different reactions involving low-valent indium, halide sources and [18]crown-6 poly-ethers; so, products such as **6.3** – **6.5** appear to be somewhat of a "thermodynamic sink" for these systems as the most favourable product of a mixture of these reagents.

In an attempt to prepare a mixed-metal In-Ga analog of **6.3**, a solution of **6.2** in toluene was treated with a solution of GaCl_3 in toluene. The resulting crystalline product obtained upon concentration of the reaction mixture was suitable for examination by single-crystal diffraction and was characterized as $[\text{In}(\text{[18]crown-6})][\text{GaCl}_3\text{-OH-GaCl}_3]$ (**6.9**); the hydroxydigallate anion is clearly the result of adventitious water and fortunately allows for the isolation of diffraction quality crystals that have not been obtained for the tetrachlorogallate salt (*vide infra*). The structure of **6.9** is depicted in Figure 6.2 and consists of a "free" $[\text{In}(\text{[18]crown-6})]$ cation that appears to have very little interaction with the anion: from one face, the closest In-Cl contact is 3.244(1) Å and the three closest In-Cl distances on the other face range from 3.604(1) – 3.821(1) Å. These distances are significantly longer than those of structures reported in the CSD having covalent In-Cl bonds, which range from 2-3 Å, and apart from the closest contact, they approach or

exceed the sum of the van der Waals radii for In and Cl (3.68 Å). Furthermore, the Ga-Cl distances within the anion are consistent with those observed in non-distorted chlorogallate anions and provide no evidence for a strong cation-anion interaction.

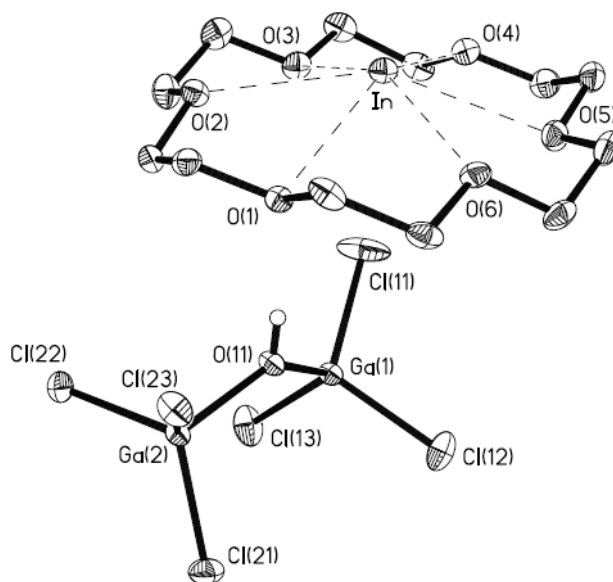


Figure 6.2: Thermal ellipsoid plot (30% probability surface) of the molecular structure of **6.9** (hydrogen atoms on the crown ether ligand are not shown for clarity). Selected bond distances (Å) and angles (°): Ga(1)–O(1), 1.863(2); Ga(2)–O(1), 1.878(2); Ga(1)–Cl(11), 2.1374(11); Ga(1)–Cl(12), 2.1539(11); Ga(1)–Cl(13), 2.1519(10); Ga(2)–Cl(21), 2.1539(10); Ga(2)–Cl(22), 2.1554(10); Ga(2)–Cl(23), 2.1463(9); In(1)–O(1), 3.089(3); In(1)–O(2), 2.939(3); In(1)–O(3), 2.852(2); In(1)–O(4), 2.841(3); In(1)–O(5), 2.878(3); In(1)–O(6), 2.901(3); In(1)–Cl(11) 3.244(1); O–H...O(1), 1.96(4); Ga(1)–O(1)–Ga(2), 130.89(14).

Undoubtedly, the most important feature of the structure of **6.9** is that the compound is clearly a salt composed of well-defined anions and not a donor-acceptor complex. Thus, in contrast to **6.3**, it is apparently not favourable for the In^I center to insert into the Ga-Cl bond of the anion and the ionic valence isomer is obtained. The structure of **6.9** thus suggests that salts of the form [In([18]crown-6)][EX₄] initially postulated by Tuck may indeed be amenable to preparation, isolation, and study.

6.2.2. Direct Routes to [In([18]crown-6)][EX₄]

Experiments employing the metathesis route outlined in Scheme 6.4 using **6.2** and either [NBu₄][AlCl₄] or [NBu₄][GaCl₄] were performed in an attempt to synthesize the mixed-metal analogues of **6.3** and to determine which valence isomer is adopted. However, the initial investigations were hindered by the inability to separate the resultant [NBu₄][OTf] by-product completely from the desired [In([18]crown-6)][ECl₄] material,^[33] and it was reasoned that an alternative approach to obtain high-purity material was required. Thus, using the mixed valent nature of "In₂X₄" as a model, it was hypothesized that the reaction of InCl with ECl₃ would afford the salt [In][ECl₄], and which could be further treated with crown ethers to provide a direct route to the desired complexes (Scheme 6.3), eliminating the complications of metathesis reactions using **6.2**. In order to probe the viability of the approach, it was decided to first investigate the "all-indium" system for which well-characterized products have been obtained from the methods outlined above. Thus, an equimolar mixture of InCl and InCl₃ was refluxed in toluene until no observable traces of InCl were present and, after allowing the mixture to cool to room temperature, an equimolar quantity of [18]crown-6 was added. Removal of

the volatile components of the mixture produced a colorless powder that was characterized as **6.3** as confirmed by powder X-ray diffraction studies and microanalysis.

In light of the positive outcome of this more direct route to **6.3**, the approach was employed towards synthesizing the mixed-metal analogues $[\text{In}([\text{18}]\text{crown-6})][\text{ECl}_4]$ (**6.10**: E= Al, **6.11**: Ga). Gratifyingly, the reaction of InCl and ECl₃ in refluxing toluene afforded $[\text{In}][\text{ECl}_4]$ in high yield as confirmed by the results of ¹¹⁵In, ⁷¹Ga, and ²⁷Al NMR spectroscopic investigations outlined in Table 6.2. The subsequent addition of an equimolar toluene solution of [18]crown-6 at room temperature (for Ga) or at -78°C (for Al) afforded the desired $[\text{In}([\text{18}]\text{crown-6})][\text{ECl}_4]$ complexes as colorless solids that precipitate from toluene solutions. The resultant solids were dissolved in MeCN and investigated using multinuclear NMR spectroscopy; in each of the experiments, the $[\text{In}([\text{18}]\text{crown-6})]$ cation with an ¹¹⁵In NMR resonance at ca. -1100 ppm is evident, as is the signal for the corresponding tetrachlorometallate anion. It is worth emphasizing the observation that whereas the "free" salt $[\text{In}][\text{AlCl}_4]$ disproportionate rapidly in acetonitrile, the crown ether complexed salt $[\text{In}([\text{18}]\text{crown-6})][\text{AlCl}_4]$ can be dissolved in MeCN to obtain the ¹¹⁵In NMR spectrum. Although some disproportionation occurs eventually, as evidenced by the appearance of a peak at ca. 378 ppm in the ¹¹⁵In NMR spectrum corresponding to $[\text{InCl}_4]$, this process is either slowed considerably by the presence of the crown ether, or is perhaps attributable to some remaining uncrowned $[\text{In}][\text{AlCl}_4]$. A final and unanticipated NMR spectroscopic observation that is of note concerns the donor-acceptor complex **6.3**. While **6.3** features no ¹¹⁵In NMR signals in toluene solution, when samples of **6.3** (prepared using any of the approaches described in this work) are dissolved in MeCN, signals attributable to $[\text{In}([\text{18}]\text{crown-6})]$ (-1100 ppm) and $[\text{InCl}_4]$ (365 ppm) are observed. This suggests that the donor-acceptor **6.3** and ionic

6.6 isomers are very similar in energy and that the form adopted in solution is dependent on the solvent. Finally, it is observed that none of these crowned In^I salts appears to react with chlorinated solvents in the manner exhibited by **6.2**.

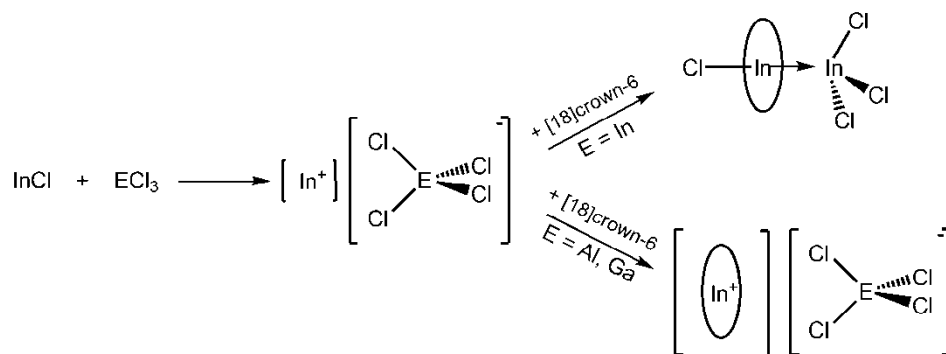
Table 6.2: Solution ¹¹⁵In NMR data for [In][ECl₄] and [In([18]crown-6)][ECl₄] salts.

Ions	[AlCl ₄]	[GaCl ₄]	[InCl ₄]
[In]	-1264 ^a	-1092	-1065
[In([18]crown-6)]	-1085	-1077	-1084

^aobtained in C₆D₆ to avoid disproportionation of the compound observed in MeCN; the resonance is actually attributable to [In(C₆D₆)_n]. Please note that the signals are quite broad and that the actual width of the signal appears to be dependent on concentration and temperature and is not easily indicative of the presence or the absence of the crown ether.

The solution ¹¹⁵In NMR data allows for the unambiguous identification of the presence of the indium(I) cation and tetrachlorometallate anions in solution; however, given the absence of crystal structures for compounds **10** and **11**, insight into the nature of these species in the solid state was also investigated. In order to obtain such information, solid-state ²⁷Al, ⁷¹Ga, and ¹¹⁵In NMR spectra of the [18]crown-6 complexes of [In][ECl₄] (E = Al, Ga, In) were obtained. As anticipated, the donor-acceptor complex **6.3** does not exhibit any observable signals in the solid-state ¹¹⁵In NMR spectrum; this is as one would predict given the quadrupolar nature of the ¹¹⁵In nucleus and the spherically asymmetric environment about each indium center. The absence of any observable signal is important because it unambiguously confirms the absence of any [InCl₄] anions in the solid state and that no signals are observed regardless of which solvent is used to

recrystallize the sample. In stark contrast, the solid-state ^{115}In NMR spectra of **10** and **11** each exhibit a signal with an isotropic chemical shift of ca. -1100 ppm and the respective solid-state ^{27}Al , and ^{71}Ga NMR spectra confirm the presence of the tetrahalo anion (isotropic chemical shifts of ca. 100 and 250 ppm, respectively). It should also be noted that the lineshape of the signal in the solid-state ^{115}In NMR spectra can clearly differentiate between In^{I} centers that are "free" or complexed by [18]crown-6, however a complete description of the results and analyses of the multinuclear solid-state NMR investigations of these compounds is being reported in a separate publication. Overall, the solution and solid-state NMR investigations clearly demonstrate that an ionic valence isomeric form of $[\text{In}([\text{18}]\text{crown-6})][\text{EX}_4]$ is favoured for $\text{E} = \text{Al}$ and Ga in both solution and the solid state, when $\text{E} = \text{In}$, the ionic form is only observed in polar solutions and the donor-acceptor isomer is always found in the solid state, as illustrated in Scheme 6.5. The reason for the differing behaviour is likely a consequence of a number of factors, one of which undoubtedly is the relative strengths of the bonds being made and broken upon changing isomers. I examined the effect of using smaller crown ethers in such systems and performed a series of computational investigations (described below) in an attempt to rationalize at least some of these observations.



Scheme 6.5: Direct synthetic route to "crowned" indium(I) complexes; the circle represents the [18]crown-6 ligand.

6.2.3. [15]crown-5 Complexes

As reported for InOTf,^[51] altering the cavity size of ligand on the univalent indium center by changing the crown ether used can have a dramatic effect on the observed structural features of the resultant complexes (as is also the case for related molecules from group 14).^[52] Perhaps most notable, is the possibility of producing sandwich-like complexes using crown ethers with smaller cavity sizes. Interestingly, while it was found previously that the addition of one equivalent of [15]crown-5 to InOTf affords the sandwich complex $[\text{In}([\text{15}]\text{crown-5})_2][\text{OTf}]$ (leaving one equivalent of InOTf uncomplexed), it has now been observed that the analogous reaction with $[\text{In}][\text{GaCl}_4]$ instead affords $[\text{In}([\text{15}]\text{crown-5})][\text{GaCl}_4]$ (**6.12**). The solid state structure of **6.12** (Figure 6.3) shows the half-sandwich nature of this solid with In- O_{crown} contacts ranging from 2.608(3)–2.777(3) Å. While the nature of the anion must play a role in favouring the crystallization of this mono-crowned "half-sandwich" species, it should be noted that In-Cl distances range from 3.731(1)–4.275(1) Å, which are even longer than the In-Cl distances observed in **6.9**. This feature is potentially attributable to the presence of a

stereochemically active "lone-pair" of electrons on the indium centre facing directly opposite the [15]crown-5 ligand. It should be emphasized that, in spite of the solid state structure, the ^{115}In NMR chemical shift of -990 ppm is virtually identical to that of $[\text{In}([\text{15}]\text{crown-5})_2][\text{OTf}]$ and suggests that a sandwich-like structure is present in solution.

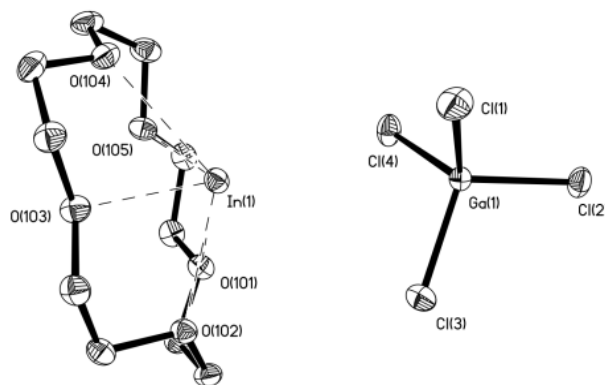


Figure 6.3: Thermal ellipsoid plot (30% probability) of the molecular structure of **6.12** (hydrogen atoms are not shown for clarity). Selected bond distances (\AA) and angles ($^\circ$): In(1)-O(101), 2.644(2); In(1)-O(102), 2.608(3); In(1)-O(103), 2.615(3); In(1)-O(104), 2.777(3); In(1)-O(105), 2.657(3); In(1)-Cl(1), 3.731(1); In(1)-Cl(4), 3.957(1); In(1)-Cl(3), 4.275(1).

It should be noted that the reaction of two equivalents of [15]crown-5 with $[\text{In}][\text{GaCl}_4]$ affords a colorless solid where the multinuclear solution NMR data (^1H , ^{13}C , ^{115}In) for this solid are identical to **6.12**, however with a distinctly different powder X-ray diffraction pattern, as illustrated in Figure 6.4. The microanalysis of this compound is

consistent with a molecular formula of $[\text{In}([\text{15}] \text{crown-5})_2][\text{GaCl}_4]$, and a test reaction of $[\text{In}][\text{GaCl}_4]$ with 1.2 equivalents of $[\text{15}] \text{crown-5}$ affords a white solid that shows characteristic peaks in the pXRD pattern equivalent to both **6.12** and the solid obtained from the reaction with two equivalents of the crown ether. While no structural data has been obtained for this species, given the solid state structure of $[\text{In}([\text{15}] \text{crown-5})_2][\text{OTf}]$, an indium "sandwich" complex with a tetrachlorogallate anion is likely.

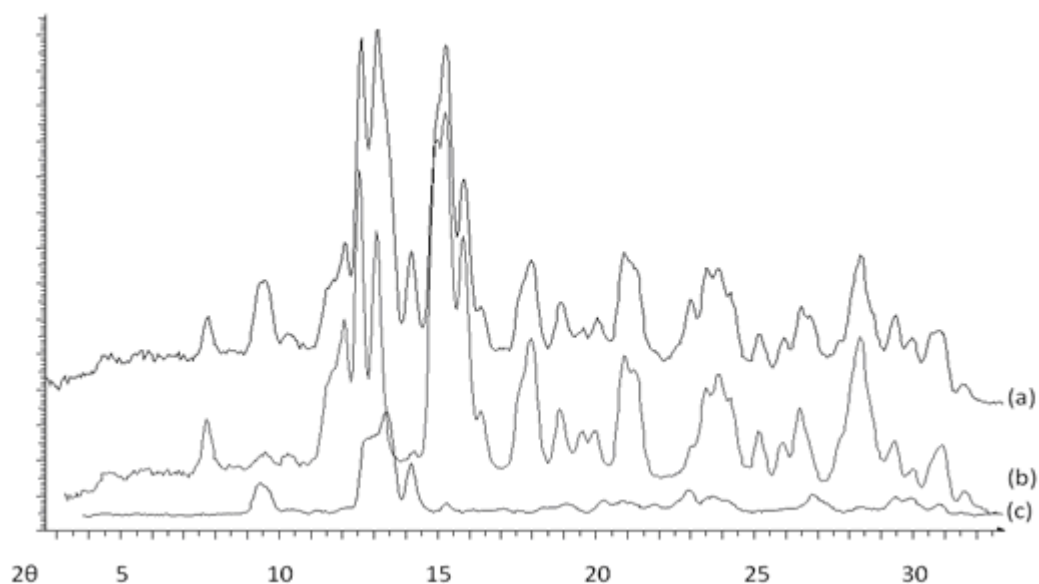


Figure 6.4: Powder X-ray diffraction patterns of: (a) $[\text{In}][\text{GaCl}_4] + 1.2 [\text{15}] \text{crown-5}$; (b) $[\text{In}][\text{GaCl}_4] + 1 [\text{15}] \text{crown-5}$; (c) $[\text{In}][\text{GaCl}_4] + 2 [\text{15}] \text{crown-5}$.

The analogous reaction of " In_2Cl_4 " with $[\text{15}] \text{crown-5}$ generated an even more surprising crystalline product. The solution phase ^{115}In NMR spectrum of the mixture features signals at ca. -1000 ppm and 365 ppm, which suggest the formation of the anticipated ions $[\text{In}([\text{15}] \text{crown-5})_2]$ and $[\text{InCl}_4]$, respectively. However, crystallization of the mixture provided the unexpected salt $[\text{In}([\text{15}] \text{crown-5})_2][\text{In}_2\text{Cl}_6]$, **6.13**, that is illustrated in Figure 6.5. Although there was no conclusive evidence for the presence of

any other In-containing products or by-products, the mixed-valent salt obtained from the reaction must have been generated by a disproportionation reaction of the starting indium halide. The formula unit of the material contains a centrosymmetric arrangement of two half-sandwich crowned In^{I} cations similar to that found in **6.12**; however, these are bridged by a dianion featuring a dinuclear In^{II} fragment that is an extremely common component of mixed-valent inorganic indium salts.^[3] The In-In bond distance of 2.724(1)Å is typical of such anions that have been reported,^[3] and the anion-cation $\text{Cl}\cdots\text{In}$ contacts are similar to those observed in **6.12**. Overall, although the structure is unique and the route through which the compound was generated remains unclear, the metrical parameters of the components are as one would anticipate.

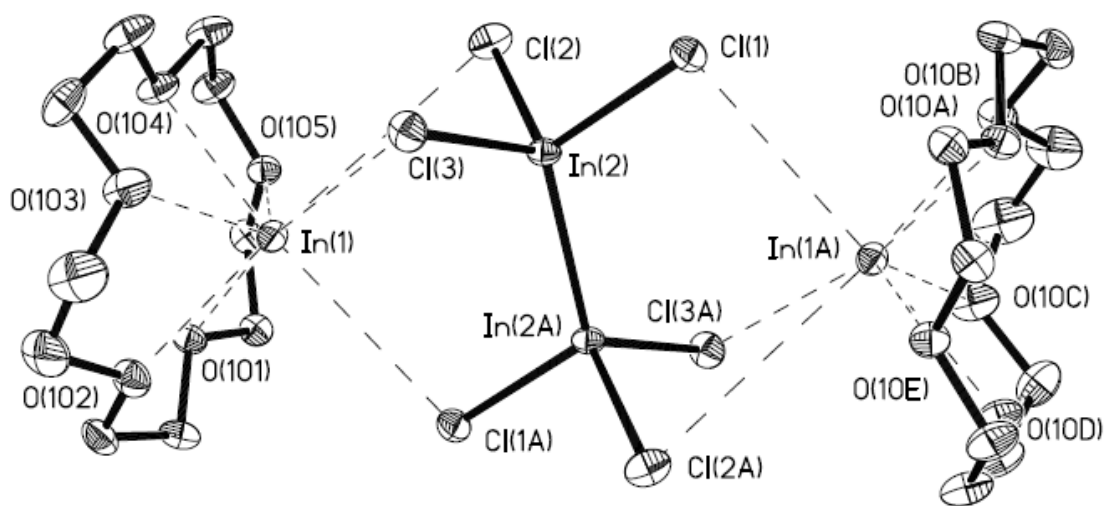


Figure 6.5: Solid state structure of **6.13** (hydrogen atoms are not shown for clarity). Selected bond distances (Å): In(2)-In(2A), 2.7242(8); In(2)-Cl(1), 2.4142(15); In(2)-Cl(2), 2.4058(15); In(2)-Cl(3), 2.4046(15); In(1)-Cl(1A), 3.6330(19); In(1)-Cl(2), 3.9999(19); In(1)-Cl(3), 3.7158(17); In(1)-O(crown) 2.608(5)-2.806(4).

6.2.4. Computational Investigations

Previous computational work by Timoshkin and Frenking assessed the relative stabilities of covalent and donor-acceptor valence isomers for a series of base-free models of the formula $EE'R_3R'$ ($R, R' = H, Cl, Me$) similar to those illustrated in Figures 6.2(b) and 6.2(c) and found that, while the covalent isomer is usually more stable, the donor-acceptor isomer is sometimes the favored form.^[53] In an effort to rationalize the differing behaviours of the various valence isomers of the $InEX_4([18]crown-6)$ systems, which appear to behave more consistently than the $[15]crown-5$ systems, a series of density functional theory (DFT) calculations was performed to ascertain the different bond energies and orbital energies of the component species. Data computed using the fully geometry-optimized structures of the "crowned" donor fragments, $X-In([18]crown-6)$ ($X = Cl, Br, I, OTf$), is compiled in Table 6.3. From the theoretical calculations attention was focused on five different properties in an attempt to identify trends and differences between the hypothetical crowned indium(I) halide complexes and the isolable crowned indium(I) triflate analog. In order to gain insight into the potential donor abilities of these crowned species it is necessary to obtain information about the "lone pair" of electrons centered on the indium atom. From Natural Bond Orbital (NBO) analyses of these species, the energy of each of the indium centered lone pair of electrons, and the percentages of s-orbital contribution to the molecular orbitals they occupy were obtained. These values can be used to predict which crowned species are likely to be the better donors: a higher energy lone pair of electrons on In, with a lower amount of s-orbital character, should correlate to that species being a better donor. Analysis of the data suggests that the trend of donor strength should be $Cl > Br > OTf > I$ given that the s-

character increases from 95.64 % (Cl) < 96.01 % (Br) < 96.51 % (OTf) < 97.02 % (I) and lone pair energies decrease from -6.065 eV (Cl) > -6.179 eV (Br) > -6.389 eV (OTf) > -6.470 eV (I). Such an inverse relationship between s-character contribution and lone pair energy is as one would anticipate on the basis of atomic orbital energies.

To assess the potential reactivity of these crowned species the energies of the highest occupied molecular orbital (HOMO) and lowest occupied molecular orbital (LUMO) were computed in order to determine the HOMO-LUMO energy gap because a smaller energy difference between the frontier orbitals is often a feature of relatively less stable species. The calculations indicate that there is only a minimal difference in the HOMO-LUMO gap between the three crowned halide species; energy differences of 4.9133, 4.9070, and 4.9035 eV were obtained for Cl, Br, and I respectively. However, in the case of the triflate analog, a significantly larger value of 5.6260 eV is observed. While this dramatic energy difference may not be causative, perhaps the larger HOMO-LUMO energy gap provides some insight into why [In([18]crown-6)][OTf] is an isolable compound, whereas no examples of [In([18]crown-6)][X] have been isolated to date and all attempts to synthesize a "crowned" halide species leads to disproportionation and isolation of complexes such as **6.3**, **6.4**, or **6.5**.

To obtain a measure of the interaction between the halide or triflate substituent and the indium center the Wiberg Bond Indices (WBI) for each complex were determined. For the halide series, it is observed that the interaction of the halogen with the indium center increases with increasing atomic number, as the bond indices were found to be 0.30 (Cl), 0.36 (Br), and 0.42 (I). This trend is understandable in the context of HSAB theory as the softer iodide anion should have more favourable interactions with the softer indium center than the harder halides. Interestingly, the WBI for the In-O_{triflate}

was calculated to be 0.11. This value is considerably lower than that for any of the halides and suggests that there is very little covalent bonding between the indium center and the triflate anion. This conclusion is consistent with the previous observations and supposition that the interaction between the indium cation and triflate anion is best described as a contact ion pair.^[32] Taken together, the results of lone-pair energies, HOMO-LUMO energy gaps and ligand-In bond indices suggest that in spite of the WBI value, chlorine is the substituent that produces the most reactive lone pair of electrons on indium and should probably provide for the strongest univalent donor.

Table 6.3: Selected data from DFT calculations for geometry optimized crowned univalent indium model compounds(see experimental for details).

Crowned In ^I model	% 5s LP ^a	E (In LP) (eV) ^b	H/L Energies (eV)	H-L Gap (eV)	WBI (In-X) ^c
Cl-In([18]crown-6)	95.64	-6.064	HOMO = -4.442 LUMO = 0.472	4.914	0.3031
Br-In([18]crown-6)	96.01	-6.179	HOMO = -4.474 LUMO = 0.433	4.907	0.3602
I-In([18]crown-6)	97.02	-6.470	HOMO = -4.545 LUMO = 0.358	4.903	0.4184
OTf-In([18]crown-6)	96.51	-6.389	HOMO = -5.385 LUMO = 0.241	5.626	0.1055
[[18]crown-6]In ⁺	99.50	-8.354	HOMO = -9.452 LUMO = -4.063	5.389	N/A

^aNBO percentage of 5s orbital character in the "lone pair" MO of electrons on In; ^bNBO energy of the "lone pair" MO of electrons on In; ^cNBO Wiberg Bond Index calculated for the In-X bond; E = Energy, H = HOMO, L = LUMO, LP = lone pair

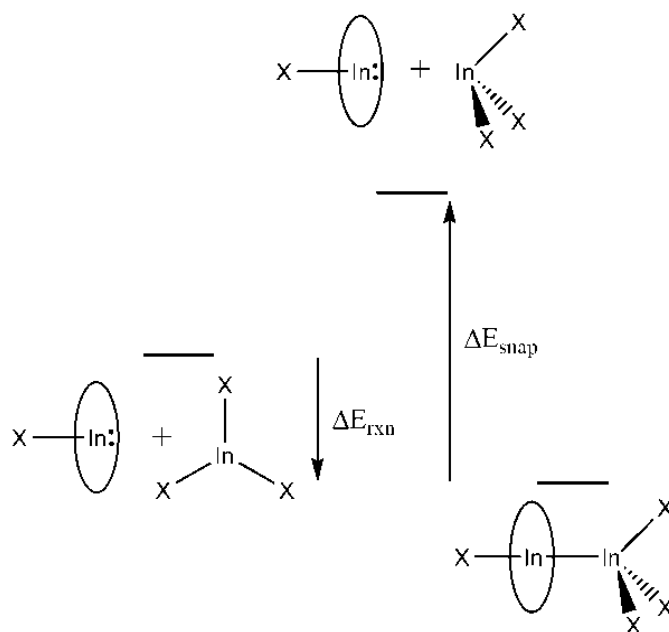
Whereas the analysis of the crowned donor species helps provide insight into the anticipated behaviour of the donor fragments, calculations were also performed on models of the donor-acceptor complexes **6.3**, **6.4**, and **6.5**, so as to garner some insights

into the nature of the compounds isolated experimentally. For the first series of calculations, models were used in which the heavy atoms were positioned on the basis of the actual metrical parameters observed in the crystal structures and the protons were placed in idealized positions (called **6.3'**, **6.4'**, and **6.5'** respectively). For comparative purposes the structure of the hypothetical donor-acceptor complex OTf-In([18]crown-6)-InCl₃ (**6.14**) was optimized also. From these calculations valuable information was obtained regarding the energy required to break the indium-indium bond and the nature of these bonds.

Prior to further analyses, it was necessary to confirm that such complexes can indeed be described reasonably as adducts of Lewis acids and bases. To this end, the nature of the indium-indium bond itself was investigated by breaking the bond both homolytically and heterolytically to determine whether these species are best described as donor-acceptor complexes or if they are better described as covalently bound according to the definition of Haaland.^[54] Calculations on **6.3'** reveal that the energy required to break the indium-indium bond in a homolytic manner is 478 kJ mol⁻¹, while by comparison it takes 398 kJ mol⁻¹ to cleave the indium-indium bond heterolytically; i.e., the cleavage of the bond into closed-shell neutral donor and acceptor fragments is, as one would anticipate, considerably easier than the cleavage of the bond into two radical ions. This result confirms that the bonds in these systems are probably best described as being indium(+1)-indium(+3) donor-acceptor in nature.

A series of calculations was performed to ascertain which complex has the strongest indium-indium donor-acceptor bond, Scheme 6.4. Again, it should be noted that the energies for **6.3'**, **6.4'**, and **6.5'** were calculated from the geometries obtained from the crystal structures and were not optimized, while a geometry optimization was

performed on the hypothetical donor-acceptor complex **6.14** prior to single point energy calculations and NBO analysis. For the halide models **6.3'** – **6.5'**, the energy required to break the indium-indium bond follows the trend suggested by the examination of the donor fragments described above: namely, the strongest donor-acceptor bond was observed for the chloride species (398 kJ mol⁻¹), with the bromide (364 kJ mol⁻¹) and iodide (322 kJ mol⁻¹) becoming progressively weaker. These values are as one would anticipate on the basis of the relative acidities of the InX₃ acceptors and also correlate with the % 5s-orbital and lone pair energies previously mentioned. It should be emphasized, however, that while these corresponding values for the triflate model **6.2'** were in between those for the bromine and iodine analogues, the indium-indium bond snapping energy for the complex **6.14** (292 kJ mol⁻¹) was found to be ca. 30 kJ mol⁻¹ smaller than for **6.5'**. This demonstrates that although the triflate complex **6.2'** should perhaps be a better donor based on the availability and energy of its "lone pair" of electrons, it actually forms a weaker indium-indium bond with indium(+3) halides than do any of the crowned indium(+1) halides. Thus the computed energies justify the experimental observation that the reaction of **6.2** with InX₃ forms **6.3**, **6.4**, or **6.5** instead of the possible mixed triflate-halide complexes such as **6.14**.



Scheme 6.6: Graphical depiction of energies determined in this work. The bond snapping energy is calculated as the difference in energy between the energies of the component donor and acceptor fragments fixed in the geometry they possess in the complex; the reaction energy is determined by the energy difference between the optimized donor and acceptor molecules and the adduct they form.

Although the bond snapping energies for the model donor-acceptor complexes were found to be quite different, the Wiberg bond indices (WBI) calculated for the indium-indium bonds in these complexes were found to be similar with values of, 0.80 (**6.3**), 0.78 (**6.4**), 0.77 (**6.5**), and 0.77 (**6.14**). Examination of the WBI for the bond between the substituent and the indium(+1) center in these complexes demonstrates that in there is always an increase in the magnitude of covalent bonding within the donor fragment upon formation of the donor-acceptor complex. While such an increase is found in every instance, it should be emphasized that the WBI between In-O_{triflate} is still only

0.18 in the case of **6.14**, suggesting that even upon formation of a donor-acceptor complex, there is remarkably little covalent interaction between the indium(+1) center and the triflate anion. Again, this observation may provide insight as to why only the all-halide complexes **6.3** – **6.5** are actually observed experimentally.

The remarkable difference between triflate- or halide-substituted univalent indium donors is further illustrated by NBO analysis of the orbital contributions to the indium-indium bonding molecular orbital, with particular focus on the composition of the indium(+1) orbital within this bonding MO. Ignoring the crown ether, from a simple valence bond perspective the central indium(+1) atom of the linear X-In-In moiety in each of these donor-acceptor complexes would probably be described as having sp hybridization. Indeed, for the halide complexes **6.3'** – **6.5'** the bonding orbital contribution from the indium(I) center is approximately 50 % s-orbital and 50 % p-orbital in nature, with **6.5'** (52 %s and 48 %p) having the largest variation from that ideal composition. In stark contrast, for the triflate model **6.14** the composition of the indium(+1) bonding MO is found to be 91 % s-orbital and only 9 % p-orbital in nature. The lack of p-orbital character from the indium(+1) center would be expected to result in less effective overlap between the indium(+1) and indium(+3) MOs and perhaps help to explain the low energy required to break the indium-indium bond in **6.14** relative to the halide species.

One final aspect of these complexes that was calculated is the overall reaction energy for the process of combining the donor and acceptors to form the indium-indium complex. These energies were obtained by comparing the energies of the fully optimized XIn([18]crown-6) and InX₃ donors and acceptors with that of the observed donor-acceptor complex that they produce. The reaction energies again suggest that the chloride

complex is the most energetically favourable as the formation reaction energy is -154 kJ mol^{-1} , while those for the bromide and iodide analogs are -145 and -117 kJ mol^{-1} respectively. Although the reaction energy obtained for the triflate donor-acceptor complex **6.14** was found to be -185 kJ mol^{-1} , it should again be clarified that **6.14** is a hypothetical complex which has a fully-optimized geometry, while the geometries of the halide donor-acceptor species were obtained from the crystal structures. This geometry optimization lowers the energy of the donor-acceptor complex and generates a more exergonic reaction than those obtained for the halide series.

Table 6.4: Computational results for indium-indium donor-acceptor complexes. E_{snap} and

E_{rxn} are illustrated in Scheme 6.6.

Model Compounds	E_{snap} (Het) (kJ mol ⁻¹) ^a	E_{snap} (Homo) (kJ mol ⁻¹) ^b	WBI (In-In)	In(+1) MO Contr. ^c	WBI (X-In)	E_{rxn} (kJ mol ⁻¹)
6.3'	397.92	477.86	0.8003	50.57 % (s) 49.43 % (p)	0.4903	-153.72
6.4'	363.50	/	0.7838	50.83 % (s) 49.17 % (p)	0.5714	-145.10
6.5'	322.13	/	0.7699	52.18 % (s) 47.82 % (p)	0.6982	-117.01
6.14	292.43	/	0.7695	91.19 % (s) 8.81 % (p)	0.1815	-184.98

^a In-In snapping energy of heterolytic cleavage; ^b In-In snapping energy of homolytic cleavage; ^c Orbital contribution on the indium(+1) atom to the In-In bonding MO.

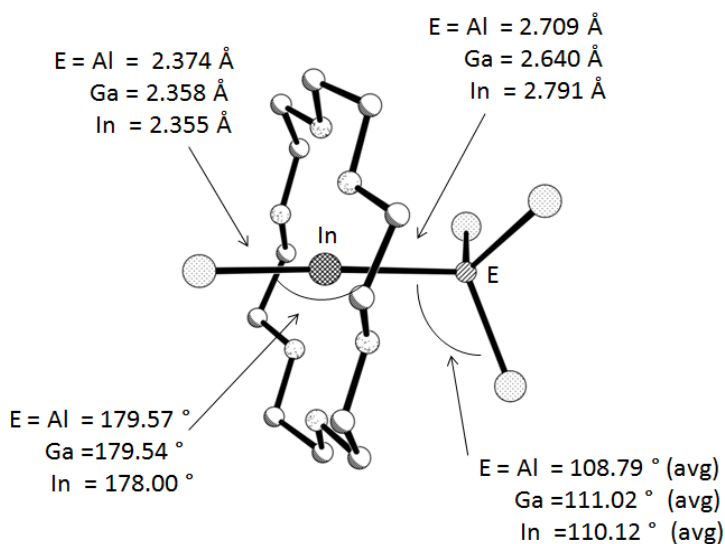


Figure 6.6: Metrical parameters of fully geometry-optimized In-E donor-acceptor complexes

The computational investigations described above provide insight into the experimental observation of indium-indium donor-acceptor complexes such as **6.3** – **6.5**; however, it was desired to rationalize the non-observation of analogous mixed group 13

metal species. To this end, full geometry optimizations and NBO analyses were performed on models of **6.3**, and the putative donor-acceptor isomers of **9** and **10**, i.e., Cl-In([18]crown-6)-ECl₃ (E = Al (**6.15**), Ga (**6.16**), In (**6.3'**_{opt})) illustrated in Figure 6.6). Selected results from the calculations are presented in Table 6.5. Although the metrical parameters and appearance of the optimized structures are as one might anticipate, it must be highlighted that the optimized In-In distance in **6.3'**_{opt} of 2.7908 Å is significantly longer than the 2.6727(7) Å distance observed experimentally for **6.3**. In spite of the longer distance, virtually all of the calculated properties of **6.3'**_{opt} remain similar to those found for the model **6.3'** that was based on the crystal structure geometry and the potential energy surface for the deformation of the In-In bond appears to be relatively flat: the difference in energy between **6.3'** and **6.3'**_{opt} is less than 5 kJ mol⁻¹. For example, even with the changes in geometry in **6.3'**_{opt} relative to **6.3'**, the orbital contributions on the indium(I) center to the In-In bonding MO remain at 50% s-orbital and 50% p-orbital. In stark contrast, changing the Lewis acid fragment from InCl₃ to ECl₃ (E = Ga, Al) results in a dramatic shift away from classical sp-hybridization to the predominately s-orbital character similar in magnitude to that calculated for the putative complex **6.14**. It is interesting to note that of all the NBO analyses performed on these complexes, none of the donor-acceptor complexes which exhibit a high In(+1) s-orbital character in their In-E bonding MO's have been amenable experimentally to identification or isolation. Thus, it appears as if the composition of the metal-metal bonding MO rather than the WBI, bond distance, or, snapping energy, etc. that appears to give the most predictive value for which complexes are more likely to be observed in the laboratory.

Table 6.5: Bond lengths, Wiberg bond indices, and MO orbital contributions for optimized donor-acceptor complexes.

Model Species ^a	In-Cl (Å)	In-Cl WBI	In-E (Å)	In-E WBI	In(+1) MO Contr. ^b
Cl-In([18]crown-6)-AlCl ₃ (6.15)	2.3733	0.4169	2.7059	0.7609	92.45 % (s) 7.55 % (p)
Cl-In([18]crown-6)-GaCl ₃ (6.16)	2.3585	0.4515	2.6395	0.7636	90.64 % (s) 9.36 % (p)
Cl-In([18]crown-6)-InCl ₃ (6.3'_{opt})	2.3545	0.4687	2.7908	0.7696	50.04 % (s) 49.96 % (p)

^a Geometry optimized model; ^b In^I orbital contribution to the In-In bonding MO.

As a final observation, given that the crystal lattice energies for each of the putative salts of the form [In([18]crown-6)][ECl₄] (E = Al, Ga, In) should be similar to each other and that the energy required to break a E-Cl bond in each of the anions is also similar, it would appear likely that the adoption of the valence isomeric donor-acceptor structure in the case of the all indium system must be attributable to the relative favorability of the In-In bond. The reason for the relative preference for In-In rather than In-Al or In-Ga bonds appears to be related to the composition of the metal-metal bonding MO and a complete energy decomposition analysis of these species may be informative.

6.3 Conclusion

The reaction of [In([18]crown-6)][OTf] with indium(+3) halides (for Cl, Br and I) consistently generates "donor-acceptor" complexes that are valence isomers of forms observed for the corresponding indium(+2) halides in the presence or absence of other types of donors. Single-crystal X-ray structures of each of these complexes confirm the viability and reproducibility of this new valence isomeric form of "InX₂" in the presence of the [18]crown-6 ligand. Although such donor-acceptor complexes may be obtained from various routes, these species can be produced in high purity through the reaction of

InX and InX₃ in the presence of [18]crown-6 ethers. Attempts to prepare mixed group 13 metal variants provide instead the first examples of structurally-characterized salts containing a "free" [In([18]crown-6)] cation. Multinuclear NMR (²⁷Al, ⁷¹Ga, ¹¹⁵In) confirms the ionic nature of the mixed metal variants in both solution and the solid state and reveals that the "ionic" isomer [In([18]crown-6)][InCl₄] is actually observable but only in polar solution. The properties of donor-acceptor complexes derived from "crowned" In^I donors and In^{III} acceptors have been elucidated using computational methods that provide a rationale for the observation of the all-halide In-In complexes and the non-observation of triflate-containing complexes or mixed metal complexes. Finally, both the experimental and computational investigations highlight and rationalize the different behaviour observed for triflate- and halide-substituted univalent indium species.

6.4 Experimental Section

6.4.1 General Procedures

All manipulations were carried out using standard Schlenk techniques and solvents were dried using a series of Grubbs'-type columns^[55] and degassed prior to use. Starting materials were purchased from either Strem or Aldrich and used without further purification. Melting points were obtained using an Electrothermal[®] melting point apparatus on samples sealed in glass capillaries under dry nitrogen. Solution phase NMR spectra were recorded at room temperature on a Bruker Avance 300 MHz spectrometer. Chemical shifts are reported in ppm, relative to external standards (SiMe₄ for ¹H and ¹³C NMR, In⁺³(OH₂)₆ or [NBu₄][InCl₄] for ¹¹⁵In NMR, Al⁺³(OH₂)₆ for ²⁷Al NMR, and Ga⁺³(OH₂)₆ for ⁷¹Ga NMR). Solid-state NMR experiments were obtained using a Varian InfinityPlus spectrometer equipped with a 9.4 T Oxford wide-bore magnet – selected

isotropic chemical shift data are reported herein however a detailed description of the experimental conditions employed and the analyses performed will be presented in another publication. InOTf and [In([18]crown-6)][OTf] were prepared according to reported procedures.^[56] While [In][EX₄] and related salts have been previously reported,^[31, 57, 58] a more facile solution phase synthetic route to these materials is reported. Microanalyses were performed using a Perkin Elmer 2400 Series II C, H, N analyzer in the Centre for Catalysis and Materials Research at the University of Windsor.

6.4.2 Synthetic Procedures

Reactions of [In([18]crown-6)][OTf] with InX₃

In a typical experiment, toluene (40 mL) was added to InX₃ and [In([18]crown-6)][OTf] in a 100 mL Schlenk flask and stirred overnight. All volatile components were removed under reduced pressure and the product is obtained as a colourless powder. Crystals of donor-acceptor complexes were obtained from slow concentration of toluene solutions. Given the necessarily-mixed nature of the resultant products, isolated and percentage yields are not necessarily meaningful in these reactions. Powder X-ray diffraction experiments suggest that the donor-acceptor complexes **6.3** – **6.5** are the only crystalline materials present in the isolated products.

Synthesis of [In][InCl₄]

Toluene (30 mL) was added to InCl₃ (0.513 g, 2.32 mmol) and InCl (0.350 g, 2.32 mmol) in a 100 mL Schlenk flask and refluxed overnight, or until no traces of InCl were visible. All volatile components were removed under reduced pressure and the product is obtained as a colourless powder (0.746 g, 86 % yield). ¹¹⁵In NMR (toluene), no signal observed; ¹¹⁵In NMR (MeCN): $\delta = -1065, 375$

Synthesis of [In][GaCl₄]

Toluene (30 mL) was added to GaCl₃ (0.876 g, 4.97 mmol) and InCl (0.750 g, 4.97 mmol) in a 100 mL Schlenk flask and refluxed overnight, or until no traces of InCl were visible. All volatile components were removed under reduced pressure and the product is obtained as a colourless powder (1.340 g, 82 % yield). ¹¹⁵In NMR (toluene), δ = -1258; ¹¹⁵In NMR (MeCN) δ = -1092; ⁷¹Ga NMR (MeCN): δ = 250

Synthesis of [In][AlCl₄]

Toluene (30 mL) was added to AlCl₃ (0.251 g, 1.89 mmol) and InCl (0.284 g, 1.89 mmol) in a 100 mL Schlenk flask and refluxed overnight, or until no traces of InCl were visible. All volatile components were removed under reduced pressure and the product is obtained as a colourless powder (0.376 g, 70 % yield). ¹¹⁵In NMR (toluene): δ = -1264; ²⁷Al NMR (toluene): δ = 102; ²⁷Al SS-NMR: δ_{iso} = 100

Synthesis of [In([18]crown-6)][AlCl₄]

Toluene (30 mL) was added to AlCl₃ (0.251 g, 1.89 mmol) and InCl (0.284 g, 1.89 mmol) in a 100 mL Schlenk flask and refluxed overnight, or until no traces of InCl were visible. The solution was then cooled to -78 °C and a toluene (10 mL) [18]crown-6 (0.500 g, 1.89 mmol) solution was added to the reaction mixture. Immediately upon addition of [18]crown-6 a colour change was observed. The reaction mixture was allowed to warm to room temperature and all volatile components were removed under reduced pressure and the product is obtained as a colourless powder after washing with pentane (0.875 g, 84.5 % yield). ¹¹⁵In NMR (MeCN): δ = -1085; ²⁷Al NMR (MeCN): δ = 104; ¹¹⁵In SS-NMR: δ_{iso} = -1115; ²⁷Al SS-NMR: δ_{iso} = 100 Anal. Calcd. C% 25.81 (26.30), H% 4.91 (4.41)

Synthesis of [In([18]crown-6)][GaCl₄]

Toluene (30 mL) was added to GaCl₃ (0.333 g, 1.89 mmol) and InCl (0.284 g, 1.89 mmol) in a 100 mL Schlenk flask and refluxed overnight, or until no traces of InCl were visible. The solution was then brought to room temperature and a toluene (10 mL) [18]crown-6 (0.500 g, 1.89 mmol) solution was added to the reaction mixture. All volatile components were removed under reduced pressure and the product is obtained as a colourless powder after washing with pentane (0.994 g, 89 % yield). ¹H NMR (CD₃CN): δ = 3.629 (s, CH₂); ¹³C NMR (CD₃CN): δ = 70.30; ¹¹⁵In NMR (MeCN): δ = -1077; ⁷¹Ga NMR (MeCN): δ = 250; ¹¹⁵In SS-NMR: δ_{iso} = -1115; ⁷¹Ga SS-NMR: δ = 246; Anal. Calcd. C% 24.50 (24.40), H% 3.93 (4.10)

Synthesis of [In([15]crown-5)][GaCl₄]

A toluene (5 mL) solution of [15]crown-5 (0.351 g, 1.59 mmol) was added to a toluene (15 mL) solution of [In][GaCl₄] (0.520 g, 1.59 mmol). All volatile components were removed under reduced pressure and the product is obtained as a colourless powder after washing with pentane (0.890 g, 98 % yield). ¹H NMR (CD₃CN): δ = 3.701 (s, CH₂); ¹³C NMR (CD₃CN): δ = 69.80; ¹¹⁵In NMR (CD₃CN): δ = -990; Anal. Calcd. C% 22.66 (21.97), H% 3.66 (3.69)

Synthesis of [In([15]crown-5)₂][GaCl₄]

A toluene (5 mL) solution of [15]crown-5 (0.629 g, 2.86 mmol) was added to a toluene (15 mL) solution of [In][GaCl₄] (0.466 g, 1.43 mmol). All volatile components were removed under reduced pressure and the product is obtained as a colourless powder after washing with pentane (1.022 g, 93 % yield). ¹H NMR (CD₃CN): δ = 3.649 (s, CH₂); ¹³C NMR (CD₃CN): δ = 69.80; ¹¹⁵In NMR (CD₃CN): δ = -990; Anal. Calcd. C% 30.92 (31.32), H% 4.57 (5.25)

Synthesis of [In([15]crown-5)]₂[In₂Cl₆]

A toluene (5 mL) solution of [15]crown-5 (0.351 g, 1.59 mmol) was added to a toluene (15 mL) solution of [In][InCl₄] (0.592 g, 1.59 mmol). All volatile components were removed under reduced pressure and the product is obtained as a crystalline material via slow concentration of a toluene solution of the colourless powder obtained from the reaction.

6.4.3. Crystallographic Investigations

Each subject crystal was covered in Nujol[®], mounted on a goniometer head and rapidly placed in the dry N₂ cold-stream of the low-temperature apparatus (Kryoflex) attached to the diffractometer. The data were collected using the SMART software^[59] on a Bruker APEX CCD diffractometer using a graphite monochromator with MoK α radiation ($\lambda = 0.71073 \text{ \AA}$). A hemisphere of data was collected using a counting time of 10 or 30 seconds per frame at -100 °C. Data reductions were performed using the SAINT-Plus software^[60] and the data were corrected for absorption using SADABS.^[61] Each structure was solved by direct methods using SIR97^[62] and refined by full-matrix least-squares on F^2 with anisotropic displacement parameters for the heavy atoms using SHELXL-97^[63] and the WinGX^[64] software package, the solution were assessed using tools in PLATON, and thermal ellipsoid plots were produced using SHELXTL^[65] For compound **6.3**·[**18**]crown-**6**, the SQUEEZE routine was used to remove a significantly-disordered toluene molecule, for compound **6.5**, the [18]crown-6 ligand was modeled using a 2-position disorder model (refined to occupancies of 51% and 49%) in which the ligand atoms were refined isotropically and constrained to have identical thermal parameters. Details of the data collection and refinement are provided in Tables 6 and 7.

CCDC 688038-688040 and 792956-792960 contain the supplementary crystallographic data for this paper. These data can be obtained free of charge from The Cambridge Crystallographic Data Centre via www.ccdc.cam.ac.uk/data_request/cif.

Powder X-ray diffraction experiments were performed with a Bruker D8 Discover diffractometer equipped with a Hi-Star area detector using Cu K α radiation ($\lambda = 1.54186$ Å). Powder XRD pattern simulations were performed using Mercury CSD 2.2.^[66] For known compounds, these patterns were simulated on the basis of relevant data contained in the Cambridge Structural Database.^[67]

Table 6.6: Crystallographic Information for **6.3**, **6.3·CH₂Cl₂**, **6.3·[18]crown-6**, and **6.4**

Compound No.	6.3	6.3·CH₂Cl₂	6.3·[18]crown-6	6.4
CCDC No.	688039	688040	792956	688038
Empirical formula	C ₁₂ H ₂₄ Cl ₄ In ₂ O ₆	C ₁₃ H ₂₆ Cl ₆ In ₂ O ₆	C ₁₈ H ₃₆ Cl ₄ In ₂ O ₉	C ₁₂ H ₂₄ Br ₄ In ₂ O ₆
Formula weight	635.75	720.68	767.91	813.59
Temperature	173(2) K	173(2) K	173(2) K	173(2) K
Wavelength	0.71073 Å	0.71073 Å	0.71073 Å	0.71073 Å
Crystal system	Monoclinic	Monoclinic	Triclinic	Orthorhombic
Space group	<i>P</i> 2 ₁ / <i>n</i>	<i>P</i> 2 ₁ / <i>c</i>	<i>P</i> -1	<i>Pna</i> 2 ₁
Unit cell dimensions	a = 8.6788(12) Å b = 17.046(2) Å c = 14.525(2) Å $\alpha = 90^\circ$ $\beta = 95.011(2)^\circ$ $\gamma = 90^\circ$	a = 14.0025(14) Å b = 8.6592(9) Å c = 21.242(2) Å $\alpha = 90^\circ$ $\beta = 104.9460(10)^\circ$ $\gamma = 90^\circ$	a = 8.6372(9) Å b = 12.8034(14) Å c = 14.2347(16) Å $\alpha = 89.9820(10)^\circ$ $\beta = 88.7630(10)^\circ$ $\gamma = 88.8560(10)^\circ$	a = 15.6431(17) Å b = 10.0116(11) Å c = 14.0846(16) Å $\alpha = 90^\circ$ $\beta = 90^\circ$ $\gamma = 90^\circ$
Volume (Å ³)	2140.5(5)	2488.5(4)	1573.5(3)	2205.8(4)
Z	4	4	2	4
Density (calculated) g·cm ⁻³	1.973	1.924	1.621	2.450
Absorption coefficient (mm ⁻¹)	2.676	2.522	1.842	9.358
F(000)	1240	1408	764	1528
Crystal size	0.20 x 0.10 x	0.20 x 0.10 x 0.1	0.20 x 0.20 x	0.50 x 0.30 x

(mm ³)	0.05		0.10	0.20
Theta range for data collection	2.39 to 27.50°	1.51 to 27.50°	1.43 to 27.50°	2.42 to 28.26°
Index ranges	-11 ≤ h ≤ 11 -21 ≤ k ≤ 22 -18 ≤ l ≤ 18	-18 ≤ h ≤ 17 -10 ≤ k ≤ 11 -26 ≤ l ≤ 27	-11 ≤ h ≤ 11 -16 ≤ k ≤ 16 -18 ≤ l ≤ 17	-20 ≤ h ≤ 20 -13 ≤ k ≤ 13 -18 ≤ l ≤ 18
Reflections collected	18466	27066	17480	23698
Independent reflections	4253 [R _{int} = 0.0978]	5658 [R _{int} = 0.0482]	6959 [R _{int} = 0.0309]	5139 [R _{int} = 0.0237]
Completeness to theta = 27.50°	86.5 %	99.1 %	96.4 %	96.6 %
Absorption correction		Semi-empirical from equivalents		
Max. and min. Transmission	0.875 and 0.744	0.777 and 0.674	0.831 and 0.725	0.154 and 0.099
Refinement method		Full-matrix least-squares on F ²		
Data / restraints / parameters	4253 / 0 / 217	5658 / 0 / 244	6959 / 0 / 298	5139 / 1 / 218
Goodness-of-fit (S ^b) on F ²	0.728	1.064	1.033	1.073
Final R indices [I > 2σ(I)] ^a	R1 = 0.0426 wR2 = 0.0807	R1 = 0.0347 wR2 = 0.0773	R1 = 0.0347 wR2 = 0.0730	R1 = 0.0217 wR2 = 0.0526
R indices (all data) ^a	R1 = 0.0914 wR2 = 0.0895	R1 = 0.0575 wR2 = 0.0950	R1 = 0.0482 wR2 = 0.0764	R1 = 0.0245 wR2 = 0.0535
Largest diff. peak and hole (e·Å ⁻³)	0.765 and -0.649	1.415 and -0.648	1.273 and -0.915	0.754 and -0.781

^aR1(F) = $\frac{\sum(|F_o| - |F_c|)/\sum|F_o|}{\sum(|F_o| - |F_c|)^2/\sum w(|F_o|^2)^2}$ ^{1/2}, where w is the weight given each reflection. ^bS = $[\frac{\sum w(|F_o|^2 - |F_c|^2)^2}{(n-p)}]$ ^{1/2}, where n is the number of reflections and p is the number of parameters used.

Table 6.7: Crystallographic Information for **6.5**, **6.9**, **6.12**, and **6.13**

Compound No.	6.5	6.9	6.12	6.13
CCDC No.	792957	792960	792959	792958
Empirical formula	C ₁₂ H ₂₄ I ₄ InO ₆	C ₁₂ H ₂₅ Cl ₆ Ga ₂ InO ₇	C ₁₀ H ₂₀ Cl ₄ GaInO ₅	C _{13.50} H ₂₄ Cl ₃ In ₂ O ₅
Formula weight	1001.55	748.28	546.60	602.32
Temperature	173(2) K	173(2) K	173(2) K	173(2) K
Wavelength	0.71073 Å	0.71073 Å	0.71073 Å	0.71073 Å
Crystal system	Monoclinic	Monoclinic	Monoclinic	Triclinic
Space group	<i>P2₁/n</i>	<i>P2₁/c</i>	<i>P2₁/c</i>	<i>P-1</i>
Unit cell dimensions (Å, °)	a = 10.5624(19) b = 16.074(3) c = 14.461(3) α = 90° β = 90.044(2)° γ = 90°	a = 15.998(2) b = 8.8836(13) c = 18.737(3) α = 90° β = 106.1380(10)° γ = 90°	a = 7.2783(5) b = 16.6877(11) c = 16.0592(11) α = 90° β = 101.7690(10)° γ = 90°	a = 10.2308(11) b = 10.6643(12) c = 10.6922(12) α = 71.8580(10)° β = 74.0800(10)° γ = 79.7460(10)°
Volume (Å ³)	2455.2(8)	2558.0(6)	1909.5(2)	1060.6(2)
Z	6	4	4	2
Density (calculated) (g·cm ⁻³)	2.710	1.943	1.901	1.886
Absorption coefficient (mm ⁻¹)	6.929	3.640	3.191	2.570
F(000)	1816	1464	1072	538
Crystal size (mm ³)	0.10 x 0.05 x 0.02	0.30 x 0.20 x 0.10	0.20 x 0.20 x 0.10	0.40 x 0.30 x 0.20
Theta range for data collection	1.89 to 27.50°	1.33 to 28.28°	1.78 to 27.50°	2.02 to 27.49°
Index ranges	-12 ≤ h ≤ 13 -21 ≤ k ≤ 20 -18 ≤ l ≤ 18	-20 ≤ h ≤ 20 -11 ≤ k ≤ 11 -23 ≤ l ≤ 23	-9 ≤ h ≤ 9 -21 ≤ k ≤ 21 -20 ≤ l ≤ 20	-13 ≤ h ≤ 13 -13 ≤ k ≤ 13 -13 ≤ l ≤ 13
Reflections collected	18889	27951	20949	11766
Independent reflections	5509 [R _{int} = 0.1294]	5969 [R _{int} = 0.0384]	4336 [R _{int} = 0.0411]	4670 [R _{int} = 0.0200]
Completeness to theta = 27.50°	97.8 %	94.1 %	98.6 %	95.7 %
Absorption correction		Semi-empirical from equivalents		
Max. and min. transmission	0.871 and 0.423	0.695 and 0.505	0.727 and 0.599	0.598 and 0.517
Refinement		Full-matrix least-squares on F ²		

method				
Data / restraints / parameters	5509 / 36 / 212	5969 / 0 / 257	4336 / 0 / 190	4670 / 8 / 197
Goodness-of-fit (S^b) on F^2	1.300	1.089	1.058	1.147
Final R indices [$I > 2\sigma(I)$] ^a	R1 = 0.1025 wR2 = 0.2121	R1 = 0.0310 wR2 = 0.0712	R1 = 0.0347 wR2 = 0.0635	R1 = 0.0395 wR2 = 0.1197
R indices (all data) ^a	R1 = 0.2126 wR2 = 0.2409	R1 = 0.0465 wR2 = 0.0838	R1 = 0.0468 wR2 = 0.0699	R1 = 0.0436 wR2 = 0.1286
Largest diff. peak and hole ($e \cdot \text{\AA}^{-3}$)	1.348 and -1.129	0.873 and -0.493	0.606 and -0.389	1.812 and -0.873

^a $R1(F) = \Sigma(|F_o| - |F_c|) / \Sigma|F_o|$ for reflections with $F_o > 4(\Sigma(F_o))$. $wR2(F^2) = \{\Sigma w(|F_o|^2 - |F_c|^2)^2 / \Sigma w(|F_o|^2)^2\}^{1/2}$, where w is the weight given each reflection. ^b $S = [\Sigma w(|F_o|^2 - |F_c|^2)^2] / (n-p)^{1/2}$, where n is the number of reflections and p is the number of parameters used.

6.4.4. Computational Methods

All density functional theory (DFT) calculations were performed using the B3PW91 method^[68] using the Gaussian 03^[69] or 09^[70] suites using the SHARCNET high-performance computing network (www.sharcnet.ca). Where applicable, the Stuttgart group (SDD) effective core potentials (ECP) and corresponding basis sets were used for indium and iodine atoms^[71] and the 6-31+G(d) basis set was used for all lighter atoms. Natural bond order (NBO) analyses^[72] to determine Wiberg bond indices, orbital contributions, and HOMO/LUMO energies were obtained using the routine included in the Gaussian distributions. All stationary points were confirmed to be minima exhibiting no imaginary frequencies. It should be noted that for determining the "snapping energy" of indium-indium bonds in the donor acceptor complexes **6.3**, **6.4**, and **6.5**, the geometries were obtained from the crystal structures with H atoms placed in idealized positions using the Gaussview application. It should also be noted that geometry optimizations for the nearly cylindrical molecules ligated to [18]crown-6 did not always satisfy all the

convergence criteria because of the very flat potential energy surface; in such cases frequency calculations on the lowest energy structures exhibit no imaginary frequencies; thus, these geometries were used to calculate the required single point energies.

References

- [1] In this work, formal oxidation states are indicated by using Arabic numerals whereas valence states are indicated by using Roman numerals.
- [2] G. Parkin, *J. Chem. Educ.* **2006**, *83*, 791.
- [3] J. A. J. Pardoe, A. J. Downs, *Chem. Rev.* **2007**, *107*, 2.
- [4] D. G. Tuck, *Chem. Soc. Rev.* **1993**, *22*, 269.
- [5] A. Frazer, P. Hodge, B. Piggott, *Chem. Comm.* **1996**, 1727.
- [6] D. L. Reger, *Coord. Chem. Rev.* **1996**, *147*, 571.
- [7] R. A. Fischer, J. Weiss, *Angew. Chem. Int. Ed.* **1999**, *38*, 2831.
- [8] P. Jutzi, B. Neumann, G. Reumann, L. O. Schebaum, H. G. Stammler, *Organometallics* **1999**, *18*, 2550.
- [9] J. D. Gorden, A. Voigt, C. L. B. Macdonald, J. S. Silverman, A. H. Cowley, *J. Am. Chem. Soc.* **2000**, *122*, 950.
- [10] J. D. Gorden, C. L. B. Macdonald, A. H. Cowley, *Chem. Comm.* **2001**, 75.
- [11] N. J. Hardman, P. P. Power, J. D. Gorden, C. L. B. Macdonald, A. H. Cowley, *Chem. Comm.* **2001**, 1866.
- [12] A. H. Cowley, *Chem. Comm.* **2004**, 2369.
- [13] Z. Yang, X. L. Ma, R. B. Oswald, H. W. Roesky, H. P. Zhu, C. Schulzke, K. Starke, M. Baldus, H. G. Schmidt, M. Noltemeyer, *Angew. Chem. Int. Ed.* **2005**, *44*, 7072.
- [14] S. Schulz, A. Kuczkowski, D. Schuchmann, U. Florke, M. Nieger, *Organometallics* **2006**, *25*, 5487.
- [15] T. Bollermann, G. Prabusankar, C. Gemel, R. W. Seidel, M. Winter, R. A. Fischer, *Chem.-Eur. J.* **2010**, *16*, 8846.
- [16] B. Buchin, C. Gemel, T. Cadenbach, I. Fernandez, G. Frenking, R. A. Fischer, *Angew. Chem. Int. Ed.* **2006**, *45*, 5207.
- [17] A. Kempter, C. Gemel, R. A. Fischer, *Chem. Comm.* **2006**, 1551.
- [18] Q. Yu, A. Purath, A. Donchev, H. Schnockel, *J. Organomet. Chem.* **1999**, *584*, 94.
- [19] D. Weiss, M. Winter, K. Merz, A. Knufer, R. A. Fischer, N. Frohlich, G. Frenking, *Polyhedron* **2002**, *21*, 535.
- [20] D. L. Reger, D. G. Garza, A. L. Rheingold, G. P. A. Yap, *Organometallics* **1998**, *17*, 3624.
- [21] D. L. Reger, S. S. Mason, A. L. Rheingold, B. S. Haggerty, F. P. Arnold, *Organometallics* **1994**, *13*, 5049.
- [22] K. Yurkerwich, D. Buccella, J. G. Melnick, G. Parkin, *Chem. Comm.* **2008**, 3305.
- [23] S. P. Green, C. Jones, A. Stasch, *Inorg. Chem.* **2007**, *46*, 11.
- [24] G. J. Moxey, C. Jones, A. Stasch, P. C. Junk, G. B. Deacon, W. D. Woodul, P. R. Drago, *Dalton Trans.* **2009**, 2630.
- [25] W. Uhl, M. Pohlmann, R. Wartchow, *Angew. Chem. Int. Ed.* **1998**, *37*, 961.

- [26] W. Uhl, M. Benter, S. Melle, W. Saak, G. Frenking, J. Uddin, *Organometallics* **1999**, *18*, 3778.
- [27] R. J. Wright, A. D. Phillips, N. J. Hardman, P. P. Power, *J. Am. Chem. Soc.* **2002**, *124*, 8538.
- [28] X. J. Yang, Y. Z. Wang, B. Quillian, P. R. Wei, Z. F. Chen, P. V. Schleyer, G. H. Robinson, *Organometallics* **2006**, *25*, 925.
- [29] L. A. Woodward, G. Garton, H. L. Roberts, *J. Chem. Soc.* **1956**, 3723.
- [30] M. A. Khan, D. G. Tuck, *Inorg. Chim. Acta.-Articles And Letters* **1985**, *97*, 73.
- [31] J. D. Corbett, R. K. McMullan, *J. Am. Chem. Soc.* **1958**, *80*, 4761.
- [32] C. G. Andrews, C. L. B. Macdonald, *Angew. Chem. Int. Ed.* **2005**, *44*, 7453.
- [33] B. F. T. Cooper, C. L. B. Macdonald, *Main Group Chem.* **2010**, *9*, 141.
- [34] S. M. Godfrey, K. J. Kelly, P. Kramkowski, C. A. McAuliffe, R. G. Pritchard, *Chem. Comm.* **1997**, 1001.
- [35] S. P. Green, C. Jones, A. Stasch, *Angew. Chem. Int. Ed.* **2007**, *46*, 8618.
- [36] M. S. Hill, P. B. Hitchcock, R. Pongtavornpinyo, *Dalton Trans.* **2007**, 731.
- [37] K. S. Klimek, C. Cui, H. W. Roesky, M. Noltemeyer, H. G. Schmidt, *Organometallics* **2000**, *19*, 3085.
- [38] G. Linti, M. Buhler, K. Y. Monakhov, T. Zessin, *Dalton Trans.* **2009**, 8071.
- [39] W. Uhl, *Coord. Chem. Rev.* **1997**, *163*, 1.
- [40] W. Uhl, M. Layh, W. Hiller, *J. Organomet. Chem.* **1989**, *368*, 139.
- [41] B. F. T. Cooper, C. G. Andrews, C. L. B. Macdonald, *J. Organomet. Chem.* **2007**, *692*, 2843.
- [42] R. G. Pearson, *J. Am. Chem. Soc.* **1963**, *85*, 3533.
- [43] I. A. Kahwa, D. Miller, M. Mitchel, F. R. Fronczek, R. G. Goodrich, D. J. Williams, C. A. Omahoney, A. M. Z. Slawin, S. V. Ley, C. J. Groombridge, *Inorg. Chem.* **1992**, *31*, 3963.
- [44] I. A. Kahwa, D. Miller, M. Mitchel, F. R. Fronczek, *Acta Crystallogr. Sect. C: Cryst. Struct. Commun.* **1993**, *49*, 320.
- [45] N. S. Fender, S. S. Finegan, D. Miller, M. Mitchell, I. A. Kahwa, F. R. Fronczek, *Inorg. Chem.* **1994**, *33*, 4002.
- [46] A. V. Mudring, F. Rieger, *Inorg. Chem.* **2005**, *44*, 6240.
- [47] F. Rieger, A. V. Mudring, *Inorg. Chem.* **2005**, *44*, 9340.
- [48] M. J. Taylor, D. G. Tuck, *J. Chem. Soc.: Dalton Trans.* **1981**, 928.
- [49] M. A. Khan, D. G. Tuck, *Acta Crystallogr. Sect. B: Struct. Sci.* **1982**, *38*, 803.
- [50] L. A. Kloo, M. J. Taylor, *J. Chem. Soc.: Dalton Trans.* **1997**, 2693.
- [51] B. F. T. Cooper, C. L. B. Macdonald, *J. Organomet. Chem.* **2008**, *693*, 1707.
- [52] R. Bandyopadhyay, B. F. T. Cooper, A. J. Rossini, R. W. Schurko, C. L. B. Macdonald, *J. Organomet. Chem.* **2010**, *695*, 1012.
- [53] A. Y. Timoshkin, G. Frenking, *J. Am. Chem. Soc.* **2002**, *124*, 7240.
- [54] A. Haaland, *Angew. Chem. Int. Ed. Eng.* **1989**, *28*, 992.
- [55] A. B. Pangborn, M. A. Giardello, R. H. Grubbs, R. K. Rosen, F. J. Timmers, *Organometallics* **1996**, *15*, 1518.
- [56] B. F. T. Cooper, C. L. B. Macdonald, *New J. Chem.* **2010**.
- [57] G. Meyer, T. Staffel, M. Irmler, *Thermochimica Acta* **1990**, *160*, 63.
- [58] J. D. Corbett, R. K. McMullan, *J. Am. Chem. Soc.* **1956**, 2906.
- [59] SMART, Bruker AXS Inc., Madison, WI, **2001**.
- [60] SAINTPlus, Bruker AXS Inc., Madison, WI, **2001**.

- [61] SADABS, Bruker AXS Inc., Madison, WI, **2001**.
- [62] WINGX, A. Altomare, M. C. Burla, M. Camalli, G. Cascarano, C. Giacovazzo, A. Guagliardi, M. A. G. G., G. Polidori, R. Spagna, CNR-IRMEC, Bari, **1997**.
- [63] SHELXL-97, G. M. Sheldrick, Universitat Gottingen, Gottingen, **1997**.
- [64] L. J. Farrugia, *Journal of Applied Crystallography* **1999**, 32, 837.
- [65] SHELXTLG. M. Sheldrick, Bruker AXS Inc., Madison, WI, **2001**.
- [66] C. F. Macrae, I. J. Bruno, J. A. Chisholm, P. R. Edgington, P. McCabe, E. Pidcock, L. Rodriguez-Monge, R. Taylor, J. van de Streek, P. A. Wood, *Journal of Applied Crystallography* **2008**, 41, 466.
- [67] F. H. Allen, *Acta Crystallogr. Sect. B: Struct. Sci.* **2002**, 58, 380.
- [68] A. D. Becke, *Journal Of Chemical Physics* **1993**, 98, 5648.
- [69] Gaussian 03, Revision D.01, M. J. Frisch, G. W. Trucks, H. B. Schlegel, G. E. Scuseria, M. A. Robb, J. R. Cheeseman, J. A. Montgomery, T. Vreven, K. N. Kudin, J. C. Burant, J. M. Millam, S. S. Iyengar, J. Tomasi, V. Barone, B. Mennucci, M. Cossi, G. Scalmani, N. Rega, G. A. Petersson, H. Nakatsuji, M. Hada, M. Ehara, K. Toyota, R. Fukuda, J. Hasegawa, M. Ishida, T. Nakajima, Y. Honda, O. Kitao, H. Nakai, M. Klene, X. Li, J. E. Knox, H. P. Hratchian, J. B. Cross, V. Bakken, C. Adamo, J. Jaramillo, R. Gomperts, R. E. Stratmann, O. Yazyev, A. J. Austin, R. Cammi, C. Pomelli, J. W. Ochterski, P. Y. Ayala, K. Morokuma, G. A. Voth, P. Salvador, J. J. Dannenberg, V. G. Zakrzewski, S. Dapprich, A. D. Daniels, M. C. Strain, O. Farkas, D. K. Malick, A. D. Rabuck, K. Raghavachari, J. B. Foresman, J. V. Ortiz, Q. Cui, A. G. Baboul, S. Clifford, J. Cioslowski, B. B. Stefanov, G. Liu, A. Liashenko, P. Piskorz, I. Komaromi, R. L. Martin, D. J. Fox, T. Keith, A. Laham, C. Y. Peng, A. Nanayakkara, M. Challacombe, P. M. W. Gill, B. Johnson, W. Chen, M. W. Wong, C. Gonzalez, J. A. Pople, **2003**.
- [70] Gaussian 09, Revision A.02, M. J. Frisch, G. W. Trucks, H. B. Schlegel, G. E. Scuseria, M. A. Robb, J. R. Cheeseman, G. Scalmani, V. Barone, B. Mennucci, G. A. Petersson, H. Nakatsuji, M. Caricato, X. Li, H. P. Hratchian, A. F. Izmaylov, J. Bloino, G. Zheng, J. L. Sonnenberg, M. Hada, M. Ehara, K. Toyota, R. Fukuda, J. Hasegawa, M. Ishida, T. Nakajima, Y. Honda, O. Kitao, H. Nakai, T. Vreven, J. Montgomery, J. A., J. E. Peralta, F. Ogliaro, M. Bearpark, J. J. Heyd, E. Brothers, K. N. Kudin, V. N. Staroverov, R. Kobayashi, J. Normand, K. Raghavachari, A. Rendell, J. C. Burant, S. S. Iyengar, J. Tomasi, M. Cossi, N. Rega, N. J. Millam, M. Klene, J. E. Knox, J. B. Cross, V. Bakken, C. Adamo, J. Jaramillo, R. Gomperts, R. E. Stratmann, O. Yazyev, A. J. Austin, R. Cammi, C. Pomelli, J. W. Ochterski, R. L. Martin, K. Morokuma, V. G. Zakrzewski, G. A. Voth, P. Salvador, J. J. Dannenberg, S. Dapprich, A. D. Daniels, Ö. Farkas, J. B. Foresman, J. V. Ortiz, J. Cioslowski, D. J. Fox, Gaussian, Inc., Wallingford CT, **2009**.
- [71] A. Bergner, M. Dolg, W. Kuchle, H. Stoll, H. Preuss, *Mol. Phys.* **1993**, 80, 1431.
- [72] A. E. Reed, L. A. Curtiss, F. Weinhold, *Chem. Rev.* **1988**, 88, 899.

Chapter 7: Ligand and Anion Effect on Low Oxidation State Indium Complexes

7.1 Introduction

The ability of indium in the +1 oxidation state to act a Lewis acid (and base) has been under investigation for many years. As discussed in Chapter 1, attempts to ligate indium(+1) centers typically leads to disproportionation resulting in loss of indium metal and the production of higher oxidation state ligated species.^[1-3] As discussed in previous chapters the Macdonald research group has previously shown that the more stable indium(+1) salt, InOTf, forms a monomeric donor-stabilized species in the presence of appropriately sized crown ethers.^[4, 5] In the case of [In([18]crown-6)][OTf], this was the first observed monomer in which the In(+1) center acts as an acceptor; more typically, oligomeric clusters are observed in the solid state for related E(+1) halide complexes.^[1, 6] As discussed in Chapter 6, complexes incorporating In(+1) halides into cyclic ether ligands appear to only be stable in the presence of Lewis acids during the formation of In(I)-In(III) donor-acceptor complexes. Jones et al. showed in 2007 that it is possible to isolate donor-stabilized InBr at low temperatures ($-30^{\circ}\text{C} < T < -20^{\circ}\text{C}$), however, disproportionation to $\text{In}_2\text{Br}_4 \cdot 2\text{tmeda}$ (tmeda = tetramethylethylenediamine) is observed above this temperature. Similar attempts to coordinate tmeda to InI resulted in the formation of the mixed valent indium cluster, $\text{In}_6\text{I}_8(\text{tmeda})_4$.^[1]

In several cases it has been possible to isolate neutral low oxidation state indium compounds using anionic ligands in which the negative charge is incorporated into the organic framework. It is likely that these species are able to be isolated as a result of either steric hindrance of possible disproportionation pathways, such as in the case of $\text{In}(\text{C}_6\text{H}_3\text{-2,6-Trip}_2)$ (Trip = $\text{C}_6\text{H}_2\text{-2,4,6-}^i\text{Pr}_3$),^[7] electronic stabilization, as is likely for

Cp*In,^[8] or a combination of the two, such as in the cases of molecules such as In(nacnac) and indium trispyrazolylborates and their derivatives.^[9-15]

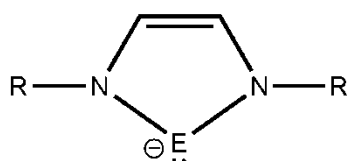
Overall, the observation of a low oxidation state indium salt forming a complex with a neutral ligand remains rare. The previously-mentioned cyclic ether complexes have recently been joined by series of diiminopyridine ligands (also featuring InOTf as the acceptor) as some of the only examples available in the literature that form stable, monomeric, low oxidation state species at ambient temperature.^[16, 17] One electronic feature common to both the stable cyclic ether complexes and the diiminopyridine complexes is the lack of strong covalent bonding interactions between the ligand and the indium center.^[17]

It is worth noting that the nature of the anion is also clearly important factor in the stability of such complexes. As has been discussed, univalent indium halides are not capable of being stabilized as acid-free entities using crown ethers (or dimpy ligands); however, univalent triel salts with very non-interacting anions appear to be more amenable to the formation of stable adducts. For example, Krossing et al. reported a low valent gallium salt that acts as a Lewis acid to triphenylphosphine donors.^[18]

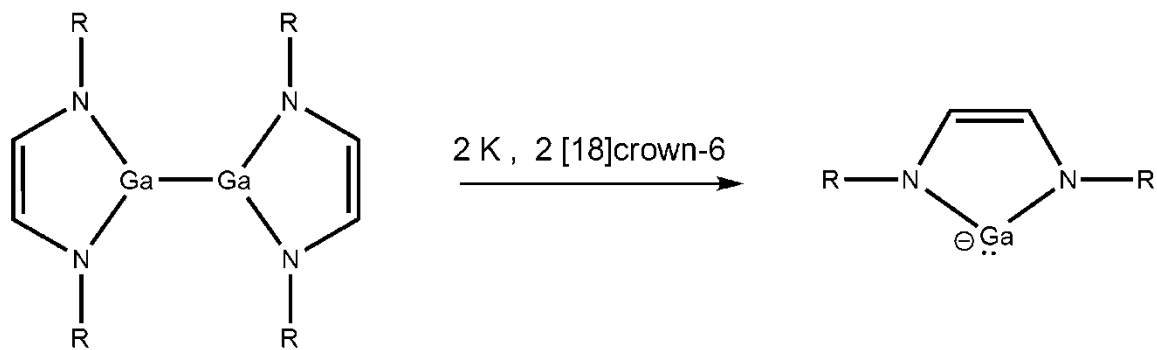
Importantly, the fluorinated aluminate non-coordinating anion (NCA) in this salt lacks any localized bonding interaction with the triel center in this salt. The related indium salt of the same NCA was prepared by Scheer et al. and allowed for indium coordination by weakly nucleophilic polyphosphide ligands.^[19] This chapter will analyse the role of the ligand and anion in formation of Lewis adducts with low oxidation state triel centers.

7.2. Reactivity of Triel Centers Towards Diazabutadiene Ligands

Several computational investigations into group 13 N-heterocyclic carbene (NHC) analogues have focused on analyses of group 13 diazabutadiene (DAB) complexes, Scheme 7.1, and suggest that the bonding between indium and the nitrogen atoms of the DAB ligand is primarily ionic in nature.^[20-23] Anions of this type are typically synthesized by reduction of existing dimers (or their isomers in the case of Ga) and cleavage of an E-E bond.^[24]



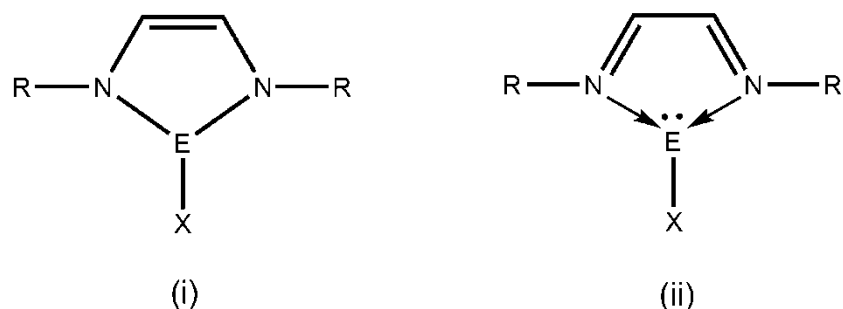
Scheme 7.1: Group 13 NHC analogues



Scheme 7.2: Synthesis of a gallium NHC analogue

The nature of the bonding between the metal center and the DAB fragment in a formal complex of a neutral DAB ligand and a neutral univalent group 13 species has the potential to be described by two different extreme canonical structures as illustrated in Scheme 7.3. These two potential bonding motifs between a DAB ligand and an E-X species include a covalent interaction where the "lone pair" of electrons is formally transferred to the DAB ligand or the formation of a donor-acceptor complex where the

"lone pair" remains associated with the metal center. The presence and location of the substituent on E in such a neutral complex will have an effect on the reactivity and stereochemistry of the "lone pair" of electrons associated with the metal center and thus will have an impact on the nature of the bonding and electron distribution within the complex. The substituent may have both electronic and steric implications as it has the potential to provide the triel center with more electron density and fill coordination sites that could otherwise be occupied by the electron pair.

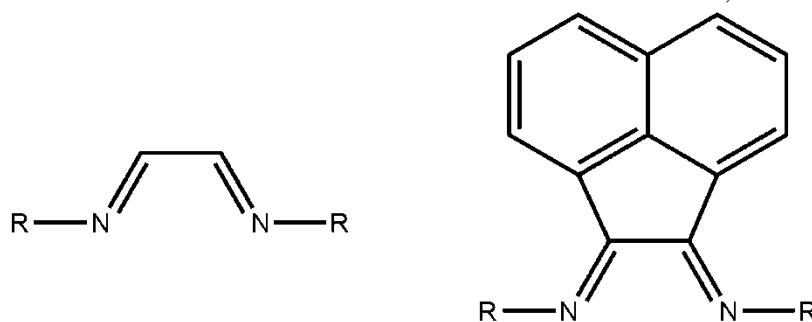


Scheme 7.3: Potential canonical forms for DAB complexes of E-X species; (i) ligand reduction and covalent bonding; (ii) donor-acceptor complex formation

In light of the poor solubility of the indium(I) halides, and their propensity towards disproportionation upon reactions with Lewis bases (and the previously discussed successful isolation of diiminopyridine indium triflate complexes), the more stable and soluble InOTf reagent was selected for the attempts to synthesize indium(I) diimine complexes. Thus, equimolar amounts of InOTf and either DAB or BIAN ligand were allowed to react in toluene solutions, Table 7.1.

Table 7.1: Diimine reactions with InOTf

Ligand Employed	Colour Observed	Microanalysis
^{Mes} BIAN	deep red / purple	Calc: C – 54.72; H – 4.15; N – 4.12 Obs: C – 52.17; H – 4.25; N – 3.79
^{Mes} DAB	orange	Calc: C – 47.27; H – 4.83; N – 4.79 Obs: C – 48.11; H – 4.69; N – 4.80
^{Diip} BIAN	orange	Calc: C – 58.12; H – 5.27; N – 3.66 Obs: C – 57.59; H – 5.21; N – 3.31
^{Diip} DAB	orange	Calc: C – 52.10; H – 6.03; N – 4.19 Obs: C – 52.85; H – 6.42; N – 4.14



Scheme 7.4: ^RDAB and ^RBIAN Ligands

Although characteristic color changes were observed in all cases upon reaction, conclusive spectroscopic or structural information into the nature of these complexes has remained elusive. Attempts at obtaining high quality crystals suitable for single crystal X-ray diffraction studies were unsuccessful in all cases; however, the crystallographic investigation of small, poor-quality crystalline material isolated from the reaction of InOTf with ^{Mes}DAB yielded a structure, depicted in Figure 7.1, that is sufficient to establish the connectivity and general features of the complex. Interestingly, the resulting structure features a non-planar, three coordinate complex in a distorted but clearly pyramidal geometry. The observed shape implies a vacancy that is consistent with the presence of a stereochemically-active "lone pair" of electrons on the indium center and

suggests that the preferred bonding motif for this complex is not a covalent reduction of the DAB ligand, but rather, the formation of a donor acceptor complex.

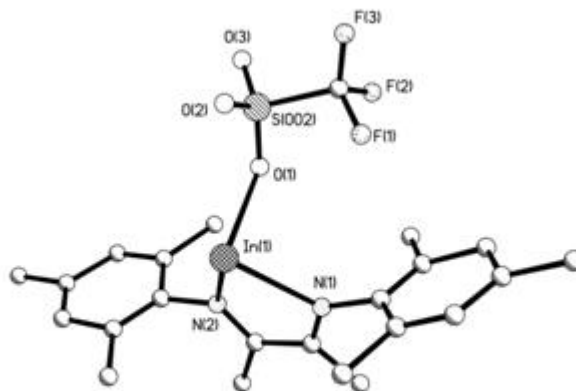


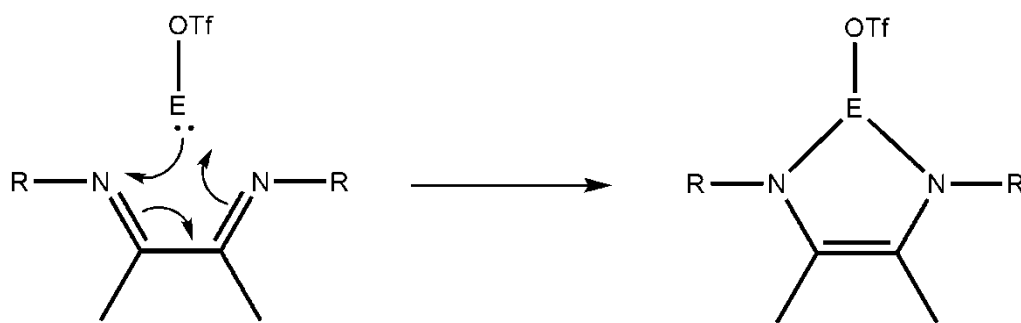
Figure 7.1: Low quality solid state structure of $\text{InOTf} \cdot \text{MesDAB}$. Selected bond distances (Å): $\text{In}(1)\text{-N}(1)$, 2.5091(4); $\text{In}(1)\text{-N}(2)$, 2.4925(4); $\text{In}(1)\text{-O}(1)$, 2.4617(4); $\text{N}(1)\text{-C}(1)$, 1.2274(2); $\text{N}(2)\text{-C}(2)$, 1.2814(2); $\text{C}(1)\text{-C}(2)$, 1.5100(3); $\text{S-O}_{(\text{range})}$, 1.417-1.441.

An important distinction between this DAB complex and diiminopyridine complexes reported by Richeson and co-workers is that the steric properties of the diiminopyridine ligands prohibit any interaction between the indium center and the triflate anion; thus, no direct comparison can be made between certain structural characteristics (i.e., coordination number, etc.). In addition, the low quality of the structure also makes a detailed examination of metrical parameters unwise.

Because the structural evidence obtained experimentally cannot be used to draw comparisons to other imine complexes, the computational analysis of DAB complexes of E-X species was pursued in order to provide insight into the nature of bonding in these

systems. As previously discussed, Richeson et al. report very little covalent interaction between the diiminopyridine ligand and the indium center; in addition, they have further investigated these species computationally and propose that the lower the 5s orbital contribution to the HOMO of the diiminopyridine complex, the more stable it will be.^[17] This conclusion is related to the proposition in Chapter 6 that the greater 5s character associated with the indium center should produce the most stable species; any apparent difference in the interpretation is simply a result of considering the situation in terms of the molecule rather than the indium atom. It is anticipated that Natural Bond Order (NBO), Wiberg Bond Index (WBI), and other computational analyses will allow for the rationalization of the similarities and differences between the two related complexes.

Initial geometry optimizations were performed on the model complexes of the form $EOTf \cdot^H DAB$ ($E = Ga, In$) in order to establish the ideal structures adopted by these two species. The gallium analogues were calculated in order to probe the viability of the "ligand reduction" pathway, Scheme 7.5, given that the oxidation of $Ga(+1)$ to $Ga(+3)$ is considerably more favourable than for the indium analogue.



Scheme 7.5: Formal ligand reduction during the complexation of EOTf species by DAB ligands

The resulting B3PW91 optimized structures, Figure 7.2, show that a pyramidal geometry is favoured for both the indium and gallium analogues. While the ideal structure for the indium analogue agrees with the low quality crystal structure, the pyramidal shape exhibited in the gallium analogue is somewhat surprising given the aforementioned unfavorability of monovalent gallium relative to the trivalent alternative. Summation of the angles around the metal center for the two model compounds provides a total of 269° for indium and 307° for gallium, highlighting the much more pyramidal environment at the indium center.

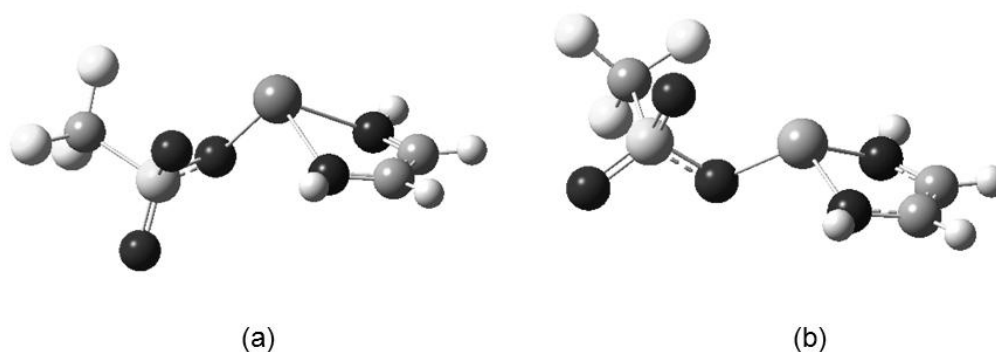


Figure 7.2: Optimized structures of EOTf^HDAB; (a) E = In, (b) E = Ga

Examination of the charges associated with the EOTf fragment and the DAB ligand reveals the degree of charge transfer from the metal center to the ligand. As expected, the gallium analogue has a higher degree of charge transfer to the DAB ligand, a -0.705 charge for E = Ga; while the ligand charge is found to be -0.349 for E = In. The degree of charge transfer is also evident upon NBO analyses, as a "lone pair" of electrons is still associated with the indium center, while no "lone pair" is present in the NBO output for the gallium analogue. For most of the computational analyses, models in

which hydrogen atoms were used as the substituents on the nitrogen were employed to minimize the calculation times, and allow comparisons between metal centers and anions. However, test calculations using a full model $\text{InOTf} \cdot \text{MesDAB}$ demonstrate that the substituent on nitrogen plays a large role on the electronic properties of the system; in this case, the charge transfer from the InOTf to the ligand drops to a negligible 0.043. The charge attributed to the ligand for two putative ionic $[\text{E}(\text{DAB})^x]$ complexes ($x = +1$ or -1) were calculated in order to compare the values of the triflate complexes to systems with and without ligand reduction. Thus, calculations were performed on the model complexes $[\text{E}(\text{DAB})^+]$, and the group 13 NHC analogue, $[\text{E}(\text{DAB})^-]$. The resulting charges on the DAB ligand moiety for the cationic models were found to be 0.104 (In) and 0.147 (Ga), while those in the anionic models were found to be -1.374 and -1.344 for indium and gallium respectively. The calculations illustrate the presence of a "lone pair" of electrons on the triel centre in both cases, with the two extra electrons added to the anionic system being primarily transferred to the DAB ligand.

An analysis of the metrical parameters of the calculated complexes, particularly the carbon-carbon and carbon-nitrogen bond distances, allows some insight into the effect of charge transfer into the ligand. As electron density is transferred from the metal center to the ligand based LUMO the bond distances should reflect this. The observed bond distances for the $[\text{E}(\text{DAB})^+]$ cations help illustrate the lack of charge transfer to the ligand as the C-C bond distance for each metal was found to be 1.494 Å and the C-N distances were found to be 1.274 Å (E = In) and 1.275 Å (E = Ga). The longer C-C distance is consistent with the presence of a single bond, while the shorter C-N distance is indicative of a double bond. The E-N bond distances were found to be 2.558 Å (E = In) and 2.306 Å

(E= Ga) which is to be expected based on the size increase from gallium to indium. The addition of two electrons to the system in $[E(DAB)^-]$ affords C-C bond distances of 1.370 Å (E= In) and 1.366 Å (E= Ga), C-N bond distances of 1.384 Å (E= In,Ga), and E-N distances of 2.174 Å (E= In) and 1.971 Å (E= Ga). The elongation of the C-N bonds and the contraction of the C-C bond are expected based on the reduction of the ligand. Interestingly, the E-N bond distances are much shorter in the anionic species, reflecting the increased covalent nature of the bonding between the triel center and the nitrogen atoms. Having analysed the metrical parameters of these ions, comparisons to the EOTf complexes can now be discussed. For the indium complex, InOTf·DAB, the bond distances were found to be, C-C 1.431 Å, C-N 1.313 Å, and In-N 2.270 / 2.230 Å and are comparable to the distances found in the $[E(DAB)^+]$ complex with exception of the much shorter In-N distance which is found to lie between the values obtained for the cation and anion. The increased metal-to-ligand charge transfer observed in the gallium complex is reflected in the metrical parameters as the bond distances were found to be; C-C 1.384 Å, C-N 1.360/1.361 Å, and E-N 1.905/1.910 Å, and are much closer to those observed for the $[E(DAB)^-]$ anion than the cation. The metrical parameters from the calculation performed on the experimentally isolated complex, InOTf·^{Mes}DAB, showed close correlation to the $[E(DAB)^+]$ cation and illustrates the lack of charge transfer to the ligand for this species as the bond distances were found to be, C-C 1.500 Å, C-N 1.290 Å, and E-N 2.445/2.447 Å.

As part of the investigation of the properties of "crowned" indium donors in Chapter 6, it was noted that the counter-anion/substituent on In played a role in the energy and availability of the "lone pair" of electrons on the indium center. Since a chloride

substituent was found to give the highest energy electron pair for those species, calculations into DAB complexes of E-Cl were performed in order to ascertain the effects of altering the group bound to the triel element. The optimized geometries for these species are depicted in Figure 7.3.

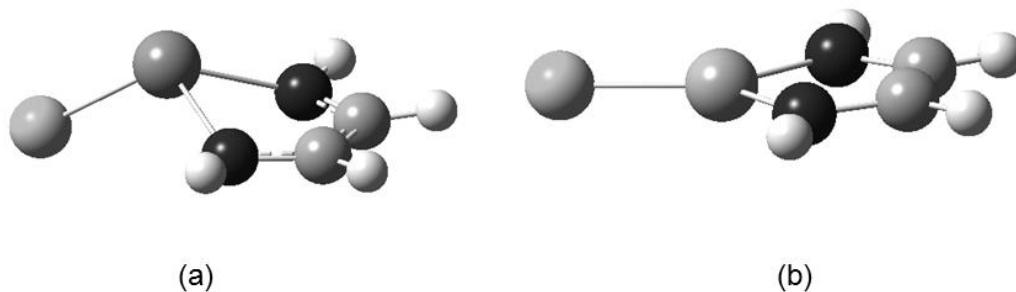


Figure 7.3: Optimized structures of $ECl \cdot {}^HDB$; (a) $E = In$; (b) $E = Ga$

While the optimized indium structure appears to be moving closer to a planar arrangement, the geometry at the metal center is still pyramidal and clearly a complete reduction of the HDB ligand has not occurred. However, for the gallium analogue a planar geometry is observed at the metal center, further illustrating the effect that substituents play in the relative reactivity of the "lone pair" of electrons in $E(+1)$ species. While the indium analogue is not completely reduced, it should be noted that the NBO output for $InCl \cdot {}^HDB$ does not identify a "lone pair" associated with the indium center. Looking at the charge associated with the DAB ligand in these chloride complexes, one sees an increase in charge transfer to the ligand from the triflate analogues. For $E = In$, the charge transfer increases from -0.349 to -0.586, while for $E = Ga$, it increases from -0.705 to -1.020, meaning that exchanging a triflate anion for a chloride anion results in an increase in charge transfer of 0.237 (68% increase) and 0.315 (45% increase),

respectively. The increased charge transfers observed in the ECl complexes are reflected in the metrical parameters when compared to the EOTf complexes as this results in a slight elongation of the C-N bonds, 1.339 Å, and slight contraction of the C-C and E-N bonds to 1.404 Å and 2.155 respectively when E = In. For E = Ga the distances are found to be C-C, 1.358 Å, C-N, 1.395 Å, and E-N, 1.837 Å and are similar to those found for the [E(DAB)]⁻ anion. One interesting feature to note is that even with the symmetry of a putative InCl·DAB complex constrained to be C_{2v}, the reduction of the ligand to form a planar complex did not occur, the DAB ligand and the InCl fragments instead separated in space, and the "lone pair" of electrons remained associated with the indium center.

Analysis of the highest occupied molecular orbital (HOMO) for ECl·DAB species, Figure 7.4, illustrates the increased interaction of the gallium atom with the DAB ligand compared to the indium analogue. In fact, the appearance of the molecular orbital for the gallium analogue is as one would anticipate if the 2 e⁻ charge transfer from the metal to the ligand is complete.

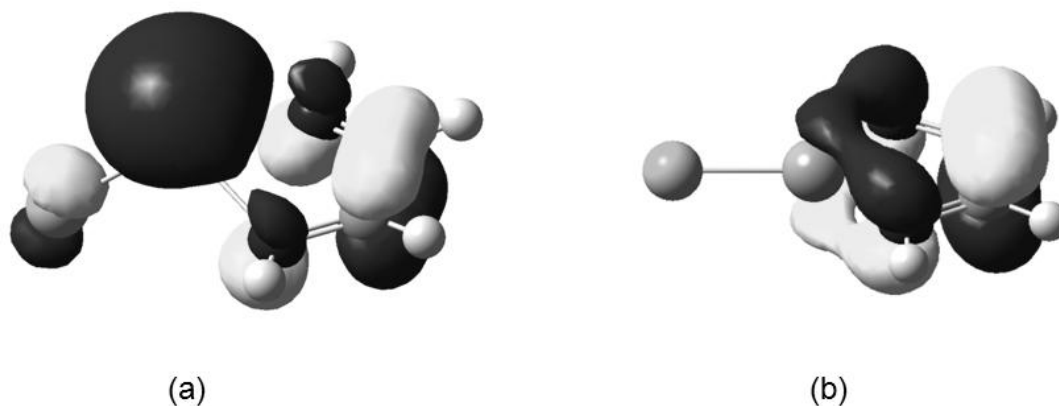


Figure 7.4: Highest Occupied Molecular Orbital of; (a) $\text{InCl} \cdot \text{H DAB}$; (b) $\text{GaCl} \cdot \text{H DAB}$

One further feature of these complexes worth discussing are the Wiberg bond indices (WBI) obtained for the bonds between the metal center and the substituents. A comparison of these values allows for a few observations. The WBI between the metal center E and the nitrogen atoms of the DAB ligand are significantly increased when the substituent on the nitrogen center is changed from a mesityl group to a hydrogen atom. This is particularly important to note given that any synthetic targets are likely to be made from N-aryl or N-alkyl R^{DAB} ligands and thus will have a lower degree of covalency than suggested by these computational studies. Indeed, much like the isolated diiminopyridine complexes reported by Richeson, the WBI for the $\text{InOTf} \cdot \text{Mes}^{\text{DAB}}$ complex is found to be relatively small at ~ 0.14 . As anticipated, changing the metal substituent from [OTf] to [Cl] results in a large increase in the WBI observed between the metal center and the anion. Coupled with the increase in charge transfer to the ligand, the increase of the WBI observed between the DAB ligand and the metal center illustrates the importance of the metal substituent on the strength of the metal-ligand interaction. This conclusion is not entirely unexpected, as higher oxidation state species are more

likely to bond in a covalent manner (on the basis of electronegativity arguments). While complete oxidation of the metal center is not achieved in most cases, the increased covalency of the bonding correlates to the increased positive charge associated with the metal center.

Table 7.2: Lone pair and WBI data of DAB species

Model	E(In LP) (eV)	%s character	WBI E-X	WBI E-N
GaCl ^H DAB	N/A	N/A	0.842	0.725 / 0.725
GaOTf ^H DAB	N/A	N/A	0.3621	0.664 / 0.663
InCl ^H DAB	N/A	N/A	0.5946	0.562 / 0.562
InOTf ^H DAB	-6.456	87.24	0.1968	0.441 / 0.424
InOTf ^{Mes} DAB	-6.746	94.36	0.133	0.144 / 0.141

Although the WBI values observed between the metal center and the nitrogen atoms may be inflated due to the presence of hydrogen substituents on nitrogen, one may draw the conclusion that an increased degree of covalent interaction between the metal center and its substituents has been found to increase the energy of the "lone pair" of electrons and subsequently change the observed optimized structures. Further analyses of the effects of anions on the lone pair energy are presented in the next section.

7.3. Role of the Anion in [In([18]crown-6)][A] species

As discussed earlier, there appears to be a correlation between a higher energy "lone pair" of electrons on a low oxidation state triel center and increased covalent interaction with the ligand/anion. Chapter 6 features calculations into the donor properties of hypothetical "crowned" indium(+1) halides and the known monomeric salt [In([18]crown-6)][OTf]. While it has been found experimentally that attempts to ligate

indium(+1) halides (or to generate them *in situ*) leads to rapid disproportionation, comparisons to the known triflate salt shows that looking at the "lone pair" energies, HOMO-LUMO gaps, and WBI of "crowned" indium species, may allow for the prediction of which salts are likely to be amenable to experimental isolation. Therefore, a series of calculations were performed on a wide variety of model $[\text{In}([\text{18}]\text{crown-6})][\text{A}]$ salts with a selection of common anions and the results are shown in Table 7.3. While the sandwich complex formed with $[\text{15}]\text{crown-5}$ (discussed in Chapter 3) has no interaction with its triflate anion, the cation has been included for LP energy and HOMO-LUMO gap comparisons. It should be mentioned that by itself no single calculated value appears to provide a complete insight into the stability of the resultant complex. For example, the "lone pair" energy of the $[\text{In}([\text{18}]\text{crown-6})][\text{A}]$ complex in which $\text{A} = \text{I}$ is lower than that when $\text{A} = \text{OTf}$. However, the iodide salt is not a stable monomeric species whereas the triflate salt is. Therefore, it is perhaps wiser to consider all three properties as a whole when drawing conclusions, i.e., a complex with a low LP energy, larger HOMO-LUMO gap, and small In-X WBI would perhaps be the most likely species to be isolated experimentally.

Analyses of the data started with the two salts that have been isolated experimentally, $\text{A} = \text{OTf}$, TFA, and were found to have very similar properties as both the triflate and trifluoroacetate salts have a LP energy less than -6.0 eV, a HOMO-LUMO gap greater than 5.2 eV, and a WBI less than 0.13. While this sample size is not large enough to draw conclusive limits to what can be obtained experimentally, it is perhaps a good starting point to direct future synthetic targets. The data suggest that perhaps the best targets for synthesis are an acetate salt and fluorinated alkoxides as the anions that best mirror the conditions of the isolated triflate and trifluoroacetate salts are when $\text{A} =$

OCF₃, OC₃F₆H, and acetate. The general trend observed in the data is that an increased WBI between the indium center and the anion leads to a decreased HOMO-LUMO gap and a higher LP energy.

Table 7.3: Computational data for a series of "crowned" indium salts

Species	E (In LP) (eV) ^a	H-L Gap (eV)	WBI (In-X) ^b
[In([18]crown-6) ⁺]	-10.717	5.388	N/A
[In([15]crown-5) ₂ ⁺]	-9.644	5.866	N/A
[In([18]crown-6)][OTf]*	-6.389	5.626	0.106
[In([18]crown-6)][TFA]*	-6.034	5.264	0.129
[In([18]crown-6)][CH ₃]	-4.999	3.599	0.385
[In([18]crown-6)][NH ₂]	-5.088	4.004	0.292
[In([18]crown-6)][NMe ₂]	-5.072	3.879	0.264
[In([18]crown-6)][OH]	-5.261	4.376	0.224
[In([18]crown-6)][OMe]	-5.093	4.293	0.208
[In([18]crown-6)][OPh]	-5.441	4.587	0.162
[In([18]crown-6)][OCF ₃]	-5.942	5.310	0.132
[In([18]crown-6)][PH ₂]	-5.823	3.854	0.448
[In([18]crown-6)][PMe ₂]	-5.787	3.360	0.434
[In([18]crown-6)][SH]	-5.936	4.473	0.367
[In([18]crown-6)][SiH ₃]	-5.805	3.935	0.520
[In([18]crown-6)][SMe]	-5.917	4.252	0.357

[In([18]crown-6)][Acetate]	-5.534	4.881	0.147
[In([18]crown-6)][OC ₃ F ₆ H]	-5.360	4.827	0.151

^aNBO energy of the "lone pair" MO of electrons on In; ^bNBO Wiberg Bond Index calculated for the In-X bond; *Isolated experimentally

7.4 Conclusions

A series of reactions was performed with InOTf and a variety of α -diimines. While definitive structural evidence remains lacking, a low quality crystal structure and computational analyses shows a distorted pyramidal geometry at the indium center with the "lone pair" of electrons associated with the indium center. However, calculations suggest that this lone pair of electrons can be "activated" by incorporating an anion with an increased degree of covalent interaction with the metal center. Analyses on a series of "crowned" indium salts shows that, in general, the energy of the "lone pair" of electrons increases and the HOMO-LUMO gap decreases as the Wiberg bond index between the indium center and the anion increases. This suggests that attempts to isolate stable materials would be best undertaken using non-coordinating anions, and substituents that favour more ionic bonding.

7.5 Experimental

7.5.1 General Procedures

All manipulations were carried out using standard Schlenk techniques and solvents were dried using a series of Grubbs'-type columns and degassed prior to use. Melting points were obtained using an Electrothermal[®] melting point apparatus on samples sealed in glass capillaries under dry nitrogen. Solution phase NMR spectra were recorded at room temperature on a Bruker Avance 300-MHz spectrometer. Chemical shifts are reported in

ppm, relative to external standards (SiMe₄ for ¹H and ¹³C NMR). InOTf and ^{Mes}DAB (and all other ligands) were prepared according to reported procedures.

7.5.2 Synthetic Procedures

General reactions of InOTf with diimines

In a typical experiment (20 mL) of toluene was added to InOTf (0.200 g, 0.758 mmol) and a toluene (15 mL) diimine (0.758 mmol) solution was added. The mixture was stirred overnight and volatile components were removed under reduced pressure and the product was obtained as a powder. In the case of ^{Mes}DAB crystals were obtained from slow concentration of a toluene solution, however were of low quality and are only used to establish connectivity.

Synthesis of InOTf·^{Mes}DAB

InOTf (0.200 g) and ^{Mes}DAB (0.242 g) yielded 0.372 g (84.2 %) of an orange powder. Anal. Calcd. Calc: C% 48.11 (47.27), H% 4.69 (4.83), N% 4.80 (4.79). ¹H NMR (C₆D₆): δ = 1.997 (CH₃, 12H); 2.052 (CH₃, 6H); 2.218 (CH₃, 6H); 6.843 (CH, 4H)

Synthesis of InOTf·^{Diip}DAB

InOTf (0.212 g) and ^{Diip}DAB (0.326 g) yielded 0.470 g (87.4 %) of an orange powder. Anal. Calcd. C% 52.85 (52.10), H% 6.42 (6.03), N% 4.14 (4.19). ¹H NMR (C₆D₆): δ = 1.171 (CH₃, 24H); 2.146 (CH₃, 6H); 2.863 (CH, 4H)

Synthesis of InOTf·^{Mes}BIAN

InOTf (0.200 g) and ^{Mes}BIAN (0.315 g) produced 0.436 g (84.7 %) of a deep red/purple powder. Anal. Calcd. C% 52.17 (54.72), H% 4.25 (4.15), N% 3.79 (4.12). Low solubility in C₆D₆.

Synthesis of InOTf·^{Diiip}BIAN

InOTf (0.200 g) and ^{Diiip}BIAN (0.378 g) produced 0.502 g (86.8 %) of an orange powder. Anal. Calcd. C% 57.59 (58.12), H% 5.21 (5.27), N% 3.31 (3.66). Low solubility in C₆D₆.

7.5.3 Computational Methods

All density functional theory (DFT) calculations were performed using the B3PW91 method using the Gaussian 03 or 09 suites using the SHARCNET high-performance computing network (www.sharcnet.ca). Where applicable, the Stuttgart group (SDD) effective core potentials (ECP) and corresponding basis sets were used for indium atoms and the 6-31+G(d) basis set was used for all lighter atoms. Natural bond order (NBO) analyses to determine Wiberg bond indices, orbital contributions, and HOMO/LUMO energies were obtained using the routine included in the Gaussian distributions. All stationary points were confirmed to be minima exhibiting no imaginary frequencies. It should also be noted that geometry optimizations for the nearly cylindrical molecules ligated to [18]crown-6 did not always satisfy all the convergence criteria because of the very flat potential energy surface; in such cases frequency calculations on the lowest energy structures exhibit no imaginary frequencies thus these geometries were used to calculate the required single point energies.

References

- [1] S. P. Green, C. Jones, A. Stasch, *Angew. Chem., Int. Ed.* **2007**, *46*, 8618.
- [2] M. L. Cole, C. Jones, M. Kloth, *Inorg. Chem.* **2005**, *44*, 4909.
- [3] M. A. Khan, C. Peppe, D. G. Tuck, *Can. J. Chem.* **1984**, *62*, 601.
- [4] C. G. Andrews, C. L. B. Macdonald, *Angew. Chem., Int. Ed.* **2005**, *44*, 7453.
- [5] B. F. T. Cooper, C. L. B. Macdonald, *J. Organomet. Chem.* **2008**, *693*, 1707.
- [6] W. Uhl, *Naturwissenschaften* **2004**, *91*, 305.
- [7] S. T. Haubrich, P. P. Power, *J. Am. Chem. Soc.* **1998**, *120*, 2202.
- [8] O. T. Beachley, R. Blom, M. R. Churchill, K. Faegri, J. C. Fettinger, J. C. Pazik, L. Victoriano, *Organometallics* **1989**, *8*, 346.
- [9] M. S. Hill, P. B. Hitchcock, *Chem. Comm.* **2004**, 1818.
- [10] M. C. Kuchta, H. V. R. Dias, S. G. Bott, G. Parkin, *Inorg. Chem.* **1996**, *35*, 943.
- [11] H. V. R. Dias, W. C. Jin, *Inorg. Chem.* **1996**, *35*, 267.
- [12] K. Yurkerwich, D. Buccella, J. G. Melnick, G. Parkin, *Chem. Comm.* **2008**, 3305.
- [13] H. V. R. Dias, L. Huai, W. C. Jin, S. G. Bott, *Inorg. Chem.* **1995**, *34*, 1973.
- [14] A. Frazer, B. Piggott, M. B. Hursthouse, M. Mazid, *J. Am. Chem. Soc.* **1994**, *116*, 4127.
- [15] A. Frazer, P. Hodge, B. Piggott, *Chem. Comm.* **1996**, 1727.
- [16] T. Jurca, J. Lummiss, T. J. Burchell, S. I. Gorelsky, D. S. Richeson, *J. Am. Chem. Soc.* **2009**, *131*, 4608.
- [17] T. Jurca, I. Korobkov, G. P. A. Yap, S. I. Gorelsky, D. S. Richeson, *Inorg. Chem.* **2010**, *49*, 10635.
- [18] J. M. Slattery, A. Higelin, T. Bayer, I. Krossing, *Angew. Chem., Int. Ed.*, *49*, 3228.
- [19] S. Welsch, M. Bodensteiner, M. Dusek, M. Sierka, M. Scheer, *Chem. Eur. J.* **2010**, *16*, 13041.
- [20] H. M. Tuononen, R. Roesler, J. L. Dutton, P. J. Ragona, *Inorg. Chem.* **2007**, *46*, 10693.
- [21] N. Metzler-Nolte, *New J. Chem.* **1998**, *22*, 793.
- [22] W. W. Schoeller, S. Grigoleit, *J. Chem. Soc., Dalton Trans.* **2002**, 405.
- [23] A. Sundermann, M. Reiher, W. W. Schoeller, *Eur. J. Inorg. Chem.* **1998**, 305.
- [24] E. S. Schmidt, A. Jockisch, H. Schmidbaur, *J. Am. Chem. Soc.* **1999**, *121*, 9758.

Chapter 8: Conclusions and Future Work

The focus of a large portion of this dissertation has been on the purification and extension of the chemistry of the useful reagent InOTf and its "crowned" salts. The discovery of the synthetic procedure using indium metal allows for a direct, facile route to the salt which eliminates any halide impurities present from previously used methods. This process is found to proceed through the formation of In(+3) species followed by reduction to the In(+1) final product. The addition of one equivalent of [18]crown-6 speeds this reaction up considerably, as the crown ether "traps" indium in the +1 oxidation state and impedes the formation of the insoluble InOTf₃.

The structural and reactivity differences between InOTf complexes incorporating various crown ethers were also investigated. Use of the cyclic ether [15]crown-5 affords a 2:1 complex which is found to have significantly different reactivity than the [18]crown-6 complex. While the [18]crown-6 indium complexes were found to readily insert into the carbon-chlorine bonds of CHCl₃ and CH₂Cl₂, the sandwich nature of the complex seemingly renders the "lone pair" of electrons on the indium center inactive in terms of stereochemistry and reactivity.

The ability to remove indium from the crown ether ligand via potassium metathesis was also investigated. In all cases the [18]crown-6 ligand preferentially formed a complex with the potassium cation over the indium(+1) cation. However, control of the reactivity of the uncrowned indium center was not straightforward, and the fate of the indium cation could not be elucidated in all cases.

The mixed valent nature of E₂X₄ species was used as a model to develop a facile synthesis of [In][EX₄] salts via a "halide transfer" reaction of InCl and ECl₃. These salts were then treated with cyclic ethers to obtain ionic salts or donor-acceptor complexes

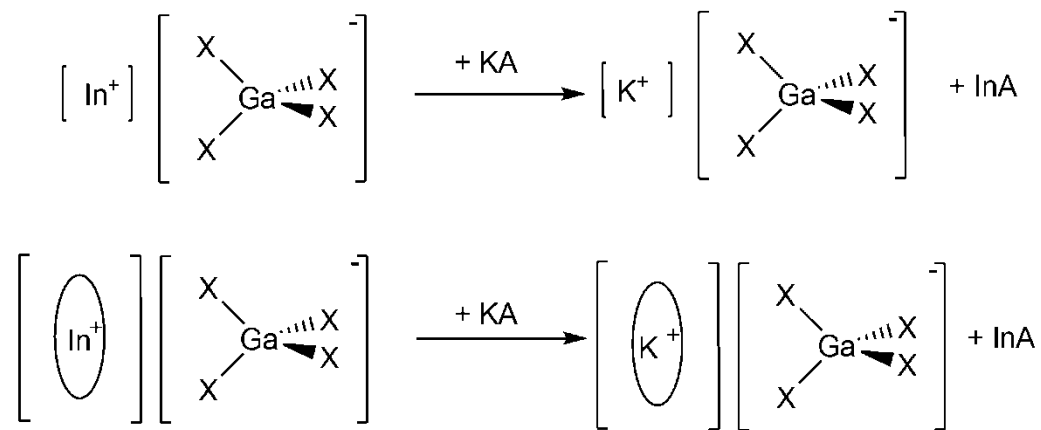
depending on the nature of element E and the cavity size of the crown ether. These compounds were also useful in illustrating the ability of solid-state ^{115}In NMR to differentiate between the various bonding environments at the indium centers. Computational analyses suggest that the anion plays a role in the energy and availability of the $\text{In}(+1)$ "lone pair" of electrons.

Experimental investigations into α -diimine complexes failed to produce definitive structural results; however, computational analyses further illustrate the importance of the bonding interaction between the ligand and the anionic substituent. The ability to stabilize low oxidation state triel centers appears to be best attained by incorporating ligands and anions that have a low degree of covalent interaction with the metal center.

Taking the knowledge learned throughout the course of this dissertation a potential direction for this project would be to use systems with non-covalent substituents to stabilize $\text{In}(+1)$ species in solution and incorporate reagents with higher degrees of covalency, such as halides, to induce reactivity. As computational analyses suggest, substituents with increased covalent nature increase the energy of the "lone pair" of electrons on the metal center and subsequently should increase the reactivity. Investigations into indium insertions via "halide activation" are currently underway in the Macdonald research group and the use of non-cyclic polyethers as stabilizing ligands are also proving fruitful.

The initial information obtained from Chapter 5, mainly ability of potassium to remove indium from cyclic ether ligand, merits further investigation of the metathesis chemistry of these species. The solubility of $[\text{In}][\text{GaCl}_4]$ and the presence of a "free" indium(+1) cation in the [15]crown-5 half-sandwich complex (reported in Chapter 6) highlight the potential this salt could have as a synthetic reagent and as a potential source

of In(+1) in solution. The ionic nature of the crowned species in solution and the solid state provides the potential that metathesis reactions with non-oxidizing, non-covalent substituents could also afford new In(+1) species (Scheme 8.1). The large number of materials synthesized via methathesis routes found in the literature frequently employ indium(+1) halides.^[1] As has been mentioned many times in this dissertation, the low solubility of these halides means that using the exceedingly more soluble [In][GaCl₄] salt would allow for these reactions to proceed in a more homogenous environment. In addition, since both the "crowned" and free potassium tetrachlorogallate salts have known crystal structures the progress of the reaction could be traced using pXRD and could allow for separation of the products by selectively crystallizing the potassium salts.^[2, 3]



Scheme 8.1: Potential metathesis reactions involving [In][GaCl₄] species.

Given the insight gained over the course of this project with regards to In(+1) reagents, and the recent discovery of a stable Ga(+1) salt by Krossing incorporating a non-coordinating anion (NCA), the ability to synthesize other low oxidation state salts of the lighter triel metals should focus on the use of non-covalent substituents and stabilizing ligands. Towards this end initial studies into the reaction of Ga₂Cl₄ with cyclic ethers have been initiated. While the gallium analogues are significantly more sensitive to

oxidation, gallium-71 NMR studies suggest that it is possible to ligate a gallium(+1) salt with [15]crown-5. The smaller size of the Ga(+1) could allow for the use of ligands that were found to be too small to complex indium, such as porphers or cryptands. Further studies into the ideal reaction conditions to ligate Ga(+1) cations are ongoing.

The mixed valent nature of E_2X_4 species has been known for decades. However, the utility of these salts as a source of E(+1) has remained underdeveloped. Some initial coordination chemistry results of [In][EX₄] salts has been presented in this dissertation; however, as these salts are significantly more soluble and stable than their EX halides their synthetic capabilities should be explored.

References

- [1] J. A. J. Pardoe, A. J. Downs, *Chem. Rev.* **2007**, *107*, 2.
- [2] M. Gorlov, A. Fischer, L. Kloo, *Acta Crystallogr. Sect. E.* **2003**, *59*, I70.
- [3] W. T. K. Chan, D. J. Eisler, D. S. Wright, *Crystengcomm.* **2008**, *10*, 1315.

Vita Auctoris

Name: Benjamin Freeman Todd Cooper

Education: New Glasgow High School, New Glasgow, NS
Mount Allison University, Sackville, NB 2001-2005 B.Sc.
University of Windsor, Windsor, ON 2005-2011 Ph.D

Publications

In addition to the following publications in peer-reviewed journals, I have co-authored a book chapter on mixed valent group 13 species in the book:

‘The Group 13 Metals Aluminium, Gallium, Indium and Thallium. Chemical Patterns and Peculiarities’

Benjamin F.T. Cooper, Hiyam Hamaed, Warren W. Friedl, Michael R. Stinchcombe, Robert W. Schurko, and Charles L.B. Macdonald. *Chemistry - A European Journal*, Accepted.

Benjamin F.T. Cooper and Charles L.B. Macdonald, *Acta Cryst.*, **2011**, E67, m233-m234

Benjamin F.T. Cooper, Charles L.B. Macdonald. *New Journal of Chemistry*, **2010**, 34, 1551-1555

Rajoshree Bandyopadhyay, **Benjamin F.T. Cooper**, Aaron J. Rossini, Robert W. Schurko, Charles L.B. Macdonald. *Journal of Organometallic Chemistry*, **2010**, 695, 7, 1012-1018

Benjamin F.T. Cooper, Charles L.B. Macdonald. *Main Group Chemistry*, **2010**, Vol. 9, No. 1-2, 141-152

Paul A. Rugar, Rajoshree Bandyopadhyay, **Benjamin F.T. Cooper**, Michael R. Stinchcombe, Paul J. Ragona, Charles L.B. Macdonald, Kim M. Baines. *Angewandte Chemie-International Edition*, **2009**, 48, 28, 5155-5158

Jonathan W. Dube, Gregory J. Farrar, Erin L. Norton, Kara L. S. Szekely, **Benjamin F.T. Cooper**, Charles L. B. Macdonald. *Organometallics*, **2009**, 28, 15, 4377-4384

Mohammad Harati, James Green, **Benjamin F.T. Cooper**, Jichang Wang. *Journal of Physical Chemistry A*, **2009**, 113(24), 6548-6551

Bhartesh Dhudshia, **Benjamin F.T. Cooper**, Charles L.B. Macdonald, Avinash N. Thadani. *Chemical Communications*, **2009**, 4, 463-465

Hiyam Hamaed, Jenna M. Pawlowski, **Benjamin F.T. Cooper**, Riqiang Fu, S. Holger Eichorn, and Robert W. Schurko. *Journal of the American Chemical Society*, **2008**, 130: 11056-11065

Benjamin F. T. Cooper and Charles L. B. Macdonald* *Journal of Organometallic Chemistry*, **2008**, 693: 1707-1711

Benjamin F.T. Cooper, Christopher G. Andrews, Charles L.B. Macdonald*. *Journal of Organometallic Chemistry*, **2007**, 692, 2843–2848

Glen G. Briand*, **Benjamin F.T. Cooper**, David B.S. MacDonald, Caleb D. Martin and Gabriele Schatte. *Inorganic Chemistry*, **2006**, 45, 8423-8429.